Acta Universitatis Agriculturae Sueciae

Doctoral Thesis No. 2024:11
Faculty of Veterinary Medicine and Animal Science

A transcriptomic tale of two worms

Evaluating *Caenorhabditis elegans* as a model for *Parascaris univalens* in drug resistance studies

Faruk Dube

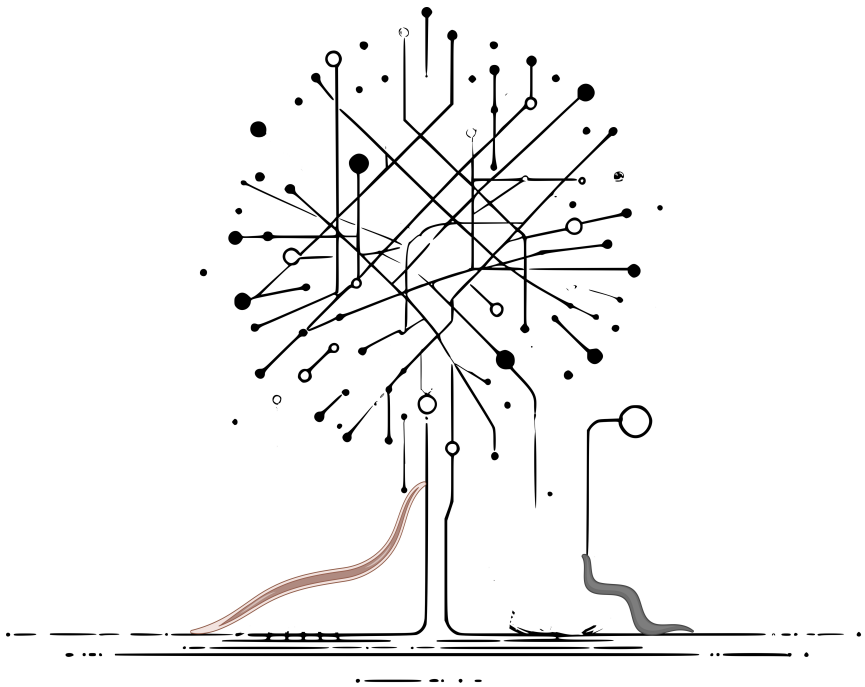

A transcriptomic tale of two worms

Evaluating *Caenorhabditis elegans* as a model for *Parascaris univalens* in drug resistance studies

Faruk Dube
Faculty of Veterinary Medicine and Animal Science
Department of Animal Biosciences
Uppsala

SLU
SWEDISH UNIVERSITY OF AGRICULTURAL SCIENCES

DOCTORAL THESIS
Uppsala 2024

Acta Universitatis Agriculturae Sueciae
2024:11

Cover: Gene network of two roundworms designed by Faruk Dube

ISSN 1652-6880
ISBN (print version) 978-91-8046-286-0
ISBN (electronic version) 978-91-8046-287-7
DOI: https://doi.org/10.54612/a.45di2f4mbp

Swedish University of Agricultural Sciences, Department of Animal Biosciences, Uppsala, Sweden

Print: SLU Grafisk service, Uppsala 2024

A transcriptomic tale of two worms

Abstract

Parascaris univalens, an equine roundworm, poses a significant threat to foals, potentially causing lethal intestinal ruptures in high infestations. Infection control relies on a limited arsenal of anthelmintic drugs like ivermectin (IVM). However, widespread resistance exacerbated by frequent treatments in foals, first year, challenges effective management. Research into the genetics of this resistance is vital, yet troubled by the parasite's complex lifecycle, large size, cultivation issues, incomplete genome, and ethical and financial constraints. The free-living nematode *Caenorhabditis elegans*, known for its simple lifecycle and well-mapped genome, offers a promising alternative model. This thesis assessed *C. elegans* as a model for studying anthelmintic resistance (AR) in *P. univalens* and other ascarids, using transcriptomics and gene co-expression networks to bypass traditional method biases and identify novel genes referred to as "core genes". The study exposed adult *P. univalens* and *C. elegans* to different IVM concentrations, revealing distinct genetic responses. *Parascaris univalens* showed core genes linked to transcriptional suppression, cell cycle inhibition, ribosomal activation, and cuticle/membrane integrity, while *C. elegans* exhibited diverse core gene involvement, especially upregulated heat shock proteins. *Caenorhabditis elegans* had more differentially expressed genes (DEGs) in xenobiotic metabolism, with Cytochrome P450s dominance compared to Short Chain Dehydrogenase/Reductases in *P. univalens* in Phase I. However, the response of Phase II metabolism genes was similar in both species. In addition, the *P. univalens* IVM response affected numerous ligand-gated ion channels compared to *C. elegans*, indicating species-specific differences. Despite no shared orthologous core genes and different IVM response functions, both species engaged similar gene families, highlighting *C. elegans* as a useful model for *P. univalens* AR studies. Yet, significant differences underline the necessity for supplementary, targeted research in specific parasitic nematodes, crucial for understanding AR mechanisms and developing more effective control strategies in equines.

Keywords: ivermectin, gene networks, RNA sequencing, anthelmintic resistance

A transcriptomic tale of two worms

Abstract

Parascaris univalens, hästens spolmask, utgör ett betydande hot mot föl. I värsta fall kan en kraftig infektion fall leda tarmruptur. Förebyggande parasitbekämpning bygger på behandling med anthelmintiska läkemedel som till exempel ivermektin (IVM). Dock har frekventa behandlingar hos föl under det första levnadsåret resulterat i en utbredd läkemedelsresistens hos *P. univalens*. För att i framtiden kunna bekämpa resistens är det viktigt att förstå de genetiska bakomliggande orsakerna. Några av de stora utmaningarna är parasiters komplexa livscykler, stora storlek och brist på metoder som möjliggör odling på laboratorier, samt ofullständiga genom. En lovande modell är den frilevande nematoden *Caenorhabditis elegans*, känd för sin enkla livscykel och väl kartlagda genom. Syftet med denna avhandling var att bedöma om *C. elegans* kan utgöra en modell för att studera anthelmintikaresistens (AR) hos *P. univalens.* Den här avhandlingen har använt sig av transkriptomik och genuttrycksnätverk för att kunna identifiera nya gener, så kallade "kärngener". Det vuxna stadiet av *P. univalens* och *C. elegans* exponerades för olika IVM-koncentrationer och därefter analyserades transkriptomet. Hos *P. univalens* hittades kärngener kopplade till transkriptionell reglering, cellcykelhämning, ribosomal aktivering och membranintegritet, medan hos *C. elegans* observerades en specifik uppreglering av heat shock proteiner. Vidare visade *C. elegans* fler differentiellt uttryckta gener involverade i xenobiotisk metabolism, och då framförallt Cytokrom P450s, jämfört med Short Chain Dehydrogenase/Reductases i *P. univalens*. Däremot hade båda arterna en likartad respons av Fas II-metabolismgener. Genuttrycket hos ligandstyrda jonkanaler visade på en tydlig artspecifik skillnad hos *P. univalen* och *C. elegans.* Sammanfattningsvis kunde inga gemensamma ortologa kärngener kopplade till IVM-exponering identifieras, men flera genfamiljer involverade i metabolism och transport svarade med ett likande mönster, vilket gör att *C. elegans* kan vara en användbar modell för *P. univalens*. Dock visar resultaten flera betydande skillnader och det är viktigt med fortsatt riktad forskning i specifika parasitiska nematoder, för att förstå de genetiska bakomliggande mekanismerna för AR.

Dedication

To *C. elegans*, my tiny yet mighty partner in the fight against parasitic worms. Your impact is larger than your size. And to my computer, who handled mountains of data without a glitch and survived countless late-night coding sessions - you both are the mighty heroes of this thesis!

Contents

List of publications

This thesis is based on the work contained in the following papers, referred to by Roman numerals in the text:

I. Dube, F., Hinas, A., Roy, S., Martin, F., Åbrink, M., Svärd, S., & Tydén, E. (2022). Ivermectin-induced gene expression changes in adult *Parascaris univalens* and *Caenorhabditis elegans*: a comparative approach to study anthelminthic metabolism and resistance *in vitro*. Parasites & vectors, 15(1), 158.

II. Dube, F., Hinas, A., Delhomme, N., Åbrink, M., Svärd, S., & Tydén, E. (2023). Transcriptomics of ivermectin response in *Caenorhabditis elegans*: Integrating abamectin quantitative trait loci and comparison to the Ivermectin-exposed DA1316 strain. PloS one, 18(5), e0285262.

III. Dube, F., Delhomme, N., Martin, F., Hinas, A., Åbrink, M., Svärd, S., & Tydén, E. (2023). Gene co-expression network analysis reveal core responsive genes in *Parascaris univalens* tissues following ivermectin exposure. PLoS one, (submitted manuscript)

IV. Dube, F., Delhomme, N., Martin, F., Hinas, A., Åbrink, M., Svärd, S., & Tydén, E. Comparative transcriptomic and gene network analysis in *Caenorhabditis elegans* and *Parascaris univalens* after ivermectin exposure, (manuscript).

Papers I-II are reproduced with the permission of the publishers.
The contribution of Faruk Dube to the papers included in this thesis was as follows:

I. Conducted data analysis and assumed primary authorship of the manuscript. Corresponded with the journal.

II. Took major part in study design and planning. Performed the experiments, data collection and analysis. Assumed primary authorship of the manuscript. Corresponded with the journal.

III. Conducted data analysis and assumed primary authorship of the manuscript. Corresponded with the journal.

IV. Conducted data analysis and assumed primary authorship of the manuscript. Corresponded with the journal.

List of tables

List of figures

Abbreviations

ABC	Adenosine triphosphate-binding cassette
AHR	Aryl hydrocarbon receptor
ALH	Aldehyde dehydrogenase
AR	Anthelmintic resistance
BLAST	Basic local alignment search tool
BZ	Benzimidazole
bZIP	Basic leucine zipper
CGC	Caenorhabditis genetics center
CYP	Cytochrome P450
DEG	Differentially expressed gene
DMSO	Dimethyl sulfoxide
DNA	Deoxyribonucleic acid
ELT	Erythroid-like transcription
FEC	Fecal egg count
FECRT	Fecal egg count reduction test
FMO	Flavin containing monooxygenase
GABA	Gamma-aminobutyric acid
GluCl	Glutamate-gated ion channel
GO	Gene ontology

GST	Glutathione S-transferase
HSP	Heat shock protein
IVM	Ivermectin
MFS	Major facilitator superfamily
ML	Macrocyclic lactone
mRNA	Messenger ribonucleic acid
nAChR	Nicotinic acetylcholine receptors
NHR	Nuclear hormone receptor
NRF2	Nuclear factor erythroid 2-related factor 2
ORA	Over-representation analysis
PCR	Polymerase chain reaction
Pgp	Permeability glycoprotein
qPCR	Quantitative polymerase chain reaction
QTL	Quantitative trait locus
RNA	Ribonucleic acid
RNA-seq	Ribonucleic acid-sequencing
SDR	Short-chain dehydrogenase/reductase
SLC	Solute carrier
spp.	Species
SVA	Swedish Veterinary Authority
TF	Transcription factor
UGT	Uridine 5'-diphospho-glucuronosyltransferase

1. Introduction

Gastrointestinal nematodes (GINs) are a significant health concern, infecting both humans and animals and leading to chronic and debilitating illnesses (Veesenmeyer, 2022; Gilleard et al., 2021). In humans, GINs affect over one billion people, contributing to roughly five million disability-adjusted life years as reported in 2010 (Pullan et al., 2014). The control of GIN in both humans and domesticated or livestock animals heavily relies on the use of anthelmintic drugs. For animals, this method of control is costly, particularly in the European ruminant livestock industry, which spends approximately €320 million annually on these treatments (Charlier et al., 2020).

Horses, like many domestic animals, are susceptible to GIN infections and commonly receive anthelmintic drugs throughout their lives. However, frequent use of these drugs fosters the development of drug-resistant nematodes, which survive treatment and pass on their resistance genes (Sangster, 1999). This has led to widespread anthelmintic resistance (AR) in various equine parasites, reviewed by (von Samson-Himmelstjerna, 2012; Nielsen et al., 2014a).

One of the most important equine parasite is *Parascaris* spp., which primarily infects foals and yearlings, often causing not only mild flu-like symptoms but also severe infestations can be fatal due to intestinal rupture (Reinemeyer, 2009). Consequently, foals are typically dewormed several times in their first year. *Parascaris* spp. resistance was initially reported in the Netherlands in 2002 (Boersema et al., 2002). Since then, resistance to multiple drug classes has been reported globally, posing a serious threat to foal health and welfare (Nielsen, 2016). While resistance among other members of the *Ascarididae* family of roundworm parasites is uncommon, there are concerning instances of resistance in *Ascaris lumbricoides*,

affecting humans (Krucken et al. 2017), and in *Ascaridia dissimilis*, a roundworm that parasitizes turkeys (Collins et al. 2019), indicating an emerging threat.

The mechanisms behind ascarid parasites' resistance to different anthelmintic drugs remain unclear. Gaining insight into these mechanisms is vital for curbing the spread of resistance and for the development of early detection markers. The recent advent of omics technologies and the publication of the *Parascaris univalens* draft genome (Wang et al., 2017) mark significant strides in understanding resistance mechanisms. Conventional candidate gene approaches are often limited by their reliance on pre-existing knowledge, leading to potential biases. In contrast, modern data-driven analytical methods (Schiffthaler et al., 2023) enable a more objective and comprehensive exploration of gene functions and interactions. These methods are instrumental in uncovering the complex gene relationships that determine drug response and resistance, free from the constraints of conventional approaches.

Research into AR in *P. univalens* is hampered by the parasite's complex life cycle and the absence of a fully annotated genome, as well as cultivation difficulties. These challenges are compounded by ethical and financial limitations, often restricting studies to *in vitro* methods using parasites from euthanized horses. Moreover, variations in gene expression between the larval and adult stages of *P. univalens* limit using larvae stage as a model (Martin et al., 2021a). In this context, the free-living nematode *Caenorhabditis elegans*, with its simpler biology, rapid life cycle, well-annotated genome, and ease of genetic manipulation (Salinas and Risi, 2018), has become an invaluable model for studying AR (Wit et al., 2021). Although *C. elegans* belongs to a different taxonomic clade, it has proven to be a useful tool in the study of AR in *P. univalens* (Janssen et al., 2015; Janssen et al., 2013; Gerhard et al., 2021). A notable example is the transfection of the *P. univalens* intestinal efflux pump gene, *pgp-9*, into *C. elegans*, was shown to confer a protective effect against ivermectin (Gerhard et al., 2021).

Given the severe health risks posed by *Parascaris* spp. and other ascarid infections, coupled with the lack of new anthelmintic drugs, the escalating resistance to existing drug classes is a major concern for both animal and human health. Consequently, identifying novel candidate genes and a

suitable model organism for ascarid research is essential to enhance our understanding and develop strategies to combat resistant parasite.

2. Background

2.1 Parascaris spp.

Parascaris spp., large nematodes of the *Ascarididae* family, represent the most pathogenic parasites in young horses (Nielsen, 2016). These helminths exhibit a cream color, with sexual dimorphism evident in size and morphology. Females typically measure 10-20 cm in length and 5 mm in diameter, while males are smaller, ranging from 10-15 cm in length with a 3-mm diameter (Wells, 1924; Clayton and Duncan, 1979b). Sexual differentiation is further marked by a posterior curl in males and the absence of visible ovaries through the cuticle in females (Wells, 1924). Notably, their eggs are round with a thick brownish shell, measuring around 100 μm in diameter (Reinemeyer and Nielsen, 2013).

Historically, the species *Parascaris equorum* was the sole agent identified in equine parasitism. However, it has been acknowledged that *Parascaris univalens*, a closely related species, also infects equines. Morphologically indistinguishable to the naked eye, these species can be differentiated by karyotyping: *P. equorum* possesses two chromosome pairs, whereas *P. univalens* has a singular pair (Goday and Pimpinelli, 1986). Contemporary research indicates a predominance of *P. univalens* in equine infections, challenging previous assumptions (Nielsen et al., 2014b; Martin et al., 2018; Martin et al., 2021c; Han et al., 2022).

Figure 1. **Adult *Parascaris univalens*** specimen displayed in a gloved hand, illustrating the species' standard cream coloration, size, and morphological features. (Photo: Faruk Dube)

2.1.1 Life-cycle and Diagnosis

Sexual reproduction in *Parascaris* spp. occurs in the host's small intestine, where females deposit eggs that are subsequently excreted into the environment via feces (Wells, 1924). Once in the external environment, particularly in pastures, these eggs develop embryonically, becoming infective larvae (Wells, 1924; Clayton and Duncan, 1979b).

When a foal ingests these eggs, the larvae hatch and penetrate the intestinal lining, migrating first to the liver and then to the lungs via the bloodstream. This migration can cause flu-like symptoms in the foal as the larvae exit the lung arterioles and capillaries, are coughed up, and re-ingested, returning to the small intestine (Clayton and Duncan, 1979b). In the intestine, *Parascaris* spp. larvae undergo rapid growth, increasing from 2-4 mm to 70-80 times their original size within 4.5 months, maturing into adult worms (Clayton and Duncan, 1979b). A heavy infestation can cause intestinal rupture and be fatal. The time from initial egg ingestion to the detection of eggs in faecal matter, known as the prepatent period, is crucial in understanding the dynamics of infection and diagnosis

During the prepatent period, adult worms are present and growing within the small intestine, yet their presence may not be detected by fecal egg counts (FECs). The detection of patent *Parascaris* spp. infection typically involves examining fecal samples; however, due to the long prepatent period, FECs can be negative even when worms are present. Egg output varies and may peak around four months post-infection, with a possible secondary peak around nine months (Clayton and Duncan, 1979b; Donoghue et al., 2015).

Notably, FECs do not always correlate with the actual number of roundworms present (Nielsen et al., 2010). However, transabdominal ultrasound emerges as an alternative diagnostic tool for ascarid presence in the small intestine (Nielsen et al., 2016), yet its specialized requirements limit its practicality for widespread diagnostic use.

2.1.2 Host immunity

Parascaris spp. infections are predominantly observed in young horses until around 6 to 8 months of age, at which point horses typically start to develop an age-linked immunity (Clayton and Duncan, 1979a; Fabiani et al., 2016). This trend is noted with some exceptions, notably in adult horses in tropical climates and in donkeys, where infection rates are influenced by factors such as inadequate nutrition and strenuous labor (Vercruysse et al., 1986; Getachew et al., 2008; Getachew et al., 2010; Lem et al., 2012; Hautala et al., 2019). As juvenile horses age, there is a decline in both the number of worms and the quantity of eggs shed in faces (Clayton and Duncan, 1979a; Fabiani et al., 2016; Donoghue et al., 2015). An experimental study involving eight foals and two yearlings indicated that while yearlings showed more severe respiratory symptoms, they retained their body condition. In contrast foals showed milder respiratory symptoms but experienced weight loss, hinting at an age-related difference in immune response, despite the small sample size (Clayton and Duncan, 1978). Antibody titers against whole worm antigens have been found to increase with foal age, correlating with a reduction in parasite prevalence (Bello, 1985), with immune responses also observed in lung and liver migrations (Nicholls et al., 1978; Brown and Clayton, 1979). However, there is no direct evidence of parasite mortality or fitness reduction due to the equine immune response, nor has there been molecular proof of such an immune response in horses.

The secretory products of helminths, such as microRNAs and extracellular vesicles, are implicated in immune evasion and host immune response stimulation, potentially paving the way for vaccine or diagnostic test development (Lightowlers and Rickard, 1988; Sotillo et al., 2020; Zakeri et al., 2021). In *Ascaris suum*, these extracellular vesicles harbor immunomodulatory proteins (Hansen et al., 2019), and microRNAs seem to be critical for parasite growth (Xu et al., 2013). *In vitro* studies of larval *Parascaris* spp. have identified secretory products that provoke an antibody response in foals with prior infections (Burk et al., 2014). These antibodies

are transferred from mares to foals through colostrum, although their diagnostic or vaccination efficacy is questionable as infections still occur despite their presence (Burk et al., 2016). To date, no research has specifically examined the microRNAs or extracellular vesicles of *Parascaris* spp., and further investigation is essential to fully comprehend the nature of equine immunity against this parasite.

2.2 Treatment and prevention

Given the extended prepatent period and the high risk of *Parascaris* spp. infection in most stud farms, it is common practice to administer anthelmintic drugs to foals at set intervals, often without prior faecal testing. In Sweden, the prevailing guidelines advise treatment of foals at 8-10 weeks and again at 16-18 weeks, with any subsequent treatments guided by fecal examination results (SVA, 2022). The three primary classes of anthelmintics used to combat roundworm infections in horses are macrocyclic lactones, tetrahydropyrimidines, and benzimidazoles.

2.2.1 Macrocyclic lactones

Introduced in 1981, macrocyclic lactones (MLs), a class of antiparasitic drugs originating from *Streptomyces* bacterial compounds, are renowned for their broad-spectrum efficacy against both endoparasites and ectoparasites and are extensively used in veterinary medicine (Nolan and Lok, 2012; Lanusse et al., 2009). Prominent members of this class include ivermectin (IVM) and moxidectin, belonging to the avermectin and milbemycin subclasses, respectively (Nolan and Lok, 2012).

Glutamate-gated chloride channels (GluCls) exhibit higher sensitivity to MLs at lower concentrations compared to gamma-aminobutyric acid (GABA) receptors, indicating they are the primary target for the drug (Beech et al., 2010b). These channels are mainly located on nerve and muscle cell membranes (Martin et al., 2002), and their drug binding affinity varies with the homo- or hetero-pentameric structure of their subunits (Wolstenholme and Neveu, 2022a). In *C. elegans*, four genes, *avr-14*, *avr-15*, *glc-1*, and *glc-3* are identified as encoding α-subunits sensitive to MLs, while two others, *glc-2* and *glc-4* are considered ML-insensitive (Glendinning et al., 2011). In *P. univalens*, at least four distinct GluCl subunits, *avr-14*, *glc-2*, *glc-3*, and

glc-4 have been identified and are reported to be phylogenetically conserved among nematodes (Lamassiaude et al., 2022).

When MLs bind to these receptors, they induce an influx of chloride ions, leading to hyperpolarization of body wall muscles and depolarization of pharyngeal muscles(Pemberton et al., 2001). This results in flaccid muscle paralysis (Martin et al., 2002), impairing feeding through reduced pharyngeal pumping, hence starvation (Geary et al., 1993; Brownlee et al., 1997). Additionally, MLs may affect parasite egg production, as GABA and GluCI receptors are integral to ovipositioning processes (Fellowes et al., 2000). Beyond their primary targets, IVM also interacts with other ligand-gated channels such as nicotinic and dopamine receptors, indicating a comprehensive antiparasitic action (Krause et al., 1998; Rao et al., 2009). Furthermore, an expanded range of targets for MLs has been extensively documented reviews (Laing et al., 2017; Martin et al., 2021d). Notably, the effective concentrations for influencing these additional targets are substantially higher than the doses needed for managing nematode infections.

2.2.2 Benzimidazoles

First introduced in 1961, the benzimidazole (BZ) drug class has been widely used to treat various nematode and trematode infections (Brown et al., 1961). This drug class functions by binding to β-tubulin, altering its shape and obstructing the assembly of microtubules and other critical cell structures, leading to cellular dysfunction, starvation, and subsequent parasite death (Lacey, 1990). Nematodes typically possess multiple β-tubulin genes, or isotypes. For instance, *C. elegans* has six β-tubulin genes (Gogonea et al., 1999), but only the *ben-1* gene is targeted by BZs (Driscoll et al., 1989). In the case of the sheep parasite *Haemonchus contortus*, out of its four β-tubulin genes, isotypes 1 and 2 are linked to BZ resistance (Saunders et al. 2013). However, none of the seven β-tubulin genes in *P. univalens* were linked to BZ resistance (Martin et al., 2021b).

2.2.3 Tetrahydropyrimidines

Introduced in 1966, tetrahydropyrimidines are a class of anthelmintic compounds available in various formulations (Aubry et al., 1970). They function as agonists to L-type nicotinic acetylcholine gated ion channels (nAChR) found in the neuromuscular junctions of somatic and pharyngeal

muscle cells in parasites. These nAChRs, consisting of five subunits with variable compositions, play a key role in determining the parasite's sensitivity to anthelmintic treatment (Williamson et al., 2009). The activation of these channels by tetrahydropyrimidines causes cation influx, leading to muscle cell depolarization and subsequent spastic paralysis of the worm, which is then expelled from the host through (Martin and Robertson, 2007)

2.3 Anthelmintic Resistance

Anthelmintic resistance, defined as the heritable and typically irreversible ability of parasites to withstand drug treatment at doses normally sufficient to kill them (Sangster, 1999), poses a major threat specifically in *Parascaris* spp. The first documented evidence of AR in *Parascaris* spp. was to MLs in 2002 (Boersema et al., 2002), and such resistance has subsequently been documented globally and is now considered widespread (Reinemeyer, 2009). This drug resistance, together with the risk of fatal complications in infected foals, renders *Parascaris* spp. infection a serious challenge to the equine industry and horse health.

2.3.1 Diagnosis of AR

The Faecal Egg Count Reduction Test (FECRT) is currently the sole routine method for screening anthelmintic resistance in *Parascaris* spp. on equine farms (Nielsen et al., 2019). This method involves counting the number of *Parascaris* spp. eggs in paired fecal samples taken before and approximately 14 days after anthelmintic treatment. The average reduction in egg count reflects the drug's effectiveness (Coles et al., 1992; Nielsen et al., 2019).

For other gastrointestinal nematodes with free-living larval stages, *in vitro* methods like egg hatch tests and larval development assays are available to assess drug efficacy (Coles et al., 2006). However, there are currently no validated *in vitro* methods for diagnosing AR in *Parascaris* spp., as ascarid larvae do not hatch outside their host.

Molecular PCR-based methods, for screening mutations, have been developed to diagnose resistance in several gastrointestinal strongyles (Coles et al., 2006; Charlier et al., 2018). Yet, to apply similar methods for ascarids, a deeper understanding of the mechanisms behind AR is required.

2.3.2 Mechanisms of AR

While the precise mechanisms conferring ML resistance in *Parascaris* spp. remain unclear, our limited understanding originates primarily from studies in *C. elegans* and some other parasitic nematodes (Whittaker et al., 2017). The proposed resistance mechanisms generally encompass mutations or differential expression of genes encoding drug targets, metabolic enzymes, transporters, and key transcription factors (Whittaker et al., 2017; Doyle et al., 2022; Laing et al., 2022; Ménez et al., 2019; Matoušková et al., 2016; Matoušková et al., 2018).

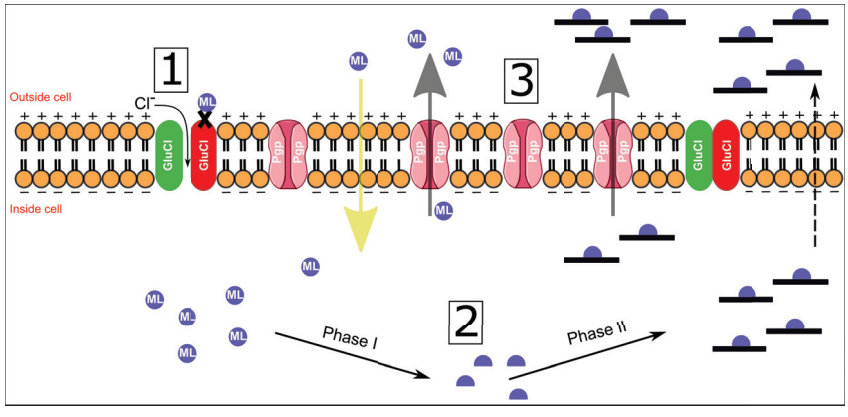

Figure 2. **Proposed anthelmintic resistance mechanisms**: 1) GluCls conformational changes, 2) increased ML drug metabolism, and 3) enhanced ML efflux via Pgps. Created by Faruk Dube in Inkscape.

Drug target

Mutation and differential expression of genes that encode drug targets are key factors in AR. For instance, concurrent mutations in the *avr-14*, *avr-15*, and *glc-1* genes in *C. elegans* resulted in a 4000-fold tolerance of IVM (Dent et al., 2000). Several strongylid parasitic nematodes share an *avr-14* orthologue, and a specific L256F mutation in this gene was linked to IVM resistance in *Cooperia oncophora* and *H. contortus* (McCavera et al., 2009; Njue et al., 2004). However, these findings could not be recapitulated in field isolates of *C. oncophora* or the closely related *Ostertagia ostertagi* (El-Abdellati et al., 2011). Moreover, mutations in the gene encoding the GABA receptor subunit, *lgc-37*, have been proposed to reduce susceptibility to MLs in *H. contortus* (Feng et al., 2002; Beech et al., 2010a). Downregulation of the *avr-14* subunit has been reported in IVM-resistant strains of the *C.*

oncophora and *O. ostertagi* (El-Abdellati et al., 2011), while decreased expression of *glc-3* and *glc-5* have been implicated in ML resistance in *H. contortus* (Williamson et al., 2011).

Metabolic enzymes

Differential expression of genes encoding enzymes involved in metabolism of xenobiotics such as drugs has been implicated in AR. Drug metabolism involves two phases. Phase I typically converts drugs into reactive compounds through oxidation, reduction, or hydrolysis. These compounds are then conjugated in Phase II with molecules like glutathione or glucose, forming soluble, inactive products for cellular excretion (Lindblom and Dodd, 2006).

Phase I enzymes, include Cytochrome P450s (CYPs), Short-chain Dehydrogenase/Reductases (SDRs), Flavin Monooxygenases (FMOs), Alcohol and Aldehyde Dehydrogenases (ALHs), Monoamine Oxidases (MAOs) and Hydrolases, but only a few of these super families have been implicated in AR so far. One such family is the CYPs, which carry out the majority of oxidative Phase I reactions (Guengerich, 2008; McDonnell and Dang, 2013). The *C. elegans* genome contains over 86 CYP genes, many of which are inducible by xenobiotics, including anthelmintic drugs (Menzel et al., 2001; Menzel et al., 2005b; Laing et al., 2010; Laing et al., 2015) (Stasiuk et al., 2019a). Constitutive overexpression of *CYP14A5* in IVM-selected *C. elegans* strains has been reported (Menzel et al., 2001). Several CYP genes have also been identified in *H. contortus* (Laing et al. 2015), and elevation of the expression of a CYP gene, *HCON_00022670* (CYP-3 family) was found in a highly BZ-resistant isolate of *H. contortus* in comparison to its susceptible counterparts (Yilmaz et al. 2017). Additionally, the expression of CYP genes in *H. contortus* is inducible by albendazole (Kellerová et al., 2020), and in *P. univalens* by ivermectin and oxibendazole (Scare et al., 2020), suggesting a potential role of Phase I enzymes in AR. The SDR superfamily, comprising enzymes that metabolize both internal and external substances, is also significant in the context of AR. The SDR genes have been reported to be upregulated in *C. elegans* following BZ exposure (Stasiuk et al., 2019a). More recently, increased expression of four SDR was reported in BZ-resistant *H. contortus* isolates compared to susceptible counterparts (Štěrbová et al., 2023). Furthermore, FMOs were reported by to play a role in the metabolism of albendazole in the liver fluke *Fasciola*

hepatica, based on the observation of elevate activity following albendazole exposure (Alvarez et al., 2005).

Phase II enzymes include the uridine 5'-diphosphoglucuronosyltransferase-glucosyltransferases (UGTs) and glutathione S-transferases (GSTs). The *C. elegans* genome contains 66 UGT (Meech et al., 2019) and 56 GST genes (Hartman et al., 2021) and some of the enzymes encoded by these genes have been implicated in AR (Matoušková et al., 2016). In *C. elegans*, several UGTs and GSTs showed increased expression in response to exposure to BZs (Stasiuk et al., 2019a), and similar responses were observed in *H. contortus* exposed to albendazole (Kellerová et al., 2020). Notably, a UGT gene was found to be consistently upregulated in a BZ-resistant *H. contortus* strain compared to a susceptible one (Matoušková et al., 2018), highlighting the potential significance of Phase II enzymes in the development of AR.

Membrane transporters

Membrane transporters, often referred to as Phase III in xenobiotic metabolism and detoxification, play a crucial role in expelling drugs from cells (Lindblom and Dodd, 2006; Hartman et al., 2021). In this thesis, this classification is extended to include transporters involved in drug import/uptake. Notably, two primary transporter families interact directly with drugs: ATP-binding cassette transporters (ABCs) and solute carrier proteins (SLCs). The ABC transporters typically facilitate drug export, while SLCs are primarily involved in compound uptake, albeit with some exceptions (Girardi et al., 2020). Transporters contribute to drug resistance by either increasing drug efflux or decreasing drug import.

The ABC family, mainly comprises of the P-glycoproteins (Pgps), the PGP-half transporter family (Hafs) and the Multidrug Resistance Protein family (Mrps) (Sheps et al., 2004), of which some have been implicated in drug resistance. Pgps, especially, have received considerable attention regarding AR, particularly for MLs (Xu et al., 1998; Dicker et al., 2011b; Raza et al., 2016b). In *P. univalens*, ten genes within the Pgp family have been identified, with *pgp-2* and *pgp-9* showing interaction with IVM (Gerhard et al., 2020). Despite higher constitutive expression in adult worms than larvae, no drug-induced expression was observed in *P. univalens* (Martin et al., 2021a). Conversely, other studies have reported different findings, such as increased expression of *pgp-11.1* in *Parascaris* spp. being correlated with reduced IVM sensitivity (Janssen et al., 2013), and its

transgenic expression in *C. elegans* leading to decreased susceptibility to the drug (Janssen et al., 2015). Similarly, in multidrug-resistant *Teladorsagia circumcincta*, an increased constitutive expression of *tci-pgp-9* has been noted (Dicker et al., 2011b). In *C. elegans*, inactivating of specific Pgps like *pgp-2*, *pgp-5*, *pgp-6*, *pgp-7*, *pgp-12*, and *pgp-13* resulted in increased sensitivity to IVM (Ardelli and Prichard, 2013a).

The SLC family includes the major facilitator superfamily (MFS), a large group of membrane transporters involved in transporting endogenous substances and drugs across membranes in both prokaryotes and eukaryotes (Höglund et al., 2011). The SLC transmembrane transporters have been implicated in resistance to cytotoxic drugs in humans (Girardi et al., 2020). In bacteria, upregulation of MFS transporter genes has been associated with drug efflux and resistance (Fluman and Bibi, 2009). However, the roles of these transporters in anthelmintic drug metabolism and resistance have not been extensively investigated to date.

Key transcription factors

Transcription factors (TFs) and regulatory mechanisms that activate specific detoxification responses to xenobiotics are broadly conserved across species. Key among these are nuclear hormone receptors (NHRs), the aryl hydrocarbon receptor (AHR), the basic leucine zipper (bZIP) protein, and nuclear factor erythroid 2-related factor 2 (NRF2). These regulators are central to an organism's adaptive response to foreign compounds, modulating gene expression in detoxification pathways (Hartman et al., 2021).

In *C. elegans*, *daf-12* is a well-studied NHR with roles in development, aging, and metabolism. However, a direct connection between *daf-12* and the detoxification of organic xenobiotics remains unestablished, despite observations of reduced expression of some detoxification genes, such as CYPs, GSTs, and UGTs in long-lived *daf-12* mutant strains (Hoffmann and Partridge, 2015). In contrast, *nhr-8* has been identified as a critical regulator of xenobiotic detoxification, essential for activating genes in response to xenobiotic exposure and necessary for IVM resistance in *C. elegans*. In the same study, n*hr-8* mutant worms showed decreased expression of several detoxification genes from Phase I, II, and III, including Pgps and CYPs, which are known to influence IVM tolerance, resulting in reduced ABC transporter-mediated drug efflux (Ménez et al., 2019).

Recently, the basic helix-loop-helix/Per-Arnt-Sim (bHLH/PAS) protein gene, *cky-1* has been linked to IVM resistance in both *C. elegans* and *H. contortus* (Laing et al., 2022; Doyle et al., 2022). Contrasting with *nhr-8*, the downstream targets of *cky-1* in the detoxification process or resistance are not yet clearly identified, indicating an area for further research.

2.3.3 Challenges studying AR in *P. univalens*

Studying AR in *P. univalens* is challenging due to the parasite's intricate life cycle, the difficulties associated with its culture, and the lack of a comprehensively annotated genome. Ethical considerations and financial limitations also add complexity to conducting *in vivo* studies. As a result, much of the current research on AR in *P. univalens* is performed *in vitro*, often utilizing parasites obtained from horses that have been slaughtered or euthanized (Scare et al., 2020; Martin et al., 2020; Janssen et al., 2013). Additionally, while studies have examined the larval stage of *P. univalens*, variations in gene expression between the larval and adult stages in response to drug treatments add another layer of complexity to the research (Martin et al., 2021a). As a *de facto* model for Clade V parasitic nematode research, *C. elegans* offers a viable alternative for AR studies in Clade III nematodes such as *P. univalens*.

2.4 Caenorhabditis elegans as model of AR

Caenorhabditis elegans, a minuscule free-living nematode approximately 1 mm in length, comparable to a printed comma, is transparent, facilitating the observation of individual cells under a microscope. This nematode thrives in laboratory settings, either on agar plates or in liquid culture, feeding on *E. coli* bacteria. As a predominantly hermaphroditic organism, *C. elegans* can generate up to 300 offspring in just three to four days, making it exceptionally useful for genetic experiments and studies (Brenner, 1974). The occasional presence of males (less than 1% in lab strains) enables straightforward crossbreeding to produce new recombinant strains.

With the shorter life cycle, *C. elegans* is conducive to rapid experimental turnaround. Researchers utilize targeted genome editing to create novel strains by altering specific genes (Paix et al., 2015). The ability to cryopreserve these nematodes without accumulating mutations ensures the

long-term preservation of genetic material for ongoing studies (Brenner, 1974).

The *C. elegans* genome, approximately 100 Mb across six chromosomes, comprises around 20,000 protein-coding genes and presents a relatively complete chromosomal-level assembly (Harris et al., 2020). This detailed genomic structure, combined with its cryopreservation capabilities, renders *C. elegans* an invaluable model for sustained genetic research.

Crucially, the genome of *C. elegans* shares about 70% similarity with *A. suum* (Jex et al., 2011), making it an appropriate model for studying, *P. univalens*. Notably, *P. univalens* demonstrates a strong genomic synteny with *A. suum*, with an 88% similarity (Wang et al., 2017) This notable genetic similarity enables researchers to apply insights from *C. elegans* to understand the genetics, biology, and particularly the mechanisms of AR in ascarid parasites like *P. univalens*. The model is especially valuable in contexts where direct research on *P. univalens* is limited by practical, financial or ethical barriers. The shared drug target sites between *C. elegans* and parasitic nematodes further enhance its relevance as a model organism for exploring AR strategies in ascarid parasites.

3. Aims of the thesis

The rise of anthelmintic resistance in *Parascaris univalens*, a parasitic nematode that imposes significant health burdens in horses, challenges the effectiveness of existing drugs. Investigating the genetic underpinnings of this resistance is crucial but is hindered by practical, financial, and ethical challenges inherent in working with parasitic nematodes. Consequently, there is a pressing need for an alternative research model.

The overall aim of the thesis was evaluate *C. elegans* as a model for *P. univalens* in drug resistance studies and identify candidate genes that underlie ivermectin response and possibly resistance.

The specific aims are:

- **Study I:** Compare the expression of 15 selected candidate genes in *P. univalens* and *C. elegans* post *in vitro* IVM exposure, to draw parallels in their genetic responses.
- **Study II:** Investigate gene expression in an adult *C. elegans* post *in vitro* IVM exposure and compare findings to data from Abamectin-QTL and IVM-resistant *C. elegans* DA1316 strain to discern genes associated with ML resistance.
- **Study III:** Leverage a data-driven gene network approach to examine gene expression and identify core IVM responsive genes in nerve-rich anterior region and the metabolically active intestinal tissue of adult *P. univalens* worms post *in vitro* IVM exposure.
- **Study IV:** Critically evaluate *C. elegans* as a model for *P. univalens* and other ascarids in AR studies.by comparing core IVM-responsive genes and differentially expressed genes involved in xenobiotic metabolism, transport, and as drug targets.

4. Materials and Methods

This chapter summarizes the materials and methods employed in this thesis. More thorough delineations can be found in the corresponding papers.

4.1 Study overview

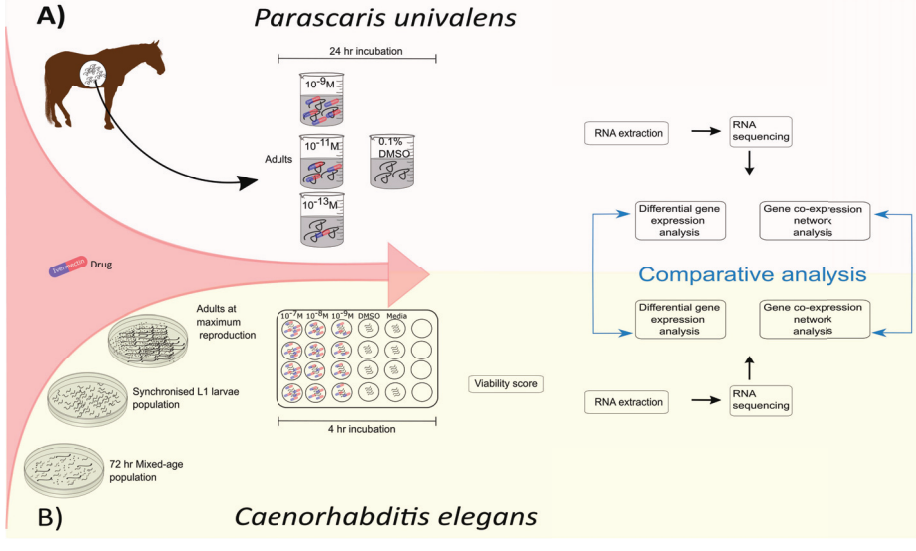

Figure 3. **Experimental setup for assessing the impact of IVM on gene expression in *Parascaris univalens* (A) and *Caenorhabditis elegans* (B).** For *P. univalens*, adult worms were incubated with IVM at concentrations of 10^{-13}, 10^{-11}, and 10^{-9} M, and a control (media $^{+\ DMSO}$) for 24 hours. In contrast, *C. elegans* populations—adults at maximum reproduction, were treated with 10^{-9}, 10^{-8}, 10^{-7} M IVM and a control for 4 hours, followed by viability assessments. Post-treatment, RNA was extracted and sequenced from both species to perform differential gene expression analysis and gene co-expression network analysis.

4.2 Study populations

The *P. univalens* worms used for the *in vitro* exposures in **Study I, III**, and **IV** were collected in partnership with the University of Iceland. They were retrieved from the intestines of approximately six-month-old foals slaughtered at an abattoir in Selfoss, Iceland in 2017 and 2019. The foals originated from three farms in southern Iceland and had no prior anthelmintic treatment.

The *C. elegans* nematodes utilized for the *in vitro* exposures in **Study I**, **II**, and **IV** consisted of the wild-type N2 Bristol strain acquired from the Caenorhabditis Genetics Center (CGC).

4.3 *In vitro* worm exposure

To explore the response, *P. univalens* and *C. elegans* were exposed to anthelmintic drug IVM *in vitro*. Subsequently, the changes in gene expression post-exposure were analyzed to assess the impact of the drug on these organisms.

Synchronized adult *C. elegans* nematodes at peak production were cultured in M9 media supplemented with 10^{-7}, 10^{-8}, 10^{-9} M IVM (Sigma-Aldrich) or media containing DMSO (control). The IVM was dissolved in dimethyl sulfoxide (DMSO) to a final concentration of 0.025% in the culture media. All treatments were prepared in quadruplicate supplemented with 1 mg/ml OP50 *E. coli* bacteria and incubated for 4 hours at 20°C. After exposure, behavior assays including pharyngeal pumping, thrashing, and dispersal were performed based on the methodology of (Johnson et al., 2009) with minor modifications (**Study I**). The worms were then pelleted and flash frozen in liquid nitrogen. **Study I** utilized 10^{-8} and 10^{-9} M IVM concentrations, **Study II** and **Study IV** only used 10^{-7} and 10^{-8} M IVM based on previous results.

Adult *P. univalens* were cultured in triplicate in tissue culture media supplemented with 10^{-9}, 10^{-11}, 10^{-13} M IVM or media containing DMSO (control) for 24 hours at 37°C. The IVM was dissolved in DMSO to a final concentration of 0.1% in the culture media. After exposure, adult worms were dissected and preserved in RNAlater (Invitrogen). Although **Study I** used all concentrations, **Study III** and **Study IV** only utilized 10^{-9} and 10^{-11} M IVM based on preceding data.

4.4 Molecular evaluation and bioinformatics

4.4.1 RNA extraction and library preparation

In **all studies**, the samples were first ground in Trizol reagent (Invitrogen, Carlsbad, USA). using a pestle and then suspended in Chloroform and the resulting aqueous phase was processed using the NucleoSpin® RNA Plus Kit (Macherey Nagel, Düren, Germany) following the manufacturer's guidelines to extract the RNA. RNA quality and quantity checks were performed using the RNA ScreenTape kit on TapeStation 4150 (Agilent, Santa Clara, USA)

The TruSeq stranded mRNA library preparation kit (Illumina Inc., San Diego, USA) was utilized for polyA selection and preparation of sequencing libraries. One microgram of RNA from each sample was used as input for the kit protocol.

4.4.2 Quantitative RT-PCR

In **Study I**, the 10 most DEGs in *P. univalens* were identified at each IVM concentration. Genes shared across multiple concentrations were also considered. Using BiomaRt and WormBase ParaSite (Howe et al., 2017), candidate genes were selected based on: 1) having a *C. elegans* orthologue, 2) known as drug targets or involved in xenobiotic metabolism, transport, or gene regulation.

4.4.3 RNA sequencing and differential gene expression

In **all studies**, libraries of the samples were paired-end sequenced for 150 cycles on NovaSeq 6000 equipment (Illumina Inc., San Diego, USA).

Read quality was assessed and differentially expressed genes (DEGs) were identified using the DESeq2 R package (Love et al., 2014), applying criteria of an adjusted p-value < 0.05 and a Log2 fold change (Log2FC) ≥ 0.5 or ≤ -0.5, as recommended by (Schurch et al., 2016).

4.4.4 Gene ontology enrichment analysis

Gene Ontology enrichment analysis was utilized to identify biological themes and processes that were over-represented among DEGs compared to

chance expectation. This pathway-level analysis provides biological context to interpret the lists of affected genes.

In **all studies**, over-representation analysis (ORA) of DEGs was performed using the Gene Ontology (GO) database via the gprofiler2 R package (Kolberg et al., 2020).The analysis utilized genes with non-zero read counts as the statistical background. *P. univalens* or *C. elegans* was set as the organism of interest. In **Study III** and **IV**, the *highlight* parameter was enabled to identify key *driver* GO terms by clustering semantically similar terms and selecting the most informative ones. While full results were tabulated, only *driver* terms were visualized for easier interpretation.

4.4.5 Network construction and core gene identification

To enable more robust gene co-expression network analysis, additional RNA-seq datasets were incorporated from other studies for a total of 28 *P. univalens* worms (**Study III**) and 25 *C. elegans* worm pools (**Study IV**).

Using variance stabilized counts for genes with non-zero expression, consensus gene co-expression networks were built with Seidr (Schiffthaler et al., 2023) by aggregating outputs from 10 inference methods. Networks underwent refinement via gold-standard based backbone retention to reduce noise and improve interpretability. The optimal consensus network was selected based on the highest Area under the curve statistic.

The Leiden algorithm (Traag et al., 2019) detected co-expression modules, which were tested for significance based on enrichment of DEGs. Within significant modules, centrality metrics identified core genes, prioritizing those overlapping DEGs in the top 5% for further examination.

5. Main results and discussion

This chapter summarizes the main findings from **Study I-IV**.
Descriptions that are more thorough can be found in the corresponding papers.

5.1 Study I: Comparative study of Ivermectin effect on gene expression in Adult *P. univalens* and *C. elegans*

In **Study I**, we examined the transcriptional response of adult *P. univalens*, particularly its nerve-rich anterior end, to IVM at concentrations of 10^{-9}, 10^{-11}, and 10^{-13} M, alongside a control group. This led to the identification of 1065 differentially expressed genes (DEGs). The study aimed to evaluate *C. elegans* as a model for understanding AR in *P. univalens*, focusing on 15 orthologous genes encompassing a drug target, xenobiotic metabolism enzymes (Phase I and II), transporters, and a transcription factor (Table 1). The methodology was based on quantitative PCR (qPCR), with RNA sequencing conducted exclusively for *P. univalens*.

Adjustments in IVM concentrations were necessary for *C. elegans* due to its higher tolerance, resulting in 10^{-7}, 10^{-8}, and 10^{-9} M. At 10^{-7} M, *C. elegans* worms were immobile, leading to their exclusion from qPCR analysis focused on sub-lethal effects.

In *P. univalens*, IVM significantly altered gene expression of candidate genes, in contrast to minimal changes in *C. elegans*, despite evident dose-dependent behavioral effects (Figure 3). The *lgc-37* gene, a GABA receptor subunit and potential IVM target, showed increased expression in *P. univalens*, aligning with prior findings (Martin et al., 2020) and mutations

associated to AR (Feng et al., 2002). This suggests *lgc-37*'s importance in IVM response, meriting further research.

Table 1. Relative gene expression in log2 fold change in *Parascaris univalens* after exposure to 10^{-13}, 10^{-11}, and 10^{-9} M ivermectin for 24 hours, and for *Caenorhabditis elegans* after exposure to 10^{-9} and 10^{-8} M IVM for 4 hours

		P. univalens			***C. elegans***	
Group	**Gene**	**10^{-13} M**	**10^{-11} M**	**10^{-9} M**	**10^{-9} M**	**10^{-8} M**
Target	*lgc-37*	0.64	-0.57	3.44	0.01	0.09
	pkc-1	-0.43	2.10	1.90	-0.26	0.04
Phase I	*dhs-2*	0.42	1.43	1.14	-0.17	-0.06
	dhs-4	-0.10	-0.07	0.00	-0.27	-0.11
	dhs-27	1.25	1.99	1.59	-0.20	-0.11
	F13D11.4	-1.20	-1.68	-1.61	-0.33	-0.52
Phase II	*C13A2.7*	-0.01	-0.24	1.37	-0.26	-0.60
	ugt-54	-1.43	-1.18	-1.41	0.04	0.01
TF	*nhr-3*	1.31	2.00	2.36	-0.31	-0.20
Transporter	*cup-4*	-2.44	-1.93	-2.34	-0.37	-0.23
	F17C11.12	-0.67	4.44	-0.20	-0.22	-0.27
	hmit-1.2	1.95	2.20	1.52	-0.08	0.11
	hmit-1.3	1.95	2.20	1.52	-0.12	0.07
	slc-17.2	-3.27	-0.22	-3.76	-0.19	0.02
	Y71G12B.25	1.97	-1.42	1.01	-0.39	-0.07
Other	*F08F8.7*	0.62	0.00	0.00	0.00	0.14

Post-IVM exposure in *P. univalens*, downregulation was noted in genes linked to MFS transport proteins, *slc-17.2* and *F17C11.12,* and the ligand-gated ion channel gene, *cup-4*. The role of MFS genes in parasitic worms remains to be elucidated, although their involvement in drug resistance is established in bacteria and yeast (Paulsen et al., 1996) and humans (Girardi et al., 2020). Beyond potential efflux functions, MFS transporters also mediate cellular uptake of glucose and other saccharides (Yan, 2013). Given that IVM causes pharyngeal paralysis and subsequent starvation in worms (Arena et al., 1995; Avery and Horvitz, 1990; Geary et al., 1993), we speculate the observed decreases in MFS expression could reflect reduced demand for glucose and nutrient transporters under starvation conditions triggered by IVM exposure. Further studies are required to elucidate the

mechanisms linking IVM induced starvation and MFS gene regulation in parasitic nematodes.

Despite prior implication in AR and drug response in parasitic nematodes (Dicker et al., 2011b; Raza et al., 2016a; Xu et al., 1998), no differential expression of Pgp efflux pumps was found in *P. univalens*, consistent with previous studies (Gerhard et al., 2020; Janssen et al., 2013; Scare et al., 2020; Martin et al., 2021a).

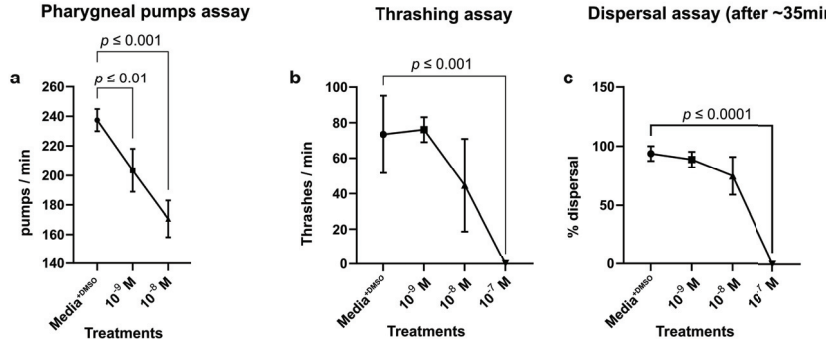

Figure 4. **Behavioural assays for *Caenorhabditis elegans***. **A)** Pharyngeal pumps per minute, **B)** body thrashes per minute, and **C)** dispersal after IVM exposure, 10^{-9} 10^{-8}, 10^{-7} M, and control (media^{+DMSO}). Mean number (± standard error, SE) of viability scores in treatments were compared to those of the control in a one-way ANOVA (Dunnett's multiple comparisons test) to elucidate significant differences

Differential expression of Phase I detoxification enzymes was observed in *P. univalens* after *in vitro* IVM exposure, with varied transcriptional responses across different genes. In contrast, *C. elegans* displayed a consistent minor decrease in expression of SDR genes *dhs-2*, *dhs-4*, *dhs-27*, and *F13D11.4* across IVM exposures. Although not yet fully characterized, SDRs are known to play a role in anthelmintic drug metabolism in helminths (Cvilink et al., 2009a; Cvilink et al., 2009b; Prchal et al., 2015; Solana et al., 2001; Stuchlíková et al., 2018). Specifically, increased expression of the *C. elegans* SDR gene *dhs-23* has been reported in a benzimidazole (BZ) resistant strain after *in vitro* exposure to BZ derivatives (Stasiuk et al., 2019b).This suggests SDR induction may contribute to anthelmintic resistance in nematodes.

Regarding Phase II enzymes, a decrease in *ugt-54* expression was noted in *P. univalens* after IVM exposure, with no significant transcriptional response observed in *C. elegans*. This pattern mirrors previous findings on other UGT family members in *P. univalens* exposed to different anthelmintic

drug classes (Martin et al., 2020; Scare et al., 2020). These results highlight the potential importance of UGT enzymes in IVM metabolism and anthelmintic resistance in *P. univalens*, warranting further investigation.

Additionally, the transcription factor *nhr-3* showed increased expression in *P. univalens* but a slight decrease in *C. elegans* post-IVM exposure. This aligns with studies demonstrating *nhr-8*'s role in upregulating P-glycoprotein and Phase I enzyme genes in *C. elegans* and *H. contortus* (Ménez et al., 2019). These insights point to the importance of NHRs' transcriptional regulation in nematode responses to IVM exposure.

5.2 Study II: Ivermectin-induced genes in wild-type *C. elegans* map to abamectin QTL and ivermectin-resistant strain

The *C. elegans* samples from all IVM exposure conditions (10^{-7}, 10^{-8}, 10^{-9} M) and control in **Study I**, were RNA-sequenced in **Study II**. Despite observable phenotypic effects at 10^{-9} M IVM in **Study I**, no significant DEGs were detected at this exposure level. After dropping the 10^{-9} M samples and reanalyzing, 615 DEGs were identified, 95% of which occurred at 10^{-7} M IVM. Comparison to a previous study's 152 DEGs in an IVM-resistant *C. elegans* strain (DA1316) (Laing et al., 2012b) revealed 31 common DEGs. Notably, 19 DEGs, including the folate transporter FOLT-2 (*folt-2*) and transmembrane transporter *T22F3.11*, displayed opposite regulation patterns between the sensitive and resistant strains. FOLT-2, exhibiting a 4-fold average downregulation in DA1316 but 4-fold upregulation here, is involved in active folate uptake (Balamurugan et al., 2007), a B-class vitamin central in the synthesis of nucleotides and amino acids (Stokstad, 1990). As other eukaryotes, *C. elegans* require dietary folate (Brzezińska et al., 2000), the *folt-2* induction potentially reflects compensatory uptake due to IVM-impaired feeding (Wolstenholme and Rogers, 2005). The mechanisms and implications of the divergent *folt-2* expression between resistant and sensitive strains warrant further elucidation. The transmembrane transporter *T22F3.11* was upregulated in DA1316 but downregulated here, implicating a possible IVM efflux role. Additionally, DA1316-specific DEGs could highlight other resistance candidates.

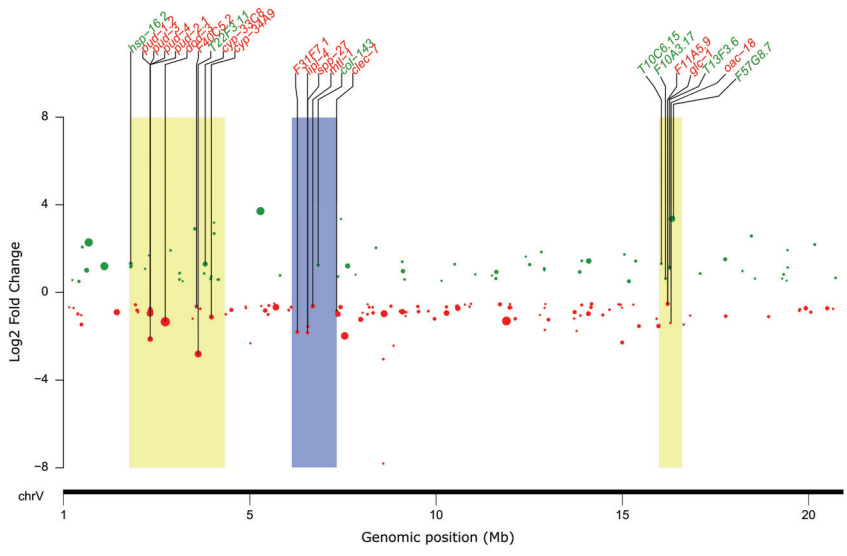

Figure 5. **Differentially expressed genes of IVM-exposed *C. elegans* N2 strain map to Abamectin-QTL on chromosome V.** The DEGs are represented by green (upregulated) and red (downregulated) dots, with the size of the dot representing the -log10 (*adj*. *p-value*) of expression, where the larger the dot, the more significantly expressed. The x-axis represents chromosome V and the y-axis represents the Log2 fold change. The karyoplot shows DEGs (labeled in green and red) mapped to abamectin-QTL VL, VC, and VR represented by yellow, blue, and yellow boxes, respectively.

Mapping the 615, IVM-associated DEGs onto recently defined Abamectin quantitative trait loci (QTL) regions (Evans et al., 2021) revealed 45 overlapping DEGs (Figure 4). Comparisons to the QTL study's proposed candidates showed only three common genes: *glc-1*, *folt-2*, and *dod-3*. While *dod-3*'s relevance is unclear, the glutamate-gated ion channel *glc-1* represents a known ML target (Ardelli and Prichard, 2013b; Ardelli et al., 2009; Cook et al., 2006; Dent et al., 2000; Cully et al., 1994). The other the putative drug target *lgc-26* encoding ion channel subunits were downregulated in the IVM 10^{-7} M concentration. The role of *lgc-26* in ML response remains unknown in *C. elegans*, but other cys-loop GABA receptor members have been implicated in the ML response of parasitic nematodes. For example, *lgc-37* was upregulated in the horse roundworm parasite, *P. univalens* after IVM exposure in **Study I** and the *lgc-54* in the sheep parasite *Teladorsagia circumcincta* was reported as potential candidate in IVM resistance through genome-wide studies (Choi et al., 2017) although challenged by Evans et al. (2021). Other differentially expressed ion channel

genes were the calcium channel *cca-1* and the potassium chloride cotransporter *kcc-2*, which were both downregulated after IVM exposure. The *cca-1* gene regulates pharyngeal pumping in *C. elegans* by enabling action potential initiation via calcium influx (Shtonda and Avery, 2005; Steger et al., 2005). As IVM slows pumping by activating GluCls (Wolstenholme and Rogers, 2005), we expected potential *cca-1* upregulation to compensate, however, the observed downregulation suggests alternate mechanisms may be involved. The *kcc-2* cotransporter mediates inhibitory GABA signaling by controlling neuronal chloride gradients (Bellemer et al., 2011). As IVM causes paralysis via similar GluCl activation, *kcc-2*'s specific role is unclear but merits further exploration, given the interconnections between chloride gradients, GABA signaling, and IVM activity. In summary, the differential regulation of channels like *cca-1* and *kcc-2* identifies additional molecular candidates potentially contributing to IVM resistance that warrant further characterization.

5.3 Study III: Gene co-expression network analysis reveal core responsive genes in *Parascaris univalens* tissues following ivermectin exposure

In this study, we employed gene co-expression network analysis (Schiffthaler et al., 2023), to identify the core genes associated with IVM response in *P. univalens*. This approach eliminates the need for biased pre-selection of candidate genes, thus facilitating the discovery of novel genes. However, gene co-expression network inferences require larger sample sizes (Langfelder and Horvath, 2008; van Dam et al., 2018) to ensure statistical robustness and wider applicability. To achieve this, we compiled RNAseq data from worm tissues collected in both a **Study I** and additional RNAseq data from (Martin et al., 2021a), resulting in a comprehensive dataset of 28 worms. Worms were subjected to 10^{-11} M and 10^{-9} M IVM concentrations *in vitro* for 24 hours. Gene count data from the worms were utilized to construct a comprehensive network. We then carried out an analysis of the transcriptional changes occurring in both the anterior end and the intestine of the worms.

Differential expression analysis showed pronounced transcriptional differences between the anterior end and intestine. The intestine displayed

substantially more IVM-induced activity. With 10^{-11} M IVM exposure, the anterior end had no enriched biological processes compared to the intestinal tissue. The intestinal tissue response involved 58% downregulation of genes regulating cellular processes like transcription and signal transduction, potentially indicating a protective, resource-conserving stress response. Concurrently, upregulated intestinal genes suggested improved peptide metabolism, ribosomal function, and energy production. These processes have also been enriched in other IVM-exposed nematodes like *H. contortus* larvae (Liu et al., 2023) and adult *Brugia malayi* (Ballesteros et al., 2016), , implying a shared strategy across species. At 10^{-9} M IVM, the intestinal tissue showed a gene expression reversal, predominantly characterized by upregulation. This was notably evident in genes associated with ion transport, cuticle structural integrity, and protein tyrosine phosphatase activity. As the cuticle is critical against environmental threats, including anthelmintics (Thompson et al., 1993; Page and Johnstone, 2007) , its permeability adaptations (Njume et al., 2022) presumably mitigate IVM efficacy. Thus, upregulation in cuticle maintenance genes likely represents a strategic protective response. Moreover, marked upregulation of tyrosine phosphatase genes, vital in cellular regulation (Zhang, 1998) highlights a potential adaptive mechanism to preserve cellular function despite IVM exposure.

Gene co-expression network analysis identified seven modules significantly associated with the response to IVM. Within these, 219 core genes were detected, largely expressed in the intestinal tissue and spanning diverse biological processes with unspecific patterns. After 10^{-11} M IVM, unlike the anterior end, the core genes in intestinal tissue exhibited clear patterns of transcriptional suppression, cell cycle inhibition, and protein synthesis and management of misfolded/unfolded proteins. The cell cycle inhibition is congruent observations with a previous a study of *B. malayi*, where gene expression changes related to meiosis were significantly downregulated 24 hours after IVM exposure (Ballesteros et al., 2016). This downregulation included genes whose RNAi phenotypes in *C. elegans* lead to developmental arrests (Ballesteros et al., 2016), suggesting a potentially conserved response mechanism across different nematode species to IVM exposure. Concurrently, were observed upregulation of core genes involved in protein synthesis and management of misfolded/unfolded proteins, are congruent with the ORA results in this study and other studies (Liu et al.,

2023; Ballesteros et al., 2016; Dicker et al., 2011a; Ruiz-May et al., 2022). Increasing the IVM concentration to 10^{-9} M induced notable shifts in the expression patterns of core genes in both tissue types. In the intestinal tissue, this elevation resulted in the upregulation of core genes implicated in maintaining cellular integrity, signal transduction, metabolism, and cuticle integrity.

We identified core genes using eigenvector centrality and betweenness metrics. Eigenvector centrality evaluates a gene's influence based on its network connections, while betweenness measures its role as a vital "bridge" in the network, underscoring the importance of these genes in network function. Typically, transcriptomic studies post-drug exposure in nematodes, including ours, reveal genes associated with drug biotransformation, like cytochrome P450s, UDP-glucuronosyltransferases, and efflux P-glycoproteins (Stasiuk et al., 2019a; Martin et al., 2020; Martin et al., 2021a; Dube et al., 2022; Dube et al., 2023; Khan et al., 2020; Scare et al., 2020; Hartman et al., 2021). Interestingly, only one core gene, *PgR014X_g126* (*alh-7*) was associated with drug metabolism, potentially indicating a shift from detoxification prioritization towards transcriptional control and cell cycling under IVM toxicity. Furthermore, three intestinal core genes changed from downregulated at lower IVM to upregulated at higher concentrations. This includes the gene *PgR028_g047 (sorb-1)*, which plays a role in muscle organization and physiology in *C. elegans* (Loveless et al., 2017), possibly promoting IVM resilience. Similarly, cuticle genes, *PgB01_g200 (gmap-1)* and *PgR046_g017 (col-37 & col-102)* followed this trend. Given *PgB01_g200 (gmap-1)*'s role in cuticle permeability (Njume et al., 2022) emphasizes potential importance of these genes under IVM exposure. Considering the phylogenetic proximity of *P. univalens* and *A. suum* (2019), along with *A. suum's* predominantly cuticular drug absorption (Thompson et al., 1993), IVM might be absorbed similarly through the cuticle of *P. univalens*. However, the differential gene expression in the current study challenges this idea of conserved uptake. Critically, the anterior end showed fewer DEGs and core genes than the intestine, despite expected GluCls abundance (Hammarlund et al., 2018; Airs et al., 2022) and known for its dominant constitutive expression (Rosa et al., 2014). This discrepancy indicates that IVM absorption in *P. univalens* might not be as straightforward as previously thought. It suggests the possibility of a dual mechanism

involving both cuticular diffusion and ingestion, rather than a singular cuticular route.

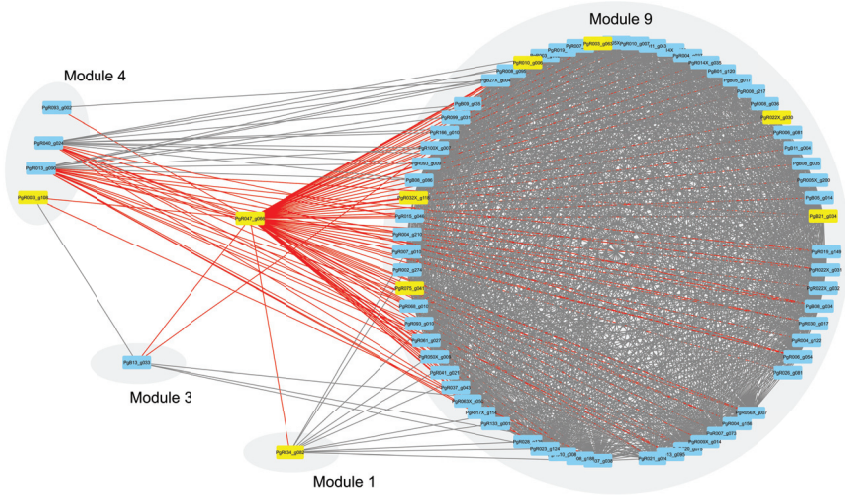

Figure 6. **Central role of non-module gene *PgR047_g066* in connecting four gene modules.** A gene network showing how *PgR047_g066* serves as a pivotal link among three distinct modules. Rectangles denote individual genes, and edges signify interactions between them. Direct first-degree neighbors to *PgR047_g066* are emphasized with red lines, while differentially expressed genes are colored yellow.

A notable 172 genes were identified as "non-modular", as they did not belong to any specific module. Among these, *PgR047_g066* (*gegf-1*), known for its calcium ion binding function as per Gene Ontology (GO), stood out as a potential intermodular gene, establishing connections with four distinct gene modules (1, 3, 4 and 9) and interacting with 71 genes (Figure 5). Overrepresentation analysis of the genes closely directly connect to *PgR047_g066* revealed its involvement in vital signalling processes, including molecular transducer, signalling receptor, and transmembrane signalling receptor activities. This is a significant discovery considering the key role of calcium signalling in nematode physiology, particularly in muscle function and neural communication (Alvarez et al., 2020), both of which are heavily influenced by IVM. Notably, a 12-fold increase in the expression of *PgR047_g066* was observed at a 10^{-9} M IVM in the intestinal tissue. Therefore, *PgR047_g066* (gegf-1) emerges as a notable gene for further exploration to elucidate its role in IVM response.

5.4 Study IV: Comparative transcriptomic and gene network analysis in *Caenorhabditis elegans* and *Parascaris univalens* after ivermectin exposure

In this study, we utilized transcriptomic data from **Study III**, which involved exposing *P. univalens* to 10^{-11} M and 10^{-9} M IVM concentrations *in vitro* for 24 hours. Similarly, data from **Study II** was used for *C. elegans*, which were exposed to 10^{-8} M and 10^{-7} M IVM concentrations i*n vitro* for 4 hours. For *P. univalens*, the analysis focused on DEGs and core genes identified from the worms subjected to the specified IVM concentrations. In the case of *C. elegans*, the study not only analysed DEGs but also utilized count data to construct a network with Seidr (Schiffthaler et al., 2023), facilitating the identification of core genes.

The overarching goal was to critically evaluate the applicability *of C. elegans* as a representative model for *P. univalens* and potentially other ascarids in the study of AR. This assessment entailed a comparative analysis of core genes in both *C. elegans* and *P. univalens* that respond to IVM, with an extended examination of DEGs involved in xenobiotic metabolism, transport, and drug targets. Through this comprehensive approach, our aim was to enhance the understanding of genetic responses to IVM in these nematode species and ascertain the efficacy of employing *C. elegans* as a model in AR research pertaining to ascarid nematodes.

The gene co-expression network analysis highlighted a marked contrast in core gene identification between *C. elegans* and *P. univalens*. In *C. elegans*, only 43 core genes were identified, compared to a significantly higher count of 219 core genes in *P. univalens*, as detailed in **Study III**. This discrepancy aligns with the differences in the number of DEGs observed post-IVM exposure, where *C. elegans* had 615 DEGs (**Study II**) and *P. univalens* had 2730 DEGs (**Study III**). The process of identifying core genes is reliant on the intersection between network module genes and DEGs, which suggests that the higher count of DEGs in *P. univalens* contributed to its increased detection of core genes. Interestingly, both species exhibit a similar ratio of core genes to DEGs, approximately 8% in *P. univalens* and 7% in *C. elegans.* A key observation in *C. elegans* was the upregulation of five heat shock protein (HSP) genes *F44E5.4*, *hsp-16.11*, *hsp-16.2*, *hsp-16.41* and *hsp-70*, which occurred in both IVM concentrations. The HSPs, widely recognized as highly conserved chaperone proteins, are typically

induced by environmental changes and stress across various organisms. (Wieten et al., 2007; Li and Srivastava, 2003). Despite limited understanding of HSPs' roles in anthelmintic drug responses and resistance in nematodes and other parasitic worms, there have been notable developments. For example, in *H. contortus*, albendazole exposure led to the upregulation of *hsp-15* and *hsp-17* (Stasiuk et al., 2019a), while a study on IVM-resistant *C. elegans* reported downregulation of *hsp-16.1*, *hsp-16.49*, and *hsp-17* following IVM exposure (Laing et al., 2012a). Furthermore, *hsp-70* was found to be upregulated in adult trematode, *Schistosoma mansoni* with decreased sensitivity to praziquantel (Abou-El-Naga, 2020). Contrastingly, no HSPs occurred as core genes in *P. univalens*, but IVM exposure resulted in the upregulation of *PgR024_g045* (*hsp-17*) and *PgB19_g032* (*hsp-43*), and downregulation of *PgB01_g096* (*hsp-12.3*) and *PgR118_g017* (*hsp-110*). This imply that HSP response to anthelmintic exposure extends beyond *C. elegans*. Interestingly, core genes in *P. univalens*' involved in the stress response were more associated with cuticle integrity and response to external stimuli (**Study III**). This disparity suggests that both *C. elegans* and *P. univalens* prioritize stress response, but in divergent ways.

Compared to *P. univalens*, *C. elegans* exhibited a greater number of DEGs involved in xenobiotic metabolism in response to IVM (Figure 7). This aligns with the hypothesis that gastrointestinal nematode parasites may possess a reduced requirement for reactive xenobiotic response pathways relative to free-living species such as *C. elegans* in facing varied environments (Zarowiecki and Berriman, 2015). Furthermore, while CYPs dominated Phase I metabolism in *C. elegans*, the SDRs were predominant in *P. univalens*. The distinct enzyme distribution mirrors baseline genetic differences, with *C. elegans* possessing over 86 CYPs and 68 SDRs (Lindblom and Dodd, 2006), contrasting typical parasites like *H. contortus* having approximately 42 CYPs and 70 SDRs (Laing et al., 2013). Such variation in background CYP and SDR numbers could drive the differing Phase I response patterns between the nematodes. Here, *cyp-35A2* uniquely showed IVM-induced downregulation, contrasting the BZ drug-induced upregulation of *cyp-35A3* previously observed in several studies (Gu et al., 2020; Menzel et al., 2001; Menzel et al., 2005a; Reichert and Menzel, 2005; Stasiuk et al., 2019a). Notably, in our study, the *cyp-35A2* gene was downregulated after IVM exposure, which contrasts with previous studies (Jones et al., 2013; Stasiuk et al., 2019a). This exemplifies differential CYP

modulation even within the same family towards different anthelmintics in *C. elegans*.

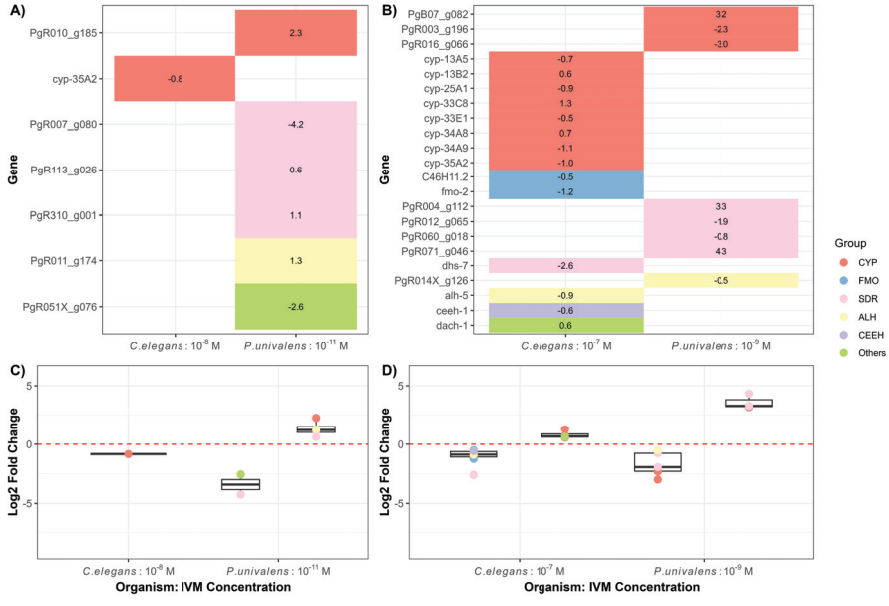

Figure 7. **Comparative analysis of Phase I gene expression responses to IVM in *C. elegans* and *P. univalens***. Panel **A**) Depicts the log2 fold changes of gene expression at a lower IVM concentration for *C. elegans* (10^{-8} M) and *P. univalens* (10^{-11} M). Panel **B**) Displays the log2 fold changes at a higher IVM concentration for *C. elegans* (10^{-7} M) and *P. univalens* (10^{-9} M). Color coding denotes various gene families/superfamilies, including Cytochrome P450 (CYP), Flavin Monooxygenase (FMO), Short Chain Dehydrogenase/Reductase (SDR), Alcohol and Aldehyde Dehydrogenase (ALH), Hydrolase (CEEH), and Others, illustrating the differential gene expression patterns between the two species at varying IVM concentrations. Panels **C)** and **D)** Show boxplots summarizing the median distribution of log2 fold changes for *C. elegans* and *P. univalens* at the corresponding lower and higher IVM concentrations, respectively, with individual genes represented as points colored according to their gene family/superfamily classification.

Further distinctions existed in Phase II metabolism, dominated by UGTs in both species but with more DEGs in *C. elegans*, increasing with IVM concentration unlike *P. univalens* (Figure 8). This likely stems from the higher baseline UGTs (66) and GSTs (56) encoded in the *C. elegans* genome (Lindblom and Dodd, 2006) compared to parasites like H. contortus (34 UGTs and 28 GSTs) (Laing et al., 2013).

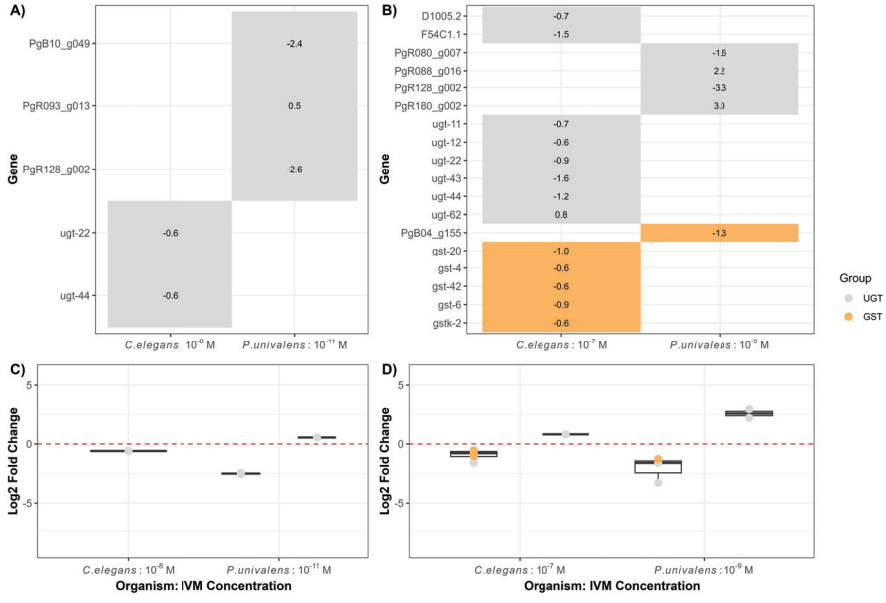

Figure 8. **Comparative analysis of Phase II gene expression responses to IVM in *C. elegans* and *P. univalens***. Panel **A**) Depicts the log2 fold changes of gene expression at a lower IVM concentration for *C. elegans* (10^{-8} M) and *P. univalens* (10^{-11} M). Panel **B)** Displays the log2 fold changes at a higher IVM concentration for *C. elegans* (10^{-7} M) and *P. univalens* (10^{-9} M). Color coding denotes various gene families/superfamilies, including Uridine 5'-diphospho-glucuronosyltransferase (UGT) and Glutathione S-transferase (GST), illustrating the differential gene expression patterns between the two species at varying IVM concentrations. Panels **C)** and **D)** Show boxplots summarizing the median distribution of log2 fold changes for *C. elegans* and *P. univalens* at the corresponding lower and higher IVM concentrations, respectively, with individual genes represented as points colored according to their gene family/superfamily classification

Parascaris univalens demonstrated a marked increase in differentially expressed ion channels compared to *C. elegans*, especially at high IVM concentrations (Figure 9). Glutamate-gated chloride channels are established IVM targets (Feng et al., 2002; Wolstenholme and Neveu, 2022b; Wolstenholme and Rogers, 2005), yet species-specific genetic variation exists as *C. elegans* has six GluCls (Glendinning et al., 2011) while *P. univalens* at least four (Lamassiaude et al., 2022). Here, *P. univalens*' *PgB06_g029* (*glc-4)* was upregulated at low IVM while *PgR005X_g138* (*glc-2)* and *PgB05_g069* (*glc-3)* were upregulated at the high IVM concentration, possibly suggesting co-activation is needed to form functional homomeric/heteromeric channels in the presence of IVM (Lamassiaude et al., 2022).

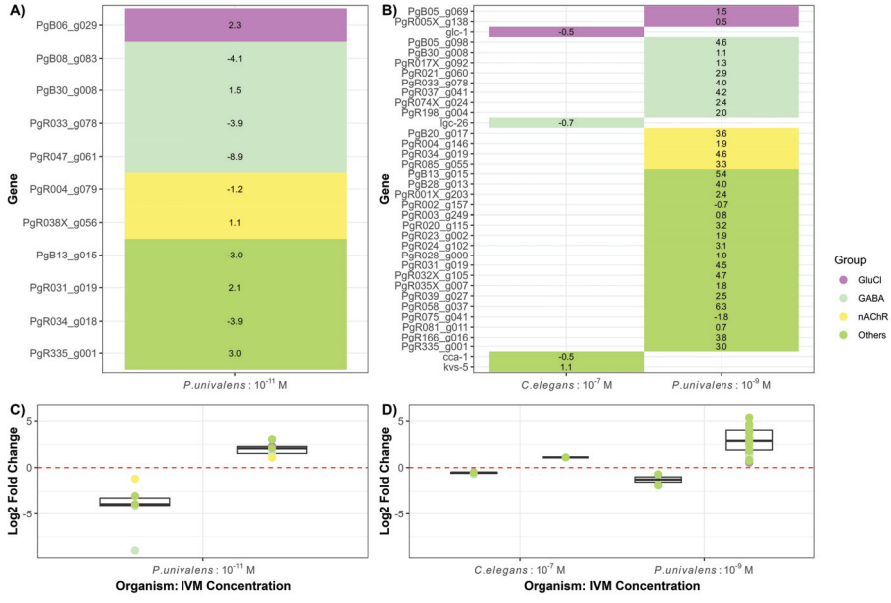

Figure 9. **Comparative analysis of gene expression responses of putative IVM targets to IVM in *C. elegans* and *P. univalens*.** Panel **A**) Depicts the log2 fold changes of gene expression at a lower IVM concentration for *C. elegans* (10^{-8} M) and *P. univalens* (10^{-11} M). Panel B) Displays the log2 fold changes at a higher IVM concentration for *C. elegans* (10^{-7} M) and *P. univalens* (10^{-9} M). Color coding denotes various gene families/superfamilies, including: Glutamate-gated ion channel (GluCl), Gamma aminobutyric acid receptor (GABA) and Nicotinic acetylcholine receptor (nAChR) and other ion channels (Others), illustrating the differential gene expression patterns between the two species at varying IVM concentrations. Panels **C)** and **D)** Show boxplots summarizing the median distribution of log2 fold changes for *C. elegans* and *P. univalens* at the corresponding lower and higher IVM concentrations, respectively, with individual genes represented as points colored according to their gene family/superfamily classification

Beyond GluCls, GABA receptors are also established IVM targets (Feng et al., 2002; Beech et al., 2010b). A striking 50-fold upregulation of the predicted GABA receptor *PgB13_g015* was observed in *P. univalens*, though its specific role requires further investigation. Additionally, four out of five nAChRs were upregulated in *P. univalens* but not *C. elegans*, indicating species-specific ion channel responses. This difference, alongside evidence of nAChRs and dopamine receptors as additional IVM targets (Krause et al., 1998; Rao et al., 2009), highlights the potential involvement of diverse ion channels in nematode xenobiotic responses.

Both nematodes showed significantly increased of differentially expressed membrane transporters at high IVM concentrations. Interestingly, the folate transporter, gene *folt-2* was upregulated in *C. elegans* at the high IVM concentration, but in contrast, its *P. univalens* orthologue *PgR036_g072* was downregulated. However, a prior study reported *folt-2* downregulation in an IVM-resistant *C. elegans* strain (Laing et al., 2012a). Notably, *folt-2* falls within a QTL associated with abamectin resistance, linking it to ML drug response (Evans et al., 2021). Gene *folt-2* is required in mediating active uptake of folate (Balamurugan et al., 2007), a B-vitamin essential for nucleotide and amino acid synthesis (Stokstad, 1990). Like other eukaryotes, *C. elegans* requires dietary folate (Brzezińska et al., 2000), thus *folt-2* induction may reflect compensatory absorption due to impaired feeding from IVM effects (Wolstenholme and Rogers, 2005). The mechanisms and implications of this divergent *folt-2* expression between IVM-sensitive versus resistant *C. elegans* strains, as well as difference from the *P. univalens* response, warrant further investigation. Elucidation of folate pathway modulation may reveal species-specific adaptations affecting IVM efficacy and resistance development.

6. Concluding remarks

This thesis has advanced our understanding of IVM response in *P. univalens* and *C. elegans* through transcriptomics and gene co-expression network analysis. This network methodology avoids the bias inherent in pre-selecting candidate genes, enabling the discovery of novel genes, referred to as "core genes". The thesis also extends to genes involved in xenobiotic metabolism, transport, and drug targets. A comparative analysis has assessed the suitability of using *C. elegans* as a model for AR research in ascarid nematodes. The key conclusions are as follows:

- **Sensitivity to IVM:** *P. univalens* exhibits greater sensitivity to IVM compared to *C. elegans*. This is inferred from the observation that concentrations of IVM lethal to *P. univalens* are only sublethal to *C. elegans*. Additionally, *P. univalens* displays over three times the number of differentially expressed genes and four times more core genes than *C. elegans* post-IVM exposure.
- **Core genes in *P. univalens* and *C. elegans*:** *P. univalens* genes show patterns of transcriptional suppression, cell cycle inhibition, ribosomal activation, and induced expression related to cuticle and membrane integrity, while core genes in *C. elegans* show unclear patterns
- **Significant core genes in *P. univalens*:** The GABA ligand-gated ion channel gene *PgR047_g061* (*lgc-37*) is identified as a core gene. Other genes such as *PgR028_g047* (*sorb-1*), *PgB01_g200* (*gmap-1*), and *PgR046_g017* (*col-37* & *col-102*) exhibit expression changes from downregulation at lower IVM concentrations to upregulation at higher concentrations, making them notable candidates for further study.

- **Significant core genes in *C. elegans*:** Five consistently upregulated heat shock protein genes *F44E5.4*, *hsp-16.11*, *hsp-16.2*, *hsp-16.41* and *hsp-70*, appeared in both IVM concentrations making them notable candidates for further study.
- **Shift in biological prioritization:** Only one core gene in *P. univalens* is associated with xenobiotic metabolism, suggesting a shift from the conventional focus on xenobiotic detoxification under toxic stress to transcription arrest, energy production, and cell cycle inhibition.
- **Non-modular calcium-signalling gene:** *PgR047_g066* (*gegf-1*) in *P. univalens*, which uniquely interconnects 71 genes across four modules, is a noteworthy candidate for further exploration.
- **Differential IVM response in xenobiotic metabolism, transport, and drug targets:**
    - *C. elegans* showed a greater number of DEGs involved in xenobiotic metabolism compared to *P. univalens*, with differences in key Phase I metabolism enzymes. Cytochrome P450s were predominant in *C. elegans*, while Short Chain Dehydrogenase/Reductases were more significant in *P. univalens*. However, Phase II genes were largely similar between the two species.
    - The response to IVM in *P. univalens* affected numerous ligand-gated ion channels, a pattern not observed in *C. elegans*, indicating pronounced species-specific differences.
    - There was an opposite expression pattern of the folate transporter gene (*folt-2*) in N2 and DA1316 strains of *C. elegans* compared to *P. univalens*. This gene, downregulated in *P. univalens* and previously identified within the abamectin-QTL, emerges as a potential candidate gene of interest.

In summary, despite no shared core gene, differential gene expression analysis revealed that similar gene families were engaged in IVM response in both *P. univalens* and *C. elegans*. This suggests that while the *C. elegans* model can provide insights into the IVM response in *P. univalens* and other ascarids, significant differences underscore the importance of complementing studies with targeted investigations in the relevant parasitic

species. This approach can lead to a more comprehensive understanding of anthelmintic resistance mechanisms.

7. Future perspective

This thesis enhances our understanding of IVM responses in *P. univalens* and *C. elegans,* paving the way for further investigation. It highlights core genes, including their differential IVM responses, and uses *C. elegans* as a comparative model, laying a foundational framework for examining AR in *P. univalens* and extending AR research in ascarid nematodes. Future research should focus on:

- **Functional analysis of core genes:** Delve deeper into the function of identified core genes in *P. univalens*, such as *PgR028_g047* (*sorb-1*), *PgB01_g200* (*gmap-1*), *PgR046_g017* (*col-37* & *col-102*), and Investigate their roles in IVM sensitivity through gene silencing studies in *C. elegans*.
- **Investigate calcium signalling in AR:** Explore the role of the non-modular calcium-signalling gene *PgR047_g066* (*gegf-1*) in IVM response. Studies could focus on its impact on calcium-mediated signalling pathways and their influence on nematode muscle function and neurotransmission under IVM exposure.
- **Comparative ion channel studies:** Given the distinct response of ligand-gated ion channels in *P. univalens* to IVM, conduct comparative studies with *C. elegans* and other ascarids to understand the species-specific ion channel adaptations that contribute to IVM sensitivity or resistance.
- **Heat shock protein functionality:** Investigate the role of upregulated heat shock proteins in *C. elegans* under IVM exposure and assess if similar mechanisms are present in *P. univalens*. This could provide insights into stress response mechanisms associated with anthelmintic exposure.

- **Study of Folate transporter genes:** Further explore the role of folate transporter genes like *folt-2* in IVM response. Investigate their expression patterns in *P. univalens* and their potential involvement in resistance mechanisms.
- **Model system refinement:** Given the differences between *P. univalens* and *C. elegans* in IVM response, refine the nematode model systems for AR research. This could involve developing more representative *in vitro* and *in vivo* models for *P. univalens*, such as the recently reported turkey ascarid, *Ascaridia dissimilis* (Collins and Andersen, 2023)

References

(2019) Comparative genomics of the major parasitic worms. *Nat Genet* 51: 163-174.

Abou-El-Naga IF. (2020) Heat shock protein 70 (Hsp70) in Schistosoma mansoni and its role in decreased adult worm sensitivity to praziquantel. *Parasitology* 147: 634-642.

Airs PM, Vaccaro K, Gallo KJ, et al. (2022) Spatial transcriptomics reveals antiparasitic targets associated with essential behaviors in the human parasite Brugia malayi. *PLoS Pathog* 18: e1010399.

Alvarez J, Alvarez-Illera P, García-Casas P, et al. (2020) The Role of Ca2+ Signaling in Aging and Neurodegeneration: Insights from Caenorhabditis elegans Models. *Cells* 9: 204.

Alvarez LI, Solana HD, Mottier ML, et al. (2005) Altered drug influx/efflux and enhanced metabolic activity in triclabendazole-resistant liver flukes. *Parasitology* 131: 501-510.

Ardelli BF and Prichard RK. (2013a) Inhibition of P-glycoprotein enhances sensitivity of Caenorhabditis elegans to ivermectin. *Vet Parasitol* 191: 264-275.

Ardelli BF and Prichard RK. (2013b) Inhibition of P-glycoprotein enhances sensitivity of Caenorhabditis elegans to ivermectin. *Veterinary Parasitology* 191: 264-275.

Ardelli BF, Stitt LE, Tompkins JB, et al. (2009) A comparison of the effects of ivermectin and moxidectin on the nematode Caenorhabditis elegans. *Vet Parasitol* 165: 96-108.

Arena JP, Liu KK, Paress PS, et al. (1995) The mechanism of action of avermectins in Caenorhabditis elegans: correlation between activation of glutamate-sensitive chloride current, membrane binding, and biological activity. *J Parasitol* 81: 286-294.

Aubry M, Cowell P, Davey M, et al. (1970) Aspects of the pharmacology of a new anthelmintic: pyrantel. *British journal of pharmacology* 38: 332.

Avery L and Horvitz HR. (1990) Effects of starvation and neuroactive drugs on feeding in Caenorhabditis elegans. *J Exp Zool* 253: 263-270.

Balamurugan K, Ashokkumar B, Moussaif M, et al. (2007) Cloning and functional characterization of a folate transporter from the nematode Caenorhabditis elegans. *Am J Physiol Cell Physiol* 293: C670-681.

Ballesteros C, Tritten L, O'Neill M, et al. (2016) The Effects of Ivermectin on Brugia malayi Females In Vitro: A Transcriptomic Approach. *PLoS Negl Trop Dis* 10: e0004929.

Beech R, Levitt N, Cambos M, et al. (2010a) Association of ion-channel genotype and macrocyclic lactone sensitivity traits in Haemonchus contortus. *Mol Biochem Parasitol* 171: 74-80.

Beech R, Levitt N, Cambos M, et al. (2010b) Association of ion-channel genotype and macrocyclic lactone sensitivity traits in Haemonchus contortus. *Molecular and Biochemical Parasitology* 171: 74-80.

Bellemer A, Hirata T, Romero MF, et al. (2011) Two types of chloride transporters are required for GABA(A) receptor-mediated inhibition in Caenorhabditis elegans. *Embo j* 30: 1852-1863.

Bello TR. (1985) The insidious invasive verminous antigens of the horse. *Journal of Equine Veterinary Science* 5: 163-167.

Boersema JH, Eysker M and Nas JW. (2002) Apparent resistance of Parascaris equorum to macrocylic lactones. *Vet Rec* 150: 279-281.

Brenner S. (1974) The genetics of Caenorhabditis elegans. *Genetics* 77: 71-94.

Brown HD, Matzuk AR, Ilves IR, et al. (1961) ANTIPARASITIC DRUGS. IV. 2-(4'-THIAZOLYL)-BENZIMIDAZOLE, A NEW ANTHELMINTIC. *Journal of the American Chemical Society* 83: 1764-1765.

Brown PJ and Clayton HM. (1979) Hepatic pathology of experimental Parascaris equorum infection in worm-free foals. *J Comp Pathol* 89: 115-123.

Brownlee DJ, Holden-Dye L and Walker RJ. (1997) Actions of the anthelmintic ivermectin on the pharyngeal muscle of the parasitic nematode, Ascaris suum. *Parasitology* 115 (Pt 5): 553-561.

Brzezińska A, Wińska P and Balińska M. (2000) Cellular aspects of folate and antifolate membrane transport. *Acta Biochim Pol* 47: 735-749.

Burk SV, Dangoudoubiyam S, Brewster-Barnes T, et al. (2014) In vitro culture of Parascaris equorum larvae and initial investigation of parasite excretory-secretory products. *Parasitol Res* 113: 4217-4224.

Burk SV, Dangoudoubiyam S, Brewster-Barnes T, et al. (2016) Equine antibody response to larval Parascaris equorum excretory-secretory products. *Vet Parasitol* 226: 83-87.

Charlier J, Rinaldi L, Musella V, et al. (2020) Initial assessment of the economic burden of major parasitic helminth infections to the ruminant livestock industry in Europe. *Preventive Veterinary Medicine* 182: 105103.

Charlier J, Thamsborg SM, Bartley DJ, et al. (2018) Mind the gaps in research on the control of gastrointestinal nematodes of farmed ruminants and pigs. *Transbound Emerg Dis* 65 Suppl 1: 217-234.

Choi YJ, Bisset SA, Doyle SR, et al. (2017) Genomic introgression mapping of field-derived multiple-anthelmintic resistance in Teladorsagia circumcincta. *PLoS Genet* 13: e1006857.

Clayton HM and Duncan JL. (1978) Clinical signs associated with parascaris equorum infection in worm-free pony foals and yearlings. *Veterinary Parasitology* 4: 69-78.

Clayton HM and Duncan JL. (1979a) The development of immunity to Parascaris equorum infection in the foal. *Res Vet Sci* 26: 383-384.

Clayton HM and Duncan JL. (1979b) The migration and development of Parascaris equorum in the horse. *International Journal for Parasitology* 9: 285-292.

Coles G, Bauer C, Borgsteede F, et al. (1992) World Association for the Advancement of Veterinary Parasitology (WAAVP) methods for the detection of anthelmintic resistance in nematodes of veterinary importance. *Veterinary Parasitology* 44: 35-44.

Coles GC, Jackson F, Pomroy WE, et al. (2006) The detection of anthelmintic resistance in nematodes of veterinary importance. *Veterinary Parasitology* 136: 167-185.

Collins JB and Andersen EC. (2023) The turkey ascarid, Ascaridia dissimilis, as a model genetic system. *International Journal for Parasitology* 53: 405-409.

Cook A, Aptel N, Portillo V, et al. (2006) Caenorhabditis elegans ivermectin receptors regulate locomotor behaviour and are functional orthologues of Haemonchus contortus receptors. *Molecular and Biochemical Parasitology* 147: 118-125.

Cully DF, Vassilatis DK, Liu KK, et al. (1994) Cloning of an avermectin-sensitive glutamate-gated chloride channel from Caenorhabditis elegans. *Nature* 371: 707-711.

Cvilink V, Szotáková B, Krízová V, et al. (2009a) Phase I biotransformation of albendazole in lancet fluke (Dicrocoelium dendriticum). *Res Vet Sci* 86: 49-55.

Cvilink V, Szotáková B, Vokrál I, et al. (2009b) Liquid chromatography/mass spectrometric identification of benzimidazole anthelminthics metabolites formed ex vivo by Dicrocoelium dendriticum. *Rapid Commun Mass Spectrom* 23: 2679-2684.

Dent JA, Smith MM, Vassilatis DK, et al. (2000) The genetics of ivermectin resistance in Caenorhabditis elegans. *Proc Natl Acad Sci U S A* 97: 2674-2679.

Dicker AJ, Nath M, Yaga R, et al. (2011a) Teladorsagia circumcincta: the transcriptomic response of a multi-drug-resistant isolate to ivermectin exposure in vitro. *Exp Parasitol* 127: 351-356.

Dicker AJ, Nisbet AJ and Skuce PJ. (2011b) Gene expression changes in a P-glycoprotein (Tci-pgp-9) putatively associated with ivermectin resistance in Teladorsagia circumcincta. *Int J Parasitol* 41: 935-942.

Donoghue EM, Lyons ET, Bellaw JL, et al. (2015) Biphasic appearance of corticated and decorticated ascarid egg shedding in untreated horse foals. *Vet Parasitol* 214: 114-117.

Doyle SR, Laing R, Bartley D, et al. (2022) Genomic landscape of drug response reveals mediators of anthelmintic resistance. *Cell Rep* 41: 111522.

Driscoll M, Dean E, Reilly E, et al. (1989) Genetic and molecular analysis of a Caenorhabditis elegans beta-tubulin that conveys benzimidazole sensitivity. *J Cell Biol* 109: 2993-3003.

Dube F, Hinas A, Delhomme N, et al. (2023) Transcriptomics of ivermectin response in Caenorhabditis elegans: Integrating abamectin quantitative trait loci and comparison to the Ivermectin-exposed DA1316 strain. *PLoS One* 18: e0285262.

Dube F, Hinas A, Roy S, et al. (2022) Ivermectin-induced gene expression changes in adult Parascaris univalens and Caenorhabditis elegans: a comparative approach to study anthelminthic metabolism and resistance in vitro. *Parasit Vectors* 15: 158.

El-Abdellati A, De Graef J, Van Zeveren A, et al. (2011) Altered avr-14B gene transcription patterns in ivermectin-resistant isolates of the cattle parasites, Cooperia oncophora and Ostertagia ostertagi. *Int J Parasitol* 41: 951-957.

Evans KS, Wit J, Stevens L, et al. (2021) Two novel loci underlie natural differences in Caenorhabditis elegans abamectin responses. *PLoS Pathog* 17: e1009297.

Fabiani JV, Lyons ET and Nielsen MK. (2016) Dynamics of Parascaris and Strongylus spp. parasites in untreated juvenile horses. *Vet Parasitol* 230: 62-66.

Fellowes RA, Maule AG, Martin RJ, et al. (2000) Classical neurotransmitters in the ovijector of Ascaris suum: localization and modulation of muscle activity. *Parasitology* 121 (Pt 3): 325-336.

Feng XP, Hayashi J, Beech RN, et al. (2002) Study of the nematode putative GABA type-A receptor subunits: evidence for modulation by ivermectin. *J Neurochem* 83: 870-878.

Fluman N and Bibi E. (2009) Bacterial multidrug transport through the lens of the major facilitator superfamily. *Biochim Biophys Acta* 1794: 738-747.

Geary TG, Sims SM, Thomas EM, et al. (1993) Haemonchus contortus: ivermectin-induced paralysis of the pharynx. *Exp Parasitol* 77: 88-96.

Gerhard AP, Krücken J, Heitlinger E, et al. (2020) The P-glycoprotein repertoire of the equine parasitic nematode Parascaris univalens. *Sci Rep* 10: 13586.

Gerhard AP, Krücken J, Neveu C, et al. (2021) Pharyngeal Pumping and Tissue-Specific Transgenic P-Glycoprotein Expression Influence Macrocyclic Lactone Susceptibility in Caenorhabditis elegans. *Pharmaceuticals (Basel)* 14.

Getachew AM, Innocent GT, Trawford AF, et al. (2008) Equine parascarosis under the tropical weather conditions of Ethiopia: a coprological and postmortem study. *Vet Rec* 162: 177-180.

Getachew M, Trawford A, Feseha G, et al. (2010) Gastrointestinal parasites of working donkeys of Ethiopia. *Trop Anim Health Prod* 42: 27-33.

Gilleard JS, Kotze AC, Leathwick D, et al. (2021) A journey through 50 years of research relevant to the control of gastrointestinal nematodes in ruminant livestock and thoughts on future directions. *Int J Parasitol* 51: 1133-1151.

Girardi E, César-Razquin A, Lindinger S, et al. (2020) A widespread role for SLC transmembrane transporters in resistance to cytotoxic drugs. *Nat Chem Biol* 16: 469-478.

Glendinning SK, Buckingham SD, Sattelle DB, et al. (2011) Glutamate-gated chloride channels of Haemonchus contortus restore drug sensitivity to ivermectin resistant Caenorhabditis elegans. *PLoS One* 6: e22390.

Goday C and Pimpinelli S. (1986) Cytological analysis of chromosomes in the two species Parascaris univalens and P. equorum. *Chromosoma* 94: 1-10.

Gogonea CB, Gogonea V, Ali YM, et al. (1999) Computational prediction of the three-dimensional structures for the Caenorhabditis elegans tubulin family. *J Mol Graph Model* 17: 90-100, 126-130.

Gu QL, Zhang Y, Fu XM, et al. (2020) Toxicity and metabolism of 3-bromopyruvate in Caenorhabditis elegans. *J Zhejiang Univ Sci B* 21: 77-86.

Guengerich FP. (2008) Cytochrome p450 and chemical toxicology. *Chem Res Toxicol* 21: 70-83.

Hammarlund M, Hobert O, Miller DM, 3rd, et al. (2018) The CeNGEN Project: The Complete Gene Expression Map of an Entire Nervous System. *Neuron* 99: 430-433.

Han L, Lan T, Lu Y, et al. (2022) Equus roundworms (Parascaris univalens) are undergoing rapid divergence while genes involved in metabolic as well as anthelminic resistance are under positive selection. *BMC Genomics* 23: 489.

Hansen EP, Fromm B, Andersen SD, et al. (2019) Exploration of extracellular vesicles from Ascaris suum provides evidence of parasite-host cross talk. *J Extracell Vesicles* 8: 1578116.

Harris TW, Arnaboldi V, Cain S, et al. (2020) WormBase: a modern Model Organism Information Resource. *Nucleic Acids Res* 48: D762-d767.

Hartman JH, Widmayer SJ, Bergemann CM, et al. (2021) Xenobiotic metabolism and transport in Caenorhabditis elegans. *J Toxicol Environ Health B Crit Rev* 24: 51-94.

Hautala K, Näreaho A, Kauppinen O, et al. (2019) Risk factors for equine intestinal parasite infections and reduced efficacy of pyrantel embonate against Parascaris sp. *Vet Parasitol* 273: 52-59.

Hoffmann JM and Partridge L. (2015) Nuclear hormone receptors: Roles of xenobiotic detoxification and sterol homeostasis in healthy aging. *Crit Rev Biochem Mol Biol* 50: 380-392.

Höglund PJ, Nordström KJ, Schiöth HB, et al. (2011) The solute carrier families have a remarkably long evolutionary history with the majority of the human families present before divergence of Bilaterian species. *Mol Biol Evol* 28: 1531-1541.

Howe KL, Bolt BJ, Shafie M, et al. (2017) WormBase ParaSite − a comprehensive resource for helminth genomics. *Molecular and Biochemical Parasitology* 215: 2-10.

Janssen IJ, Krücken J, Demeler J, et al. (2013) Genetic variants and increased expression of Parascaris equorum P-glycoprotein-11 in populations with decreased ivermectin susceptibility. *PLoS One* 8: e61635.

Janssen IJ, Krücken J, Demeler J, et al. (2015) Transgenically expressed Parascaris P-glycoprotein-11 can modulate ivermectin susceptibility in Caenorhabditis elegans. *Int J Parasitol Drugs Drug Resist* 5: 44-47.

Jex AR, Liu S, Li B, et al. (2011) Ascaris suum draft genome. *Nature* 479: 529-533.

Johnson JR, Ferdek P, Lian LY, et al. (2009) Binding of UNC-18 to the N-terminus of syntaxin is essential for neurotransmission in Caenorhabditis elegans. *Biochem J* 418: 73-80.

Jones LM, Rayson SJ, Flemming AJ, et al. (2013) Adaptive and specialised transcriptional responses to xenobiotic stress in Caenorhabditis elegans are regulated by nuclear hormone receptors. *PLoS One* 8: e69956.

Kellerová P, Raisová Stuchlíková L, Matoušková P, et al. (2020) Sub-lethal doses of albendazole induce drug metabolizing enzymes and increase albendazole deactivation in Haemonchus contortus adults. *Vet Res* 51: 94.

Khan S, Nisar A, Yuan J, et al. (2020) A Whole Genome Re-Sequencing Based GWA Analysis Reveals Candidate Genes Associated with Ivermectin Resistance in Haemonchus contortus. *Genes (Basel)* 11.

Kolberg L, Raudvere U, Kuzmin I, et al. (2020) gprofiler2 -- an R package for gene list functional enrichment analysis and namespace conversion toolset g:Profiler. *F1000Res* 9.

Krause RM, Buisson B, Bertrand S, et al. (1998) Ivermectin: a positive allosteric effector of the alpha7 neuronal nicotinic acetylcholine receptor. *Mol Pharmacol* 53: 283-294.

Lacey E. (1990) Mode of action of benzimidazoles. *Parasitol Today* 6: 112-115.

Laing R, Bartley DJ, Morrison AA, et al. (2015) The cytochrome P450 family in the parasitic nematode Haemonchus contortus. *Int J Parasitol* 45: 243-251.

Laing R, Doyle SR, McIntyre J, et al. (2022) Transcriptomic analyses implicate neuronal plasticity and chloride homeostasis in ivermectin resistance and response to treatment in a parasitic nematode. *PLoS Pathog* 18: e1010545.

Laing R, Gillan V and Devaney E. (2017) Ivermectin - Old Drug, New Tricks? *Trends Parasitol* 33: 463-472.

Laing R, Kikuchi T, Martinelli A, et al. (2013) The genome and transcriptome of Haemonchus contortus, a key model parasite for drug and vaccine discovery. *Genome biology* 14: 1-16.

Laing ST, Ivens A, Butler V, et al. (2012a) The transcriptional response of Caenorhabditis elegans to Ivermectin exposure identifies novel genes involved in the response to reduced food intake. *PLoS One* 7: e31367-e31367.

Laing ST, Ivens A, Butler V, et al. (2012b) The transcriptional response of Caenorhabditis elegans to Ivermectin exposure identifies novel genes involved in the response to reduced food intake. *PLoS One* 7: e31367.

Laing ST, Ivens A, Laing R, et al. (2010) Characterization of the xenobiotic response of Caenorhabditis elegans to the anthelmintic drug

albendazole and the identification of novel drug glucoside metabolites. *Biochem J* 432: 505-514.
Lamassiaude N, Courtot E, Corset A, et al. (2022) Pharmacological characterization of novel heteromeric GluCl subtypes from Caenorhabditis elegans and parasitic nematodes. *Br J Pharmacol* 179: 1264-1279.
Langfelder P and Horvath S. (2008) WGCNA: an R package for weighted correlation network analysis. *BMC Bioinformatics* 9: 559.
Lanusse C, Lifschitz A and Imperiale FA. (2009) Macrocyclic Lactones: Endectocides Compounds. *Veterinary pharmacology and therapeutics*: 1119-1144.
Lem MF, Vincent KP, Pone JW, et al. (2012) Prevalence and intensity of gastro-intestinal helminths in horses in the Sudano-Guinean climatic zone of Cameroon. *Trop Parasitol* 2: 45-48.
Li Z and Srivastava P. (2003) Heat-shock proteins. *Current protocols in immunology* 58: A. 1T. 1-A. 1T. 6.
Lightowlers MW and Rickard MD. (1988) Excretory-secretory products of helminth parasites: effects on host immune responses. *Parasitology* 96 Suppl: S123-166.
Lindblom TH and Dodd AK. (2006) Xenobiotic detoxification in the nematode Caenorhabditis elegans. *J Exp Zool A Comp Exp Biol* 305: 720-730.
Liu Y, Wang X, Luo X, et al. (2023) Transcriptomics and Proteomics of Haemonchus contortus in Response to Ivermectin Treatment. *Animals (Basel)* 13.
Love MI, Huber W and Anders S. (2014) Moderated estimation of fold change and dispersion for RNA-seq data with DESeq2. *Genome Biol* 15: 550.
Loveless T, Qadota H, Benian GM, et al. (2017) Caenorhabditis elegans SORB-1 localizes to integrin adhesion sites and is required for organization of sarcomeres and mitochondria in myocytes. *Mol Biol Cell* 28: 3621-3633.
Martin F, Dube F, Karlsson Lindsjö O, et al. (2020) Transcriptional responses in Parascaris univalens after in vitro exposure to ivermectin, pyrantel citrate and thiabendazole. *Parasit Vectors* 13: 342.
Martin F, Eydal M, Höglund J, et al. (2021a) Constitutive and differential expression of transport protein genes in Parascaris univalens larvae and adult tissues after in vitro exposure to anthelmintic drugs. *Vet Parasitol* 298: 109535.

Martin F, Halvarsson P, Delhomme N, et al. (2021b) Exploring the β-tubulin gene family in a benzimidazole-resistant Parascaris univalens population. *International Journal for Parasitology: Drugs and Drug Resistance* 17: 84-91.

Martin F, Höglund J, Bergström TF, et al. (2018) Resistance to pyrantel embonate and efficacy of fenbendazole in Parascaris univalens on Swedish stud farms. *Vet Parasitol* 264: 69-73.

Martin F, Svansson V, Eydal M, et al. (2021c) First Report of Resistance to Ivermectin in Parascaris univalens in Iceland. *J Parasitol* 107: 16-22.

Martin R, Robertson A and Wolstenholme A. (2002) Mode of action of the macrocyclic lactones. *Macrocyclic lactones in antiparasitic therapy.* CAB International Wallingford UK, 125-140.

Martin RJ and Robertson AP. (2007) Mode of action of levamisole and pyrantel, anthelmintic resistance, E153 and Q57. *Parasitology* 134: 1093-1104.

Martin RJ, Robertson AP and Choudhary S. (2021d) Ivermectin: An Anthelmintic, an Insecticide, and Much More. *Trends Parasitol* 37: 48-64.

Matoušková P, Lecová L, Laing R, et al. (2018) UDP-glycosyltransferase family in Haemonchus contortus: Phylogenetic analysis, constitutive expression, sex-differences and resistance-related differences. *Int J Parasitol Drugs Drug Resist* 8: 420-429.

Matoušková P, Vokřál I, Lamka J, et al. (2016) The Role of Xenobiotic-Metabolizing Enzymes in Anthelmintic Deactivation and Resistance in Helminths. *Trends Parasitol* 32: 481-491.

McCavera S, Rogers AT, Yates DM, et al. (2009) An ivermectin-sensitive glutamate-gated chloride channel from the parasitic nematode Haemonchus contortus. *Mol Pharmacol* 75: 1347-1355.

McDonnell AM and Dang CH. (2013) Basic review of the cytochrome p450 system. *J Adv Pract Oncol* 4: 263-268.

Meech R, Hu DG, McKinnon RA, et al. (2019) The UDP-Glycosyltransferase (UGT) Superfamily: New Members, New Functions, and Novel Paradigms. *Physiol Rev* 99: 1153-1222.

Ménez C, Alberich M, Courtot E, et al. (2019) The transcription factor NHR-8: A new target to increase ivermectin efficacy in nematodes. *PLoS Pathog* 15: e1007598.

Menzel R, Bogaert T and Achazi R. (2001) A systematic gene expression screen of Caenorhabditis elegans cytochrome P450 genes reveals CYP35 as strongly xenobiotic inducible. *Arch Biochem Biophys* 395: 158-168.

Menzel R, Rödel M, Kulas J, et al. (2005a) CYP35: xenobiotically induced gene expression in the nematode Caenorhabditis elegans. *Arch Biochem Biophys* 438: 93-102.
Menzel R, Rödel M, Kulas J, et al. (2005b) CYP35: Xenobiotically induced gene expression in the nematode Caenorhabditis elegans. *Archives of Biochemistry and Biophysics* 438: 93-102.
Nicholls JM, Clayton HM, Pirie HM, et al. (1978) A pathological study of the lungs of foals infected experimentally with Parascaris equorum. *J Comp Pathol* 88: 261-274.
Nielsen M, Mittel L, Grice A, et al. (2019) AAEP Internal Parasite Control Guidelines. Obtenido de American Association of Equine Practitioners: https://aaep. org ….
Nielsen MK. (2016) Evidence-based considerations for control of Parascaris spp. infections in horses. *Equine Veterinary Education* 28: 224-231.
Nielsen MK, Baptiste KE, Tolliver SC, et al. (2010) Analysis of multiyear studies in horses in Kentucky to ascertain whether counts of eggs and larvae per gram of feces are reliable indicators of numbers of strongyles and ascarids present. *Vet Parasitol* 174: 77-84.
Nielsen MK, Donoghue EM, Stephens ML, et al. (2016) An ultrasonographic scoring method for transabdominal monitoring of ascarid burdens in foals. *Equine Vet J* 48: 380-386.
Nielsen MK, Reinemeyer CR, Donecker JM, et al. (2014a) Anthelmintic resistance in equine parasites--current evidence and knowledge gaps. *Vet Parasitol* 204: 55-63.
Nielsen MK, Wang J, Davis R, et al. (2014b) Parascaris univalens--a victim of large-scale misidentification? *Parasitol Res* 113: 4485-4490.
Njue AI, Hayashi J, Kinne L, et al. (2004) Mutations in the extracellular domains of glutamate-gated chloride channel alpha3 and beta subunits from ivermectin-resistant Cooperia oncophora affect agonist sensitivity. *J Neurochem* 89: 1137-1147.
Njume FN, Razzauti A, Soler M, et al. (2022) A lipid transfer protein ensures nematode cuticular impermeability. *iScience* 25: 105357.
Nolan TJ and Lok JB. (2012) Macrocyclic lactones in the treatment and control of parasitism in small companion animals. *Curr Pharm Biotechnol* 13: 1078-1094.
Page A and Johnstone I. (2007) The cuticle, WormBook, ed. The C. elegans Research Community WormBook.
Paix A, Folkmann A, Rasoloson D, et al. (2015) High Efficiency, Homology-Directed Genome Editing in Caenorhabditis elegans Using CRISPR-Cas9 Ribonucleoprotein Complexes. *Genetics* 201: 47-54.

Paulsen IT, Brown MH and Skurray RA. (1996) Proton-dependent multidrug efflux systems. *Microbiol Rev* 60: 575-608.

Pemberton DJ, Franks CJ, Walker RJ, et al. (2001) Characterization of glutamate-gated chloride channels in the pharynx of wild-type and mutant Caenorhabditis elegans delineates the role of the subunit GluCl-alpha2 in the function of the native receptor. *Mol Pharmacol* 59: 1037-1043.

Prchal L, Bártíková H, Bečanová A, et al. (2015) Biotransformation of anthelmintics and the activity of drug-metabolizing enzymes in the tapeworm Moniezia expansa. *Parasitology* 142: 648-659.

Pullan RL, Smith JL, Jasrasaria R, et al. (2014) Global numbers of infection and disease burden of soil transmitted helminth infections in 2010. *Parasit Vectors* 7: 37.

Rao VT, Siddiqui SZ, Prichard RK, et al. (2009) A dopamine-gated ion channel (HcGGR3*) from Haemonchus contortus is expressed in the cervical papillae and is associated with macrocyclic lactone resistance. *Mol Biochem Parasitol* 166: 54-61.

Raza A, Kopp SR, Bagnall NH, et al. (2016a) Effects of in vitro exposure to ivermectin and levamisole on the expression patterns of ABC transporters in Haemonchus contortus larvae. *International Journal for Parasitology: Drugs and Drug Resistance* 6: 103-115.

Raza A, Kopp SR, Bagnall NH, et al. (2016b) Effects of in vitro exposure to ivermectin and levamisole on the expression patterns of ABC transporters in Haemonchus contortus larvae. *Int J Parasitol Drugs Drug Resist* 6: 103-115.

Reichert K and Menzel R. (2005) Expression profiling of five different xenobiotics using a Caenorhabditis elegans whole genome microarray. *Chemosphere* 61: 229-237.

Reinemeyer CR. (2009) Diagnosis and control of anthelmintic-resistant Parascaris equorum. *Parasit Vectors* 2 Suppl 2: S8.

Reinemeyer CR and Nielsen MK. (2013) *Handbook of equine parasite control*: John Wiley & Sons.

Rosa BA, Jasmer DP and Mitreva M. (2014) Genome-Wide Tissue-Specific Gene Expression, Co-expression and Regulation of Co-expressed Genes in Adult Nematode Ascaris suum. *PLOS Neglected Tropical Diseases* 8: e2678.

Ruiz-May E, Álvarez-Sánchez ME, Aguilar-Tipacamú G, et al. (2022) Comparative proteome analysis of the midgut of Rhipicephalus microplus (Acari: Ixodidae) strains with contrasting resistance to ivermectin reveals the activation of proteins involved in the detoxification metabolism. *J Proteomics* 263: 104618.

Salinas G and Risi G. (2018) Caenorhabditis elegans: nature and nurture gift to nematode parasitologists. *Parasitology* 145: 979-987.
Sangster NC. (1999) Anthelmintic resistance: past, present and future. *Int J Parasitol* 29: 115-124; discussion 137-118.
Scare JA, Dini P, Norris JK, et al. (2020) Ascarids exposed: a method for in vitro drug exposure and gene expression analysis of anthelmintic naïve Parascaris spp. *Parasitology* 147: 659-666.
Schiffthaler B, van Zalen E, Serrano AR, et al. (2023) Seiðr: Efficient calculation of robust ensemble gene networks. *Heliyon* 9: e16811.
Schurch NJ, Schofield P, Gierliński M, et al. (2016) How many biological replicates are needed in an RNA-seq experiment and which differential expression tool should you use? *Rna* 22: 839-851.
Sheps JA, Ralph S, Zhao Z, et al. (2004) The ABC transporter gene family of Caenorhabditis elegans has implications for the evolutionary dynamics of multidrug resistance in eukaryotes. *Genome Biol* 5: R15.
Shtonda B and Avery L. (2005) CCA-1, EGL-19 and EXP-2 currents shape action potentials in the Caenorhabditis elegans pharynx. *J Exp Biol* 208: 2177-2190.
Solana HD, Rodriguez JA and Lanusse CE. (2001) Comparative metabolism of albendazole and albendazole sulphoxide by different helminth parasites. *Parasitol Res* 87: 275-280.
Sotillo J, Robinson MW, Kimber MJ, et al. (2020) The protein and microRNA cargo of extracellular vesicles from parasitic helminths - current status and research priorities. *Int J Parasitol* 50: 635-645.
Stasiuk SJ, MacNevin G, Workentine ML, et al. (2019a) Similarities and differences in the biotransformation and transcriptomic responses of Caenorhabditis elegans and Haemonchus contortus to five different benzimidazole drugs. *International Journal for Parasitology: Drugs and Drug Resistance* 11: 13-29.
Stasiuk SJ, MacNevin G, Workentine ML, et al. (2019b) Similarities and differences in the biotransformation and transcriptomic responses of Caenorhabditis elegans and Haemonchus contortus to five different benzimidazole drugs. *Int J Parasitol Drugs Drug Resist* 11: 13-29.
Steger KA, Shtonda BB, Thacker C, et al. (2005) The Caenorhabditis elegans T-type calcium channel CCA-1 boosts neuromuscular transmission. *J Exp Biol* 208: 2191-2203.
Štěrbová K, Rychlá N, Matoušková P, et al. (2023) Short-chain dehydrogenases in Haemonchus contortus: changes during life cycle and in relation to drug-resistance. *Vet Res* 54: 19.

Stokstad ER. (1990) Historical perspective on key advances in the biochemistry and physiology of folates. *Folic acid metabolism in health and disease* 13.

Stuchlíková LR, Matoušková P, Vokřál I, et al. (2018) Metabolism of albendazole, ricobendazole and flubendazole in Haemonchus contortus adults: Sex differences, resistance-related differences and the identification of new metabolites. *Int J Parasitol Drugs Drug Resist* 8: 50-58.

SVA. (2022) *Avmaskning av häst*. Available at: https://www.sva.se/media/tilhmqmf/hastens_mag-tarmparasiter.pdf.

Thompson DP, Ho NFH, Sims SM, et al. (1993) Mechanistic approaches to quantitate anthelmintic absorption by gastrointestinal nematodes. *Parasitology Today* 9: 31-35.

Traag VA, Waltman L and Van Eck NJ. (2019) From Louvain to Leiden: guaranteeing well-connected communities. *Scientific reports* 9: 5233.

van Dam S, Võsa U, van der Graaf A, et al. (2018) Gene co-expression analysis for functional classification and gene-disease predictions. *Brief Bioinform* 19: 575-592.

Veesenmeyer AF. (2022) Important Nematodes in Children. *Pediatr Clin North Am* 69: 129-139.

Vercruysse J, Harris EA, Kaboret YY, et al. (1986) Gastro-intestinal helminths of donkeys in Burkina Faso. *Z Parasitenkd* 72: 821-825.

von Samson-Himmelstjerna G. (2012) Anthelmintic resistance in equine parasites - detection, potential clinical relevance and implications for control. *Vet Parasitol* 185: 2-8.

Wang J, Gao S, Mostovoy Y, et al. (2017) Comparative genome analysis of programmed DNA elimination in nematodes. *Genome research* 27: 2001-2014.

Wells MM. (1924) *Ascaris megalocephala*: General Biological Supply House.

Whittaker JH, Carlson SA, Jones DE, et al. (2017) Molecular mechanisms for anthelmintic resistance in strongyle nematode parasites of veterinary importance. *J Vet Pharmacol Ther* 40: 105-115.

Wieten L, Broere F, van der Zee R, et al. (2007) Cell stress induced HSP are targets of regulatory T cells: a role for HSP inducing compounds as anti-inflammatory immuno-modulators? *FEBS letters* 581: 3716-3722.

Williamson SM, Robertson AP, Brown L, et al. (2009) The nicotinic acetylcholine receptors of the parasitic nematode Ascaris suum:

formation of two distinct drug targets by varying the relative expression levels of two subunits. *PLoS Pathog* 5: e1000517.
Williamson SM, Storey B, Howell S, et al. (2011) Candidate anthelmintic resistance-associated gene expression and sequence polymorphisms in a triple-resistant field isolate of Haemonchus contortus. *Mol Biochem Parasitol* 180: 99-105.
Wit J, Dilks CM and Andersen EC. (2021) Complementary Approaches with Free-living and Parasitic Nematodes to Understanding Anthelmintic Resistance. *Trends in Parasitology* 37: 240-250.
Wolstenholme AJ and Neveu C. (2022a) The avermectin/milbemycin receptors of parasitic nematodes. *Pesticide Biochemistry and Physiology* 181: 105010.
Wolstenholme AJ and Neveu C. (2022b) The avermectin/milbemycin receptors of parasitic nematodes. *Pestic Biochem Physiol* 181: 105010.
Wolstenholme AJ and Rogers AT. (2005) Glutamate-gated chloride channels and the mode of action of the avermectin/milbemycin anthelmintics. *Parasitology* 131 Suppl: S85-95.
Xu M, Molento M, Blackhall W, et al. (1998) Ivermectin resistance in nematodes may be caused by alteration of P-glycoprotein homolog. *Mol Biochem Parasitol* 91: 327-335.
Xu MJ, Fu JH, Nisbet AJ, et al. (2013) Comparative profiling of microRNAs in male and female adults of Ascaris suum. *Parasitol Res* 112: 1189-1195.
Yan N. (2013) Structural advances for the major facilitator superfamily (MFS) transporters. *Trends in Biochemical Sciences* 38: 151-159.
Zakeri A, Whitehead BJ, Stensballe A, et al. (2021) Parasite worm antigens instruct macrophages to release immunoregulatory extracellular vesicles. *J Extracell Vesicles* 10: e12131.
Zarowiecki M and Berriman M. (2015) What helminth genomes have taught us about parasite evolution. *Parasitology* 142: S85-S97.
Zhang ZY. (1998) Protein-tyrosine phosphatases: biological function, structural characteristics, and mechanism of catalysis. *Crit Rev Biochem Mol Biol* 33: 1-52.

Popular science summary

Parascaris univalens, a species of roundworm that infects horses, particularly foals, is a major veterinary concern due to its potential to cause severe intestinal issues, sometimes with fatal consequences. The primary strategy for controlling this parasite has been the use of anthelmintic drugs like ivermectin. However, a significant challenge has emerged because these roundworms are increasingly developing resistance to these drugs. This resistance is especially problematic due to the frequent use of these treatments in foals during their first year of life.

Addressing this issue necessitates a deeper understanding of the genetic mechanisms behind this resistance. Directly studying *P. univalens* is complex, given the parasite's intricate lifecycle, substantial size, cultivation challenges in the laboratory, incomplete genome, and various ethical and financial constraints.

In this context, the study turns to the *Caenorhabditis elegans*, a much simpler non-parasitic nematode, as a model organism. The rationale behind this choice lies in *C. elegans*' straightforward lifecycle and well-characterized genetic profile, making it a potentially valuable proxy for studying anthelmintic resistance mechanisms in *P. univalens*.

Through advanced genetic analysis techniques like transcriptomics and gene co-expression networks, this research bypasses traditional limitations in studying *P. univalens* directly. It focuses on identifying core genes, essential to understanding response and possibly resistance.

When exposed to different concentrations of ivermectin, *P. univalens* and *C. elegans* exhibited distinct genetic responses *Parascaris univalens* showed alterations in genes linked to cellular control mechanisms, protein synthesis, and maintaining structural integrity. In contrast, *C. elegans* demonstrated

changes primarily in genes associated with stress responses, particularly heat shock proteins.

Notably, the study observed divergent patterns in how each species metabolized the drug. While *C. elegans* predominantly utilized Cytochrome P450 enzymes, *P. univalens* showed a preference for a different set of enzymes in its metabolic response. Despite these variations, similarities in the engagement of certain gene families across both species were observed, underscoring the utility of *C. elegans* as a model for studying anthelmintic resistance in *P. univalens*.

However, the research also underscores the significant differences in the response of the two species to ivermectin, highlighting the importance of complementing *C. elegans*-based models with targeted studies on *P. univalens*. Understanding these details is vital for developing effective strategies to manage anthelmintic resistance, thereby enhancing the health and well-being of equines.

Populärvetenskaplig sammanfattning

Hästens spolmask, *Parascaris univalens*, är en art av rundmask som infekterar föl. Arten är viktig ur en veterinärmedicinsk synvinkel eftersom den har potential att orsaka allvarlig förstoppning, ibland med dödlig utgång. Den huvudsakliga strategin för att kontrollera spolmask hos häst är genom behandling med avmaskningsmedel. På grund av en överanvändning av avmaskningsmedel har spolmasken under de senaste 20 åren utvecklat resistens mot flera substanser som används för att behandla hästar, och då framförallt ivermektin.

För att lösa problematiken med resistens och resistensutveckling hos parasiterna krävs en förståelse av de bakomliggande genetiska mekanismerna. Att direkt studera *P. univalens* är komplicerat, eftersom parasiten har en komplex livscykel och en betydande storlek, vilket leder till utmaningar vid odling i laboratorium. Parasitens genom är dessutom ofullständigt och att studera *P. univalens* hos sin naturliga värd hästen involverar även etiska och ekonomiska begränsningar.

På grund av dessa orsaker använder sig studierna i denna avhandling av *Caenorhabditis elegans*, en icke-parasitisk nematod, som modellorganism. Anledningen till detta val ligger i *C. elegans* enkla livscykel och väl karakteriserade genetiska profil, vilket gör den till en potentiellt värdefull ersättare för att studera mekanismer för resistens i *P. univalens*.

Genom avancerade genetiska analysmetoder som undersöker skillnader i uttryck av gener och nätverk av gener, kringgår denna forskning traditionella begränsningar i direktstudier av *P. univalens*. De ingående studierna fokuserar på att identifiera så kallade kärngener, som kan hjälpa oss att förstå hur *P. univalens* svarar på behandling med avmaskningsmedel och utvecklar resistens.

När *P. univalens* och *C. elegans* utsattes för olika koncentrationer av ivermektin svarade de två arterna med distinkt olika förändringar i genuttryck. Spolmasken uppvisade förändringar i gener kopplade till cellulära kontrollmekanismer, proteinsyntes och bibehållande av cellens struktur. I kontrast visade *C. elegans* främst förändringar i gener kopplade till stressrespons.

Under studierna observerades också olika mönster i hur de två arterna bröt ner läkemedlet, något som kan påverka överlevnad vid behandling. Resultaten visade att *C. elegans* och *P. univalens* använde olika enzymer för att göra sig av med främmande ämnen som avmaskningsmedel. Trots dessa variationer observerades även likheter i användandet av vissa genfamiljer hos båda arterna, vilket understryker användbarheten av *C. elegans* som modell för att studera resistens mot avmaskningsmedel hos *P. univalens*.

Resultaten från den här avhandlingen betonar dock även att det finns betydande skillnader mellan de två arternas svar på behandling med substansen ivermektin. Detta understryker vikten av att komplettera eventuell forskning utförd på *C. elegans* med studier av *P. univalens*. Att förstå dessa detaljer i parasitens svar på avmaskning är av yttersta vikt för att utveckla effektiva strategier för att hantera den allt mer vanligt förekommande resistensen mot avmaskningsmedel hos hästens spolmask, och därmed förbättra hälsan och välbefinnandet hos hästar.

Acknowledgements

The work described in this thesis has been carried out at the Department of Animal Biosciences (SLU), Uppsala, Sweden. This thesis would not have been possible without the generous funding from the **Swedish Research Council Formas** and the **Faculty of Veterinary Medicine and Animal Sciences.** Their financial support has been the backbone of this project. I extend my heartfelt thanks to the **Royal Swedish Academy of Agriculture and Forestry**, the **Department of Biomedical Sciences and Veterinary Public Health**, and **SLU** for awarding me travel grants. These grants enabled me to attend international conferences and a study visit, which have been crucial in broadening my academic horizons and networking.

I am deeply indebted to my supervisors for their invaluable guidance, support, and mentorship. **Eva Tydén**, my main supervisor, your unwavering guidance and support have been instrumental throughout this research journey. I am deeply grateful for the privilege of learning from you. **Andrea Hinas**, you introduced me to the fascinating world of *C. elegans* and guided me through every step. **Staffan Svärd**, your innovative approach and insightful interpretation of data have been instrumental in shaping this research. **Magnus Åbrink**, your guidance, input, and advice have significantly contributed to this project. **Nicolas Delhomme**, you mentored me in the computational aspects of this thesis, helping me navigate through countless coding challenges and always being available to review my work and provide resources to enhance my bioinformatics skills.

A special acknowledgment goes to **Erik Andersen** and the entire **Andersen Lab** in the USA, who hosted me for six months. The experience gained under your guidance, especially in reproducible bioinformatics and population genetics, has been invaluable.

I am fortunate to have been surrounded by an incredibly supportive group of **colleagues at the department and VHC**. Your encouragement and assistance have been a source of strength. A special thanks to **Frida Martin**, whose guidance has been akin to that of a shadow supervisor.

I would also like to express my gratitude to **Karin Troell** for helping me start my research career in Sweden and encouraging me to embark on this PhD journey.

Lastly, but most importantly, I owe a debt of gratitude to my family and friends. **Darion**, **Moses**, **Bashil**, **Auntie Violet**, **Elly**, **Bob, Allan** and **Leon** your endless love, encouragement, and belief in me has been my pillar of strength. This achievement is as much yours as it is mine. **Tewali kuzikiza!**

Thank you all for being part of my PhD journey.

I

Dube *et al. Parasites & Vectors* (2022) 15:158
https://doi.org/10.1186/s13071-022-05260-4

Parasites & Vectors

RESEARCH

Open Access

Ivermectin-induced gene expression changes in adult *Parascaris univalens* and *Caenorhabditis elegans*: a comparative approach to study anthelminthic metabolism and resistance in vitro

Faruk Dube[1*], Andrea Hinas[2], Shweta Roy[2], Frida Martin[1], Magnus Åbrink[3], Staffan Svärd[2] and Eva Tydén[1]

Abstract

Background: The nematode *Parascaris univalens* is one of the most prevalent parasitic pathogens infecting horses but anthelmintic resistance undermines treatment approaches. The molecular mechanisms underlying drug activity and resistance remain poorly understood in this parasite since experimental in vitro models are lacking. The aim of this study was to evaluate the use of *Caenorhabditis elegans* as a model for *P. univalens* drug metabolism/resistance studies by a comparative gene expression approach after in vitro exposure to the anthelmintic drug ivermectin (IVM).

Methods: Twelve adult *P. univalens* worms in groups of three were exposed to ivermectin (IVM, 10^{-13} M, 10^{-11} M, 10^{-9} M) or left unexposed for 24 h at 37 °C, and total RNA, extracted from the anterior end of the worms, was sequenced using Illumina NovaSeq. Differentially expressed genes (DEGs) involved in metabolism, transportation, or gene expression with annotated *Caernorhabditis elegans* orthologues were identified as candidate genes to be involved in IVM metabolism/resistance. Similarly, groups of 300 adult *C. elegans* worms were exposed to IVM (10^{-9} M, 10^{-8} M and 10^{-7} M) or left unexposed for 4 h at 20 °C. Quantitative RT-PCR of RNA extracted from the *C. elegans* worm pools was used to compare against the expression of selected *P. univalens* candidate genes after drug treatment.

Results: After IVM exposure, 1085 DEGs were found in adult *P. univalens* worms but the relative gene expression changes were small and large variabilities were found between different worms. Fifteen of the DEGs were chosen for further characterization in *C. elegans* after comparative bioinformatics analyses. Candidate genes, including the putative drug target *lgc-37*, responded to IVM in *P. univalens*, but marginal to no responses were observed in *C. elegans* despite dose-dependent behavioral effects observed in *C. elegans* after IVM exposure. Thus, the overlap in IVM-induced gene expression in this small set of genes was minor in adult worms of the two nematode species.

Conclusion: This is the first time to our knowledge that a comparative gene expression approach has evaluated *C. elegans* as a model to understand IVM metabolism/resistance in *P. univalens*. Genes in *P. univalens* adults that responded to IVM treatment were identified. However, identifying conserved genes in *P. univalens* and *C. elegans*

*Correspondence: faruk.dube@slu.se

[1] Division of Parasitology, Department of Biomedical Sciences and Veterinary Public Health, Swedish University of Agricultural Sciences, Box 7036, 750 07 Uppsala, Sweden
Full list of author information is available at the end of the article

involved in IVM metabolism/resistance by comparing gene expression of candidate genes proved challenging. The approach appears promising but was limited by the number of genes studied ($n = 15$). Future studies comparing a larger number of genes between the two species may result in identification of additional candidate genes involved in drug metabolism and/or resistance.

Keywords: Equine roundworm, Gene expression, Anthelmintic resistance, RNA sequencing

Introduction

The equine roundworm, *Parascaris univalens*, is one of the most important pathogenic parasites infecting foals, with a prevalence of 31–58% on stud farms [1–4]. Clinical manifestations of infection include stunted growth, respiratory symptoms, and in severe cases lethal obstruction and rupture of the small intestines [5]. In addition, *P. univalens* are known shedders of high numbers of eggs [6], and larvated eggs can remain viable on grazing fields for many years [7]. This asserts a high infection pressure on farms, resulting in foals requiring several treatments with deworming drugs during their first year [8].

Three main classes of anthelmintic drugs, benzimindzoles (BZ), tetrahydropyrimidines (THP), and macrocyclic lactones (MLs), are registered for use in horses to combat parasitic infections, including *Parascaris* spp. Macrocyclic lactones are the most commonly used drug class in veterinary medicine due to their high efficacy, low toxicity, and broad spectrum of target parasites [9]. The primary target of MLs in parasitic nematodes are glutamate-gated ion channels (GluCls), where for example the ML drug ivermectin (IVM) binds irreversibly to cause hyperpolarization of the pharynx and flaccid paralysis of muscles in the worm [10]. Development of anthelmintic resistance (AR) in *Parascaris* spp. has evolved as a result of extensive drug usage [11], and resistance to MLs is now widespread [3, 4, 11–14].

Several ML drug resistance mechanisms have been proposed, e.g. polymorphisms or changes in expression of the GluCls target and transport protein genes (see [15] for review). In addition, increased expression of genes encoding drug-metabolizing enzymes has been shown to be involved in resistance [16]. Polymorphisms cause conformational changes and alter drug-binding sites in the GluCl targets in the pathogenic nematodes *Cooperia oncophora* [17] and *Haemonchus contortus* [18]. In addition, decreased expression of drug target genes may lead to a reduction of drug-binding sites and thus reduced drug effectiveness [19, 20]. Transport protein genes, particularly encoding P-glycoproteins (Pgps) and other ATP-binding-cassette family members, have been implicated in anthelmintic drug resistance through the elimination of xenobiotic substances from the cell, thus preventing the drugs from reaching their target sites [21–24]. Multiple studies have also reported higher constitutive expressions of Pgps in resistant parasite strains compared to their susceptible counterparts [20, 21]. The metabolism of drugs is biphasic. In the first phase (Phase I), the drug is converted by oxidation, reduction, or hydrolysis to a more reactive compound that can be conjugated with an endogenous molecule such as glutathione or glucose in the second phase (Phase II). As a result, a soluble, inactive drug is generated that can be expelled from the cell [25]. Increased constitutive expression of Phase I [26] and Phase II metabolic genes [27] was reported in resistant *H. contortus* isolates after in vitro exposure with BZs. However, the exact roles of Phase I and II enzymes in development of ML resistance in parasitic nematodes remain unknown.

The genetic mechanisms underlying ML resistance in *P. univalens* are inadequately understood, and further research is hampered by the complex host-dependent life cycle. Moreover, in vivo studies using the parasite host would be more comprehensive, but are challenged by both ethical and financial constraints. Previous studies have only been conducted in an in vitro setting using live adult worms isolated from slaughtered horses or euthanized foals from research herds [28–30]. However, not only is this approach laborious and costly, but it is also inefficient because slaughter of foals is rare and the number of research herds is limited. In addition, the unnatural in vitro culture environment has been reported to have undesirable effect on gene expression of *P. univalens* [29]. Therefore, there is a need for the development of in vitro experimental models for *P. univalens*. Recently, the larval stage of *P. univalens* has been explored as a possible in vitro model, but authors reported variation in gene expression between larvae and adult *P. univalens* [31]. The free-living nematode *Caenorhabditis elegans* has been used as an in vitro model for parasitic nematodes, particularly those belonging to the same taxonomic clade, V, such as *H. contortus* [32–35]. Although *P. univalens* belongs to a different clade, III, previous studies have employed transgenic lines of *C. elegans* as models for interpretation of ML-resistance in *P. univalens* [28, 36, 37]. Factors that support *C. elegans* as a viable model for parasitic nematodes include possession of similar drug targets [38, 39] and being cheap and easy to maintain in the laboratory. In addition, *C.*

elegans has a short life cycle of 3.5 days and a plethora of powerful genetic tools for manipulation are readily available [40]. To improve the likelihood of deriving conclusions from *P. univalens* research that uses *C. elegans* as a model organism, it is necessary to assess its applicability, at the very least in terms of gene expression following xenobiotic exposure.

In the current study, we investigated differentially expressed genes (DEGs), which encode drug targets, transporters, transcription regulators, or enzymes involved in drug metabolism in adult *P. univalens* after in vitro exposure to the ML substance, IVM. We further investigated the expression profile of the *C. elegans* orthologues of the above genes in adult *C. elegans* after in vitro exposure to IVM. Our objective was to evaluate whether *C. elegans* is a suitable model for *P. univalens* by studying and comparing gene expression of selected candidate genes in *P. univalens* and *C. elegans* after in vitro IVM exposure. Our findings showed that candidate genes, including the putative drug target gene, *lgc-37*, responded to IVM in *P. univalens*, but marginal to no response was observed in *C. elegans* despite dose-dependent behavioral effects observed in *C. elegans* after IVM exposure.

Materials and methods

Parascaris univalens

Adult *P. univalens* worms collected from two anthelmintic-naïve Icelandic foals at an abattoir in Selfoss, Iceland, were exposed to IVM in vitro. A detailed account of the experimental setup has been described in Martin et al. [29]. Care was taken to choose only the largest worms (i.e. females) for the study. Briefly, worms were incubated for 24 h in cell culture media containing 0.1% DMSO supplemented with 10^{-13}, 10^{-11} or 10^{-9} M IVM. In addition, a control group (media^{+DMSO}) of unexposed worms receiving cell culture media containing 0.1% DMSO was used (Fig. 1a). The experiment was performed in three biological replicates with at least three worms in each group. One worm from each subgroup was dissected. The anterior end (pharynx, nerve cell bodies ('ganglia'), nerve ring, and part of the intestine) of the worm was cut into fine pieces and suspended in 1 ml Trizol (Invitrogen, Carlsbad, USA). After homogenization with a glass tissue grinder, chloroform was added and the aqueous phase of the homogenized suspension was isolated. The aqueous phase was advanced into NucleoSpin® RNA Plus Kit (Macherey Nagel, Düren, Germany) for RNA extraction according to the manufacturer's instruction. Before preparing sequencing libraries from 500 ng total RNA, Fragment Analyzer (Agilent, Santa Clara, USA) was used

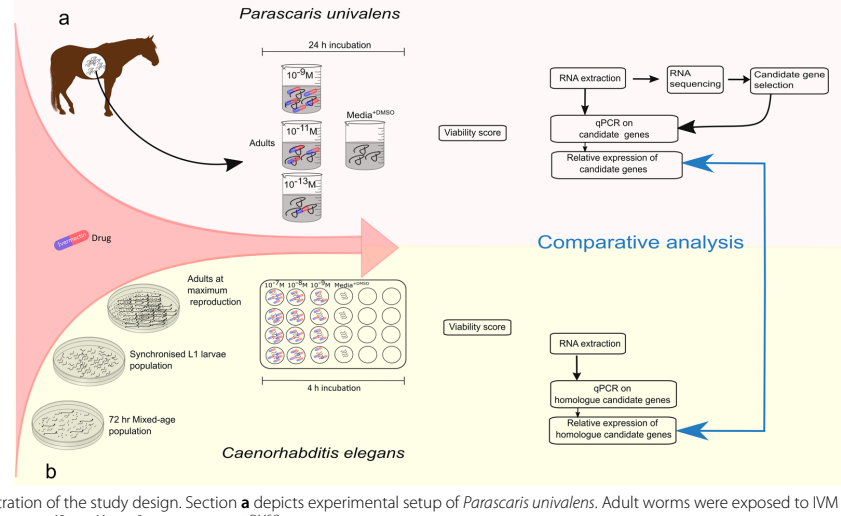

Fig. 1 Illustration of the study design. Section **a** depicts experimental setup of *Parascaris univalens*. Adult worms were exposed to IVM drug concentrations, 10^{-13}, 10^{-11}, 10^{-9} M, and media^{+DMSO} (control). After viability scoring, RNA was sequenced, candidate genes selected, and quantitative RT-qPCR performed on the selected candidate genes. Section **b** depicts experimental setup of *Caenorhabditis elegans*. Worm pools of adults at maximum reproduction were exposed to IVM drug concentrations, 10^{-9}, 10^{-8}, 10^{-7} M, and media^{+DMSO} (control). Quantitative RT-PCR was performed on the *P. univalens* orthologues of selected candidate genes. Relative gene expression of the candidates was compared between nematode species

to determine RNA concentration and quality. Illumina NovaSeq S1 flow cells and 100-bp paired end v1 sequencing chemicals were used to sequence three biological replicates per condition (Fig. 1a).

RNA sequencing analysis

Reads were quality assessed using blastp [41] in a pipeline available at https://github.com/SLUBioinformaticsInfrastructure/RNAseq_nf. Mapping and quantification of reads against the predicted reference *P. univalens* transcriptome (https://parasite.wormbase.org/Parascaris_univalens_prjna386823/Info/Index/) were performed using Salmon v.0.11.3 [42]. Salmon output was matrix-summarized using R package tximport [43] for DESeq2 v.1.22.2 R package to determine DEGs as $\log_2$foldchange). Wald test derived *P*-values from DESeq2 were modified for multiple testing using the Benjamini-Hochberg approach-based p.adjust function in R base [44]. Differentially expressed genes were defined as those with an adjusted *P*-value < 0.05. Functional annotations of DEGs were identified by a BlastP search (e-value $\leq 10^{-5}$) of their respective protein sequences against the Swiss-Prot database.

To determine the number of genes shared by different drug concentrations, gene IDs were used to build comparative Venn diagrams in R v.3.6.1 using the venn.diagram function of the VennDiagram package [45]. The get.venn.partition function was used to retrieve gene IDs corresponding to each Venn diagram partition.

Principal component analysis

To analyze differences in the response to IVM exposure among individual worms, principal component analysis (PCA) was employed using scaled read counts > 0 for 10,830 genes from each worm ($n = 12$). The prcomp function in R was used on the scaled read count to perform PCA. To determine how much variation each principal component (PC) accounts for in the data, standard deviations generated by PCA were used to compute variances. The percentage variances were visualized in a scree plot using barplot function in R. The top two PCs, which account for most variation in the data, were used to build a PCA plot using ggplot2 R package.

Selection of candidate genes

The ten most DEGs in *P. univalens* were identified for each IVM concentration and considered as potential candidate genes. In addition, genes shared by two or more IVM concentrations were considered as potential candidates. Using the BiomaRt package in R, the potential candidate gene IDs were used to retrieve their respective ontologies and *C. elegans* orthologues from WormBase ParaSite (https://parasite.wormbase.org). From the pool of potential candidates, the selection of candidate genes was based on the presence of an orthologue gene in *C. elegans* and that they were functionally characterized as drug targets or involved in at least one of the following processes: xenobiotic metabolism, metabolite transportation, and gene expression regulation.

The similarity of *P. univalens* and corresponding *C. elegans* orthologues from WormBase were verified on the I-TASSER web-server [46] using their respective amino acid sequences.

Caenorhabditis elegans

Caenorhabditis elegans culture and maintenance

Wild-type N2 Bristol strain of *C. elegans* obtained from Caenorhabditis Genetics Center (CGC) was used in this study.

Worms were grown and maintained on OP50 *Escherichia coli* seeded Nematode Growth Media (NGM) at 20 °C as per standard methods [47].

Worm synchronization

Unless otherwise stated all M9 buffer [48] used was supplemented with 0.005% Tween20 to avoid worms/embryos adhesion to plastic ware.

Caenorhabditis elegans of different life stages were cultured on 10-cm-diameter NGM agar plates for 72 h to gravid adults. Worms were harvested with ice-cold M9 buffer into 15-ml Falcon tubes and synchronized by bleaching with 1.3% NaOCl and 0.5 M KOH, according to methods described by Porta-de-la-Riva et al. [49]. Embryo floatation was performed with 60% sucrose-0.1 M NaCl mixture (ratio: 1:1) and subsequently re-suspended in M9 buffer. Hatching into L1 larvae was done on NGM agar plates without bacteria for ~20 h to obtain a synchronous L1 population.

Approximately 860 synchronized L1 larvae per 10-cm-diameter OP50 *E. coli* seeded NGM plate were incubated at 20 °C for 76 h to an adult population at maximum reproduction stage (Fig. 1b).

Caenorhabditis elegans ivermectin exposure

Synchronized N2 adults at maximum reproduction (~300 worms/ml) were initially incubated in S-complete media supplemented with 10^{-9}, 10^{-11}, 10^{-13} M IVM (+0.025% DMSO final concentration), and media^{+DMSO} (control). However, because the above-mentioned IVM concentrations had no discernible effect on the worms' behavior, the concentrations were increased to 10^{-7}, 10^{-8}, 10^{-9} M IVM (+0.025% DMSO final concentration). All treatments were set up in biological quadruplets supplemented with 1 mg/ml OP50 *E. coli* and incubated for 4 h at 20 °C (Fig. 1b).

Behavioral assays

After 4 h incubation at 20 °C, worms were phenotypically scored for each IVM concentration and control at room temperature. Scoring was based on three assays and performed with minor modifications as previously described by Johnson et al. [50].

The pharyngeal pumping assay was performed on three randomly selected worms per biological replicate. Worms were placed on 6-cm-diameter NGM plate containing a lawn of OP50 *E. coli*. Under an 80× magnification stereomicroscope (Nikon, Amstelveen, The Netherlands), the number of pharyngeal pumps per minute for each worm was counted.

The thrashing assay was performed on 12 worms, 3 randomly selected from a pool of at least 6 worms per biological replicate. Scoring was performed within their respective treatment solutions. Worms were video recorded for at least a minute. For scoring, a photographic image of the pool was taken at 0 s. Worms were randomly assigned numbers between one and *n*, where *n* is the total number of worms in the pool. Assigned numbers were randomized thrice, and three numbers were drawn. Worms with the drawn number were used for the scoring. The number of thrashings per minute was recorded. A thrash was defined as a complete sinusoidal motion from maximum to minimum amplitude and back.

In the dispersal assay, three to five worms from each treatment group were placed on the opposite edge of an OP50 lawn on a 6-cm-diameter NGM plate. Plates were scored after ~35 min based on the percentage of worms that left the inoculation spot and reached the OP50 lawn.

Caenorhabditis elegans RNA extraction, quality check, and cDNA synthesis

The remaining approximately 300 *C. elegans* worms were retrieved from the wells, washed twice in ice-cold M9 buffer, and centrifuged to pellet. The pellet was frozen in liquid nitrogen, ground with a pestle, and suspended in 900 µl Trizol (Invitrogen, Carlsbad, CA, USA) during continuous grinding. The aqueous phase of the homogenized suspension was isolated using chloroform and then advanced into the NucleoSpin® RNA Plus Kit (Macherey Nagel, Düren, Germany) for RNA extraction according to the manufacturer's instructions. RNA quality and quantity checks were performed on TapeStation 4150 (Agilent, Santa Clara, CA, USA) according to manufacturer's instructions. Two micrograms of total RNA was reverse transcribed using SuperScript™ III First-Strand Synthesis System (Invitrogen, Carlsbad, CA, USA) to generate cDNA, which was then used in the qPCR assays.

Primer design and optimization

Coding sequences (CDS) for the candidate genes were retrieved from the *P. univalens* genome (accession no. PRJNA386823) in the WormBase ParaSite database [51]. Primers were designed on an open-source online application, primer3 version 0.4.0, available at http://bioinfo.ut.ee/primer3-0.4.0/, aiming for an amplicon size of approximately 500 bp, spanning at least two exons (Additional file 4: Table S1). For genes with multiple transcripts, only CDSs for transcripts with the highest read counts in the RNA sequencing (RNAseq) data were chosen. Coding sequences were aligned in CodonCode Aligner program (version 9.0.1, CodonCode Corporation) and unique or homologous regions selected for the design of primers. Polymerase chain reaction (PCR) was performed on a thermocycler (Applied Biosystems, Waltham, MA, USA) in a reaction mix consisting of 12.5 µl ToughMix (QuantaBio, Beverly, USA), 1 µl each 10-µM primer, 9.5 µl water, and 1 µl cDNA as a template, synthesized from 1 µg *P. univalens* RNA extract. The PCR program was as follows: initial denaturation at 95 °C for 5 min, 40 cycles of denaturation at 95 °C for 45 s, 55 °C annealing temperature for 45 s, elongation at 72 °C for 1 min, and final elongation at 72 °C for 5 min. Amplicons were submitted for Sanger sequencing at Macrogen (Amsterdam, The Netherlands). Resulting sequences were quality assessed and aligned to obtain consensus sequences in CodonCode Aligner. As a validation step, BLAST searches of consensus sequences against their corresponding CDS were performed using WormBase ParaSite. Thereafter, consensus sequences were used to design Reverse Transcriptase-qPCR (RT-qPCR) primers (Additional file 4: Table S1) using the same online platform as above, aiming for an amplicon size of 75–150 bp.

Similarly, CDS of *C. elegans* orthologues were retrieved from WormBase [52] using respective gene IDs. For orthologues with splice variants, primers were designed for CDS regions that were homologous to all variants. Likewise, amplicons were Sanger sequenced at Macrogen (Amsterdam, The Netherlands) and validated by BLAST searches against their corresponding CDS in the WormBase database. Reverse Transcriptase-qPCR assays were optimized for primer concentration, annealing temperature, and efficiency (Additional file 4: Table S1).

Relative gene expression of candidate genes using reverse transcriptase qPCR

Samples and non-template controls were run in duplicate reactions of 25 µl, composed of 12.5 µl Quantitect SYBR Green PCR mix (Qiagen, Hilden, Germany), 1 µl of each 10-µM primer, 8.5 µl water, and 2 µl (dilution factor: 5) cDNA as template on a CFX96 Touch PCR machine (Bio-Rad, Solna, Sweden). The RT-qPCR program was as

follows: initial denaturation at 95 °C for 15 min, 40 cycles of denaturation at 95 °C for 15 s, assay specific annealing temperature for 30 s, and elongation at 72 °C for 30 s. For amplicon verification, a subsequent melt curve analysis was performed by temperature elevation from 60 to 95 °C, with increments of 0.5 °C for 5 s.

The Livak method [53] was used to determine the relative expression of the candidate genes. The gene expression was normalized to the geometric mean of two references genes for each species, i.e. actin, *act-5* (PgR070_g023) and flyceraldehyde-3-phosphate dehydrogenase, *gpd-1* (PgB20_g009) for *P. univalens*, and *tba-1* (tubulin, alpha) and *eif-3.C* (eukaryotic initiation factor) for *C. elegans* and related to media^{+DMSO} controls (Additional file 5: Table S2 and Additional file 6: Table S3). Gene expression was presented as $\log_2$ fold change. As a validation step, the $\log_2$ fold change values of candidate genes from RNAseq DEG analysis and RT-qPCR assays were imported into R and graphically compared in ggplot2's scatterplot.

Statistical analysis

The average counts of behavioral assays were calculated in Microsoft Excel (Additional file 7: Table S4) and then imported into GraphPad Prism [Version 9.1.0 (221)] for statistical analysis and visualization. In a one-way ANOVA with Dunnett's multiple comparisons test, average counts for the drug-treated worms were compared to media^{+DMSO} controls and graphically represented.

Log_2 fold changes of gene expression in the IVM exposed biological replicates were imported into GraphPad Prism [version 9.1.0 (221)] for each candidate gene and graphically represented. Graphical data are presented as mean values with a standard error of the mean (SEM) where applicable.

Results

Parascaris univalens RNAseq and differential gene expression

Adult *P. univalens* worms, collected from Icelandic horses, were treated with sublethal doses of IVM in vitro (10^{-13}, 10^{-11}, 10^{-9} M IVM for 24 h), and non-treated worms served as controls (see "Materials and methods"). Total RNA with RIN values ranging from 6.6 to 8.7 was sequenced on an Illumina Nova Seq. After read quality control with fastp, the number of reads per sample ranged between 63 and 132 million. Read sequences are available at https://www.ebi.ac.uk/ena [European Nucleotide Archive (ENA), accession no. PRJEB37010]. Read mapping against the reference transcriptome (https://parasite.wormbase.org/Parascaris_univalens_prjna386823/Info/Index/) yielded an average rate of 80–90% mapped reads, indicative of a high similarity between this transcriptomic data and reference transcriptome.

After PCA, 12 PCs were revealed of which PC1 and PC2 accounted for the most variation in the data, 35.5% and 14.1%, respectively (Fig. 2 and Additional file 1: Fig. S1). PC1 grouped worms into IVM treated and IVM untreated, except for worm 12. However, PC2 revealed variation in response within biological replicates but worms 1, 4 and 12 appeared away from their treatment groups (Fig. 2). Although effort was taken to select only females for the experiment, individual 2 in 10^{-11} M lacked an egg-containing uterus upon dissection. However, because this individual did not appear to be an outlier in the PCA plot (Fig. 2), it was included in the analysis.

Following DESeq2 analysis of the 1085 genes (> 0.5-fold, adj. *P*-value < 0.05) differentially expressed across the three drug concentrations, 65% (703 genes) had known functions according to Swiss-Prot annotations. Twenty-one percent of the DEGs were found in 10^{-13} M, 17% in 10^{-11} M, and 62% in 10^{-9} M (Additional file 2: Fig. S2). The overall amplitude of gene expression changes after IVM treatment was small; 84 genes were upregulated more than twofold and 147 genes were downregulated more than twofold. There was also a quite high level of variability in gene expression between the different worms.

Selection of candidate genes for further characterization was based on the presence of an orthologue in *C. elegans*, level of differential gene expression and functional characterization as drug target or involvement in at least one of the following processes: xenobiotic metabolism, metabolite transportation, or gene expression regulation. Fifteen candidate genes were selected (11 up- and 4 downregulated) and further categorized into six groups: drug target, phase I metabolic enzyme, phase II metabolic enzyme, transporter, transcription regulator, and others (Table 1). The I-TASSER web server was used to verify *P. univalens*–*C. elegans* similarity for 80% and 87% of the candidate genes based on molecular function and biological process, respectively (Table 1).

Caenorhabditis elegans behavior assays after IVM exposure

Synchronized *C. elegans* N2 adults were initially exposed to similar IVM concentrations as adult *P. univalens* (10^{-9}, 10^{-11}, 10^{-13} M). However, as there were no observable phenotypic or gene expression effects on *C. elegans* with such low IVM concentrations (data not shown), the drug concentrations were increased to 10^{-9}, 10^{-8}, 10^{-7} M, respectively.

Increased IVM concentration showed an observable effect on the worms in all behavioral assays (Fig. 3). Ivermectin exposure also showed a significant dose-dependent reduction of the number of pharyngeal pumps per

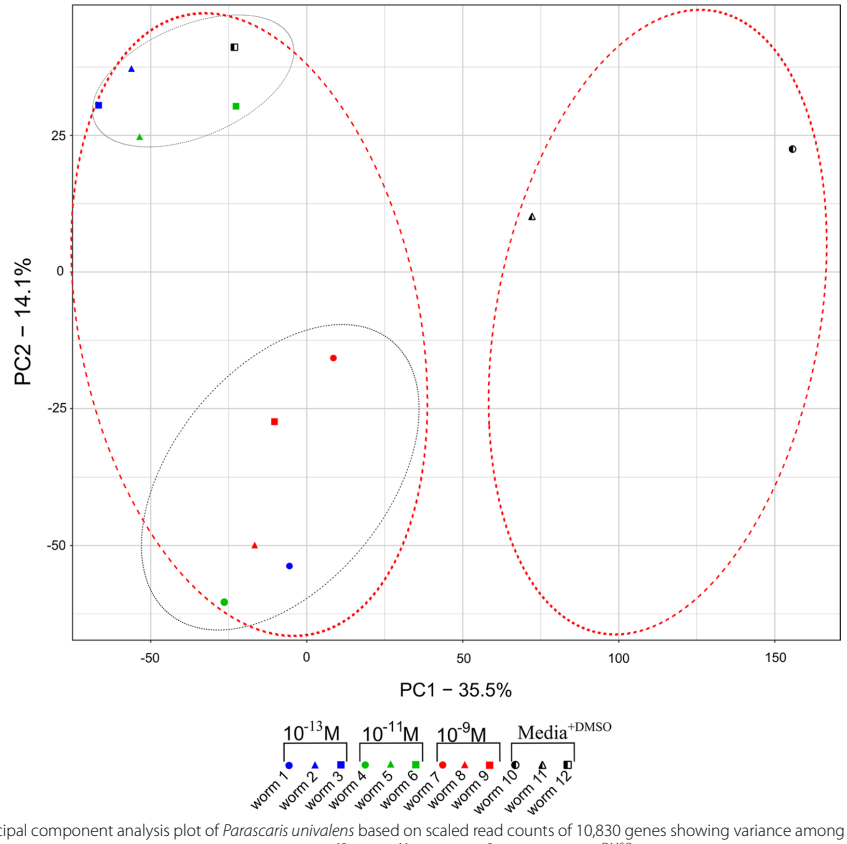

Fig. 2 Principal component analysis plot of *Parascaris univalens* based on scaled read counts of 10,830 genes showing variance among individual worms after exposure to three IVM drug concentrations (10^{-13} M, 10^{-11} M and 10^{-9} M) and media^{+DMSO} (control). PC1 and PC2 represent the largest variances in the data, further portrayed by red and black dotted ellipses, respectively

minute (Fig. 3a). In the thrashing assay, IVM concentrations (10^{-8} and 10^{-7} M) significantly reduced thrashes, with even immobile worms in the 10^{-7} M concentration demonstrated by the very low adjusted *P*-value ($P \leq 0.001$) (Fig. 3b). The dispersal assay showed a similar dose-dependent trend, but was significant only in 10^{-7} M IVM (Fig. 3c). Worms incubated in media^{+DMSO} (control) showed no observable effects and no significant behavioral differences (Fig. 3). The 10^{-7} M concentration was excluded from the qPCR assays, as we aimed for mechanisms at play only in sub-lethal conditions.

Expression of candidate genes in *P. univalens* and *C. elegans* after IVM exposure

Log_2 fold change of candidate genes from RNAseq DEG analysis appeared consistent to those from RT-qPCR, with very few exceptions (Fig. 4). To verify differential gene expression in IVM-treated *P. univalens* and *C. elegans*, RNA with RIN values ranging from 6.6 to 9.8 were used in RT-qPCR assays, and all gene expressions described below are based on these assays. For simplicity, only *C. elegans* gene names are used for both *P. univalens* and *C. elegans*. Corresponding *P. univalens* gene names can be referenced in Table 11.

In general, although IVM appears to have an effect on the expression levels of candidate genes in *P. univalens*, this effect appears to vary among individual worms, agreeing with the observations seen in the RNAseq-based PCA plot (Fig. 2). In *C. elegans*, however, even if there is a strong phenotypic effect of IVM, it has marginal to no effect on the change in expression levels of any of the 15 selected candidate genes (Figs. 5, 6, 7, 8).

Table 1 I-TASSER web server comparison of selected candidate genes' orthologues in *Caenorhabditis elegans* and *Parascaris univalens* (geneIDs begin with "Pg")

	GeneID	GO:MF[a]	GO-score[c]	GO:BP[b]	GO-score	*P. univalens* RNAseq $\log_2$ fold change		
						10^{-13} M	10^{-11} M	10^{-9} M
Drug target	*lgc-37*	GO:0004889	0.34	GO:0006811	0.73			8.20
	PgR047_g061		0.33		0.60			
Phase I enzyme	*dhs-2*	GO:0005488	0.83	GO:0055114	0.83	1.40	1.50	1.50
	PgR127_g021	GO:0004303	0.36		0.87			
	dhs-4	GO:0004316	0.73	GO:0055114	0.81		1.90	
	PgR004_g112	GO:0005488	0.83		0.83			
	dhs-27	GO:0004316	0.81	GO:0055114	0.81	1.80	1.70	1.90
	PgR007_g080		0.59		0.77			
	F13D11.4	GO:0050662	0.98	GO:0055114	0.80	− 1.50	− 1.60	− 1.10
	PgB01_g106		0.97		0.76			
Phase II enzyme	*C13A2.7*	GO:0008171	0.52	GO:0032259	0.35	1.20		1.90
	PgR018_g071	GO:0008376	0.53	GO:0043413	0.56			
	ugt-54	GO:0016758	0.70	GO:0030259	0.52	− 0.80		− 1.20
	PgB20_g050		0.72		0.62			
Transport	*cup-4*	GO:0004889	0.45	GO:0006811	0.65	− 2.80		− 2.10
	PgR075_g041		0.48		0.67			
	hmit-1.2	GO:0015168	0.36	GO:0055085	0.40	2.40	2.10	2.30
	PgR015_g078	GO:0042900	0.32		0.38			
	hmit-1.3	GO:0042900	0.36	GO:0055085	0.41	2.40	2.10	2.30
	PgR015_g078		0.32		0.38			
	slc-17.2	GO:0042900	0.57	GO:0055085	0.57	− 1.00		− 1.10
	PgR047_g023		0.57		0.61			
	Y71G12B.25	GO:0015168	0.55	GO:0055085	0.69	1.60		1.50
	PgR005X_g127		0.54		0.64			
	F17C11.12	GO:0042900	0.34	GO:0055085	0.51	− 1.00		0.70
	PgR003_g012		0.51		0.39			
Transcription regulator	*nhr-3*	GO:0003700	0.65	GO:0006355	0.65	1.2	0.90	
	PgR005X_g204		0.50		0.50			
Others	*F08F8.7*	GO:0004750	1.00	GO:0006098	0.94	8.90		
	PgR013_g129		0.99		0.67			
	pkc-1	GO:0005524	0.60	GO:0014059	0.32		1.00	0.90
	PgB05_g097		0.64		0.31			

[a] GO term: molecular function

[b] GO term: biological process

[c] Average weight assigned to the GO term, where the weights are determined using a combined measure of global and local similarity between the query and template proteins. It is a numeric value between 0 and 1, with higher values indicating more certain predictions

The GABA receptor subunit gene, *lgc-37*, a putative drug target for IVM, showed a generally increased trend in change in expression in *P. univalens* after IVM exposure (Fig. 5a); however, increments in *C. elegans* were marginal (Fig. 5b).

The change in expression profiles of the Phase I metabolic genes in *P. univalens* showed non-uniform patterns. The short chain dehydrogenases (SDR) *dhs-2* and *dhs-27* showed an increased change in expression while *F13D11.4* was decreased in *P. univalens* (Fig. 6a). The expression change of Phase II metabolic genes varied. The glucuronosyltransferase gene *ugt-54* was decreased in *P. univalens*, while transferase *C13A2.7* showed a trend of increased change in expression (Fig. 6c). However, in *C. elegans*, all genes generally appear not to be affected by the IVM exposure (Fig. 6b, d).

All investigated transport protein genes were enriched with major facilitator superfamily (MFS) members,

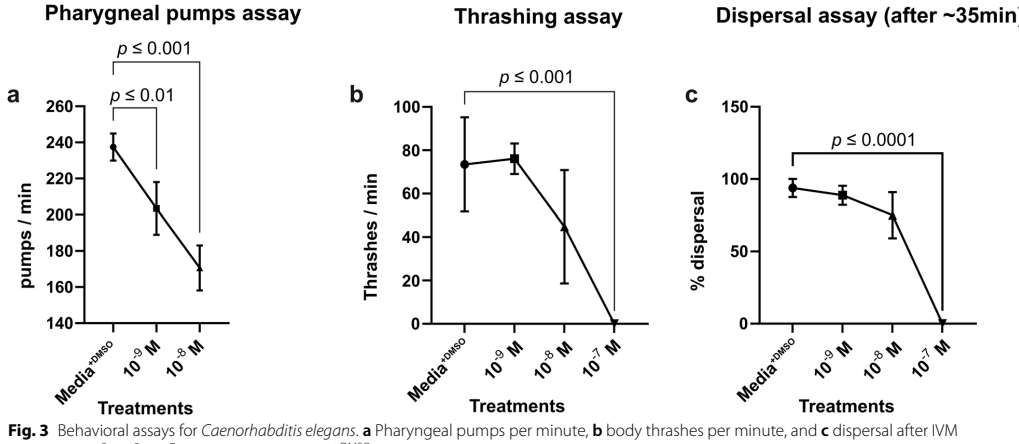

Fig. 3 Behavioral assays for *Caenorhabditis elegans*. **a** Pharyngeal pumps per minute, **b** body thrashes per minute, and **c** dispersal after IVM exposure, 10^{-9} 10^{-8}, 10^{-7} M, and control (media^{+DMSO}). Mean number (±standard error, SE) of viability scores in treatments were compared to those of the control in a one-way ANOVA (Dunnett's multiple comparisons test) to elucidate significant differences

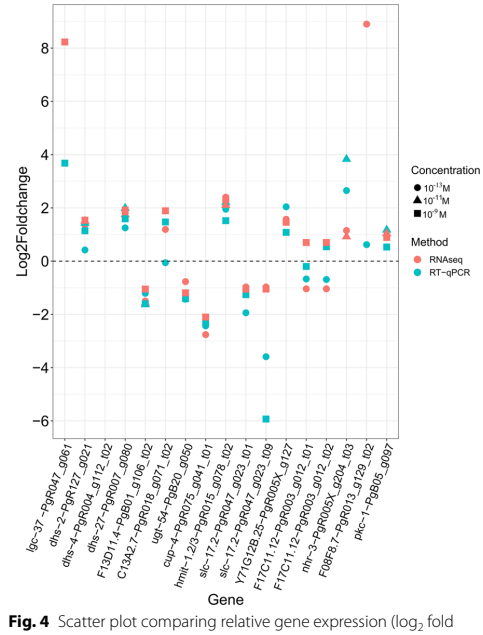

Fig. 4 Scatter plot comparing relative gene expression ($\log_2$ fold change) of *Parascaris univalens* candidate genes between two methods [RNAseq (orange) and RT-qPCR (blue)] after exposure to 10^{-13}, 10^{-11}, and 10^{-9} M IVM for 24 h

except *cup-4*, which belongs to the ligand-gated ion channel family. Overall change in expression of transport protein genes showed a decreased trend in *P. univalens* and minor to no change in *C. elegans* (Fig. 7). Genes *hmit-1.2/hmit-1.3* and *Y17G128B.25* showed an increased change in expression in *P. univalens* (Fig. 7a).

Finally, in response to IVM, transcriptional regulator, *nhr-3*, showed an increased change in gene expression trend in *P. univalens* (Fig. 8a) but marginal to no change in expression was observed in *C. elegans* (Fig. 8b).

The neural signaling protein, *pkc-1*, showed an increased change in gene expression in *P. univalens* exposed to 10^{-11} and 10^{-9} M IVM (Additional file 3: Fig. S3A), but showed little to no change was observed in *C. elegans* (Additional file 3: Fig. S3B). Only the 10^{-13} M IVM showed marginal increased change in expression of ribulose-phosphate 3-epimerase gene *F08F8.7* in *P. univalens*, and little to no change in *C. elegans* across all IVM concentration was observed in both species (Additional file 3: Fig. S3).

Discussion

Recent studies show that the equine roundworm *P. univalens* has developed resistance to the three major classes of anthelmintic drugs used and that the emergence of multidrug-resistant variants is apparent [4, 12, 54]. While the cause of drug resistance drug in parasites is poorly understood, the primary resistance mechanism to benzimidazoles has been better explored than those of other drug classes, particularly in clade V nematodes (see [15] for review). Consequently, most of the proposed

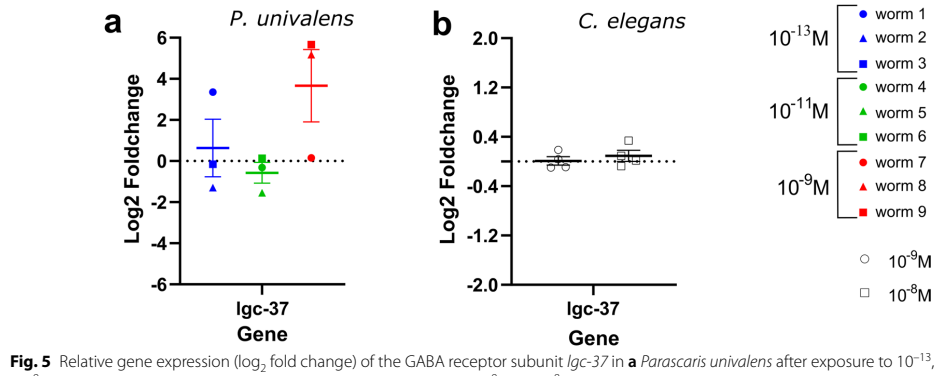

Fig. 5 Relative gene expression (log_2 fold change) of the GABA receptor subunit *lgc-37* in **a** *Parascaris univalens* after exposure to 10^{-13}, 10^{-11}, and 10^{-9} M IVM for 24 h and **b** *Caenorhabditis elegans* after exposure to 10^{-9} and 10^{-8} M IVM for 4 h

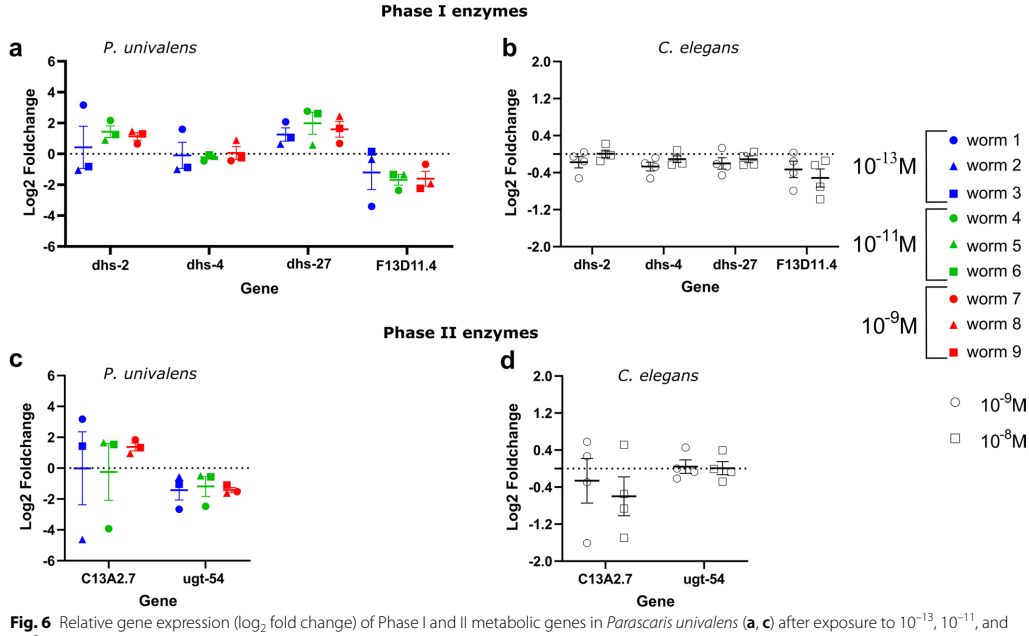

Fig. 6 Relative gene expression (log_2 fold change) of Phase I and II metabolic genes in *Parascaris univalens* (**a**, **c**) after exposure to 10^{-13}, 10^{-11}, and 10^{-9} M IVM for 24 h. Relative gene expression (log_2 fold change) of Phase I and II metabolic genes in *Caenorhabditis elegans* (**b**, **d**) after exposure to 10^{-9} and 10^{-8} M IVM for 4 h

resistance mechanisms have been derived from clade V nematodes and may therefore differ in Clade III nematodes such as *P. univalens*. It is critical to have a thorough understanding of *P. univalens* resistance mechanisms to potentiate species-specific interventions for resistance control and/or alleviation. This, however, is largely constrained by the complexity of its host-dependent life cycle and a lack of in vitro experimental models.

In this study, we evaluated the usage of *C. elegans* as a model for *P. univalens* by a comparative gene expression approach. Of the 1085 DEGs in *P. univalens* after IVM exposure, 231 DEGs had a fold change above

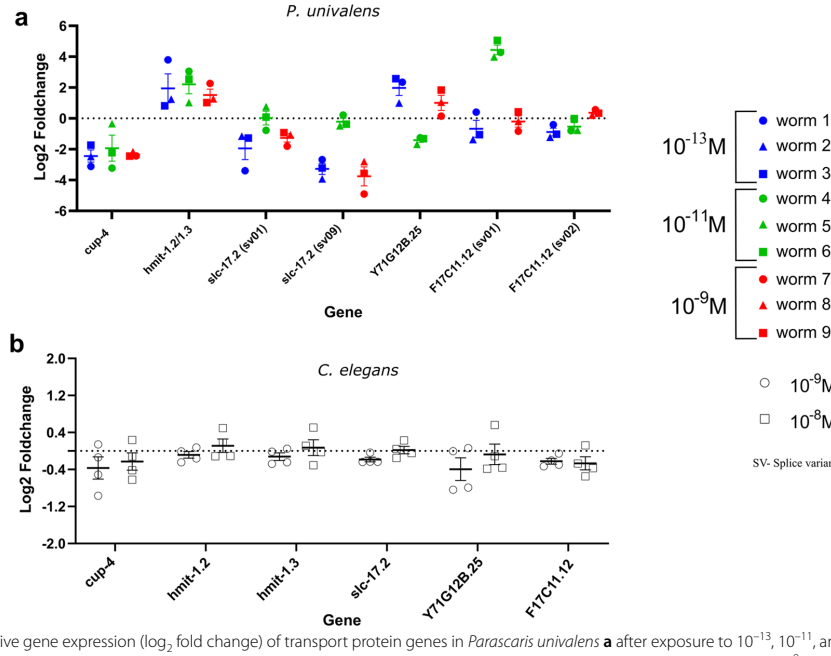

Fig. 7 Relative gene expression (log_2 fold change) of transport protein genes in *Parascaris univalens* **a** after exposure to 10^{-13}, 10^{-11}, and 10^{-9} M IVM for 24 h. Relative gene expression (log_2 fold change) of transport protein genes in *Caenorhabditis elegans* **b** after exposure to 10^{-9} and 10^{-8} M IVM for 4 h

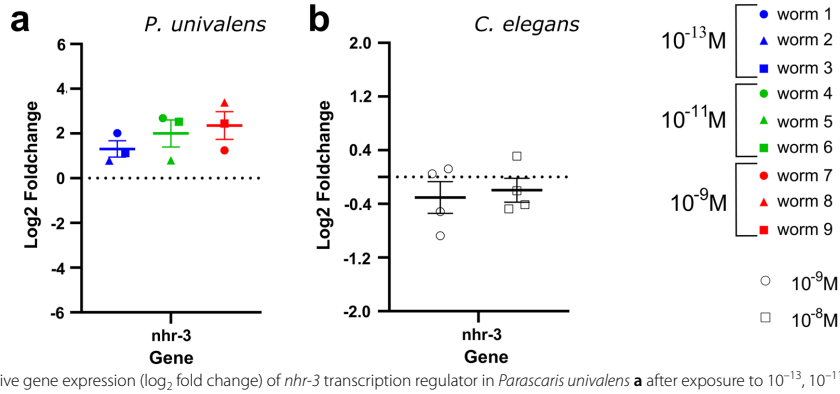

Fig. 8 Relative gene expression (log_2 fold change) of *nhr-3* transcription regulator in *Parascaris univalens* **a** after exposure to 10^{-13}, 10^{-11}, and 10^{-9} M IVM for 24 h. Relative gene expression (log_2 fold change) of *nhr-3* transcription regulator in *Caenorhabditis elegans* **b** after exposure to 10^{-9} and 10^{-8} M IVM for 4 h

twofold. This is however not unique to *P. univalens* as another clade III member, *Brugia malayi*, exposed to 10^{-7} M IVM for 24 h, demonstrated similar modest gene expression changes (14 genes upregulated and 8 genes downregulated more than twofold) [55]. While changes in gene expression greater than twofold are generally

considered more important, expression changes of up to 0.5-fold have been proposed to be as equally meaningful in RNAseq assays if the false discovery rate is < 5% (adj. *P*-value 0.05), with at least three biological replicates used and data analyzed using the Deseq2 R program [56]. All DEGs in the current study followed the above recommendation and were therefore treated equally. Fifteen DEGs were selected as candidate genes and were further evaluated and compared with orthologous genes in *C. elegans* exposed to IVM.

Although IVM affected gene expression in *P. univalens*, there was little to no response in expression of the candidate genes in *C. elegans*, despite the significant dose-dependent behavioral effect of IVM on adult *C. elegans* worms. The premises for *C. elegans* as a model for research in parasitic nematodes have been thoroughly described in other studies [40, 57–59]. For example, *Ascaris suum* and *C. elegans* share 68.9% predicted genes [60], which supports *C. elegans* as a suitable model for the *Ascarididae* family. However, despite all the above, our results show differences in expression of the selected genes between *C. elegans* and *Parascaris univalens* after exposure to IVM. This observation can be attributed to a variety of factors. *C. elegans* and *P. univalens* are members of different clades, V and III, respectively, and they also have different life cycles and evolutionary histories [61]. As a result, genes and gene families associated with parasitism are either absent or have different functions in *C. elegans* [62–64]. The chosen candidate genes in this study are a small subset (1.4%) of all the genes responding to IVM exposure in *P. univalens*. Therefore, a global transcriptomic approach comparing whole worm transcriptomes of both *C. elegans* and *P. univalens* after IVM exposure may be a better method to evaluate whether *C. elegans* can be an accurate in vitro model for *P. univalens*.

The putative IVM target, *lgc-37* (GABA receptor subunit), showed an increased expression in *P. univalens*, and Martin et al. [29] reported a similar observation. Increased expression of *lgc-37* has not been correlated to AR; however, an amino acid substitution (K169R) in *H. contortus lgc-37* transfected in *C. elegans* has been reported to exhibit reduced sensitivity to ML [65]. Taken together, these findings indicate that *lgc-37* is important and that additional research is necessary to fully understand its role in *P. univalens*' response to IVM.

In *P. univalens*, decreased expression was observed for the genes belonging to MFS-transport proteins *slc-17.2* and *F17C11.12* and the ligand-gated ion channel *cup-4* after exposure to IVM. The role of MFS genes in parasitic worms has yet to be determined, but their involvement in drug resistance in bacteria and yeast has been reported [66]. Other than the efflux role, MFSs mediate cellular uptake of glucose and other saccharides [67]. Because IVM causes worm starvation through pharyngeal paralysis [68–70], we speculate that the decreased glucose concentration, a consequence of starvation, may trigger decreased gene expression of MFS responsible for glucose or other saccharide uptake. The ATP-binding cassette transporters, primarily Pgp efflux pumps, have been implicated in resistance in parasitic nematodes [21, 22, 24]. Interestingly, we found no DEGs of Pgps in our RNAseq dataset, which is consistent with previous studies in *P. univalens* [28, 30, 31, 71]. However, other studies have reported induced gene expression of Pgps in IVM-resistant larvae of *Cooperia oncophora* [72] and multi-drug resistant larvae of *H. contortus* exposed to IVM [22].

Differential expression of several Phase I enzymes was observed in *P. univalens* after IVM exposure. Expressions of *dhs-2* and *dhs-27* were increased whereas the reverse was seen for *dhs-4* and *F13D11.4*. However, in *C. elegans*, all SDR genes showed a consistent minor decrease in expression levels. The role of SDRs in anthelmintic resistance is not well known. However, in several helminths, SDR genes have been shown to be involved in metabolic activities of BZs [73–77]. Even though we did not observe any major expressional response of SDR genes in *C. elegans* after IVM exposure, an increase in expression of *dhs-23* in a BZ-resistant strain of *C. elegans* after in vitro exposure to BZ derivatives has been reported [35].

Expression of the Phase II enzyme, *ugt-54*, was decreased in *P. univalens* after IVM exposure, but no response was observed in *C. elegans*. Similarly, decreased expression of other members of the UGT family, *ugt-3*, *ugt3a1*, *ugt-47*, and *ugt-48*, have been observed in *P. univalens* in vitro exposed to pyrantel citrate, thiabendazole, and oxibendazole [29, 30]. Although we did not observe any response of *ugt-54* in *C. elegans*, other studies have shown differential gene expression of UGTs in IVM-tolerant strain of *C. elegans* after exposure to 10^{-6} M IVM [78] and in the BZ-resistant strain of *C. elegans* after exposure to BZs [35, 79, 80]. Together, it is clear that UGTs are important in drug metabolism in both nematode species, and their role in anthelmintic resistance in *P. univalens* needs to be further elucidated.

The transcriptional regulator, *nhr-3*, showed increased change in expression in *P. univalens* after IVM exposure but a slightly decreased change in *C. elegans*. Increased expression of *nhr-8* has reported to upregulate expression of Pgps and Phase I enzyme genes in *C. elegans* and resulted in a decreased efficacy of IVM [81]. A similar effect of IVM has also been observed in *C. elegans* carrying a transgenic construct expressing *H. contortus-nhr-8* [81], suggesting that the function of *nhr-8* could be similar in different nematode species. Even though

nhr-3 does not respond in a similar way in *C. elegans* and *P. univalens*, the NHR family may play a role in AR.

Conclusion

In summary, this is the first time *C. elegans* has been evaluated as a model for *P. univalens* using a comparative gene expression approach. However, the genes selected showed dissimilar expression patterns between the two nematode species. This difference in expression could be due to caveats in the experimental design or simply the differences in life cycles of *P. univalens* and *C. elegans*. For example, due to the difficulties in obtaining live adult *P. univalens*, only three individuals were used per biological replicate in the study, compared to 300 worms for *C. elegans*. In addition, the unnatural in vitro culture environment may influence undesired behavioral changes or gene expression in *P. univalens* worms [29]. Furthermore, only 1.4% of RNAseq-derived DEGs from *P. univalens* were used as candidate genes in this study, of which some transcripts (splice variants) also showed varying expression patterns. Together, this limits the ability to draw firm conclusions regarding comparability between these two nematode species. However, with comparative genomics, using RNAseq data from IVM exposed *C. elegans* and *P. univalens*, it is plausible to find potential drug targets with similar expression in both nematodes. This could provide a better understanding of drug response mechanisms to further investigate and combat drug resistance.

Abbreviations

IVM: Ivermectin; BZ: Benzimindzoles; THP: Tetrahydropyrimidines; ML: Macrocyclic lactones; GluCls: Glutamate-gated ion channels; DEGs: Differentially expressed genes; DMSO: Dimethyl sulfoxide; PCA: Principal component analysis; PC: Principal component; ID: Identification; NaOCl: Sodium hypochlorite; KOH: Potassium hydroxide; NaCl: Sodium chloride; NGM: Nematode growth media; CDS: Coding sequences; PCR: Polymerase chain reaction; RT-qPCR: Reverse transcriptase quantitative polymerase chain reaction; ANOVA: Analysis of variance; SEM: Standard error of the mean; RIN: RNA integrity number; GABA: γ-Aminobutyric acid; SDR: Short chain dehydrogenases; MFS: Major facilitator superfamily; Pgp: P-glycoprotein.

Supplementary Information

The online version contains supplementary material available at https://doi.org/10.1186/s13071-022-05260-4.

Additional file 1: Figure S1. A screeplot showing variation explained by all principal components.

Additional file 2: Figure S2. Venn diagrams showing the number of differentially expressed genes in *P. univalens* that are shared among three IVM concentrations 10^{-13}, 10^{-11}, and 10^{-9} M. Genes with an adjusted *P*-value (Walds test and Benjamini-Hochberg procedure) < 0.05 were considered differentially expressed.

Additional file 3: Figure S3. Relative gene expression (log_2 fold change) of *pkc-1* neural signaling protein and F08F8.7 Ribulose-phosphate-3-epimerase in *Parascaris univalens* (**a**) after exposure to 10^{-13}, 10^{-11} and 10^{-9} M IVM for 24 h. Relative gene expression (log_2 fold change) of *pkc-1* neural signaling protein and *F08F8.7* ribulose-phosphate-3-epimerase in *Caenorhabditis elegans* (**b**) after exposure to 10^{-9} and 10^{-8} M IVM for 4 h.

Additional file 4: Table S1. *Parascaris univalens* and *Caenorhabditis elegans* primer sequences used in PCR assays as well as their respective amplicon sizes, annealing temperatures, and primer efficiencies.

Additional file 5: Table S2. *Parascaris univalens* RT-qPCR cycle time values and log_2 fold change calculations. IVM-13, IVM-11, IVM-9, and CD represent treatment conditions 10^{-13}, 10^{-11}, 10^{-9} M IVM, and media^{+DMSO} (control), respectively.

Additional file 6: Table S3. *Caenorhabditis elegans* RT-qPCR cycle time values and log_2 fold change calculations. IVM-9, IVM-8, IVM-7, and IVM-D represent treatment conditions 10^{-9}, 10^{-8}, 10^{-7} M IVM, and media^{+DMSO} (control), respectively.

Additional file 7: Table S4. Behavioral assays of *Caenorhabditis elegans* after exposure to 10^{-9}, 10^{-8}, 10^{-7} M IVM and media^{+DMSO} (control) for 4 h.

Acknowledgements

The authors would like to express their gratitude to Sláturfélag Suurlands in Selfoss, Iceland, for allowing us to collect parasite material and to the Institute for Experimental Pathology at Keldur at the University of Iceland in Reykjavk, Iceland, for providing laboratory space. The SNP&SEQ Technology Platform in Uppsala performed the sequencing. The facility is a joint venture between Sweden's National Genomics Infrastructure (NGI) and Science for Life Laboratory. Additionally, the Swedish Research Council and the Knut and Alice Wallenberg Foundation support the SNP&SEQ Platform. SLU Bioinformatics Infrastructure performed the bioinformatics analysis (SLUBI).

Author contributions

FD, AH, MA, SS and ET designed the study. FD, FM, ET and SR collected parasite material. FD and SR performed the experiments. FD, ET AH, MA, and SS analyzed the data. FD wrote the manuscript. FM, AH, MA, SS, ET and SR reviewed the manuscript. All authors read and approved the final manuscript.

Funding

Open access funding provided by Swedish University of Agricultural Sciences. This work was supported by the Swedish Research Council FORMAS (Grant Number: 2018-01049).

Availability of data and materials

The pipeline used for quality assessment, mapping, and quantification is available (with nextflow and docker support) at https://github.com/SLUBioinformaticsInfrastructure/RNAseq_nf. Nucleotide sequence data reported in this paper are available in the European Nucleotide Archive (ENA) under the accession number PRJEB37010 (https://www.ebi.ac.uk/ena).

Declarations

Ethics approval and consent to participate

Not applicable.

Consent for publication

Not applicable.

Competing interests

The authors declare that they have no competing interests.

Author details

[1]Division of Parasitology, Department of Biomedical Sciences and Veterinary Public Health, Swedish University of Agricultural Sciences, Box 7036, 750 07 Uppsala, Sweden. [2]Department of Cell and Molecular Biology, Uppsala University, 751 24 Uppsala, Sweden. [3]Section of Immunology, Department of Biomedical Sciences and Veterinary Public Health, Swedish University of Agricultural Sciences, Box 7036, 750 07 Uppsala, Sweden.

Received: 20 January 2022 Accepted: 29 March 2022
Published online: 05 May 2022

References

1. Laugier C, Sevin C, Ménard S, Maillard K. Prevalence of *Parascaris equorum* infection in foals on French stud farms and first report of ivermectin-resistant *P. equorum* populations in France. Vet Parasitol. 2012;188:185–9.
2. Relf VE, Morgan ER, Hodgkinson JE, Matthews JB. Helminth egg excretion with regard to age, gender and management practices on UK Thoroughbred studs. Parasitology. 2013;140:641–52.
3. Armstrong SK, Woodgate RG, Gough S, Heller J, Sangster NC, Hughes KJ. The efficacy of ivermectin, pyrantel and fenbendazole against *Parascaris equorum* infection in foals on farms in Australia. Vet Parasitol. 2014;205:575–80.
4. Alanazi AD, Mukbel RM, Alyousif MS, AlShehri ZS, Alanazi IO, Al-Mohammed HI. A field study on the anthelmintic resistance of *Parascaris* spp. in Arab foals in the Riyadh region, Saudi Arabia. Vet Q. 2017;37:200–5.
5. Cribb NC, Cote NM, Bouré LP, Peregrine AS. Acute small intestinal obstruction associated with *Parascaris equorum* infection in young horses: 25 cases (1985–2004). N Z Vet J. 2006;54:338–43.
6. Clayton HM, Duncan JL. The migration and development of *Parascaris equorum* in the horse. Int J Parasitol. 1979;9:285–92.
7. Clayton HM. Ascarids: recent advances. Vet Clin N Am Equine Pract. 1986;2:313–28.
8. Nielsen MK. Evidence-based considerations for control of *Parascaris* spp. infections in horses. Equine Vet Educ. 2016;28:224–31.
9. Shoop WL, Mrozik H, Fisher MH. Structure and activity of avermectins and milbemycins in animal health. Vet Parasitol. 1995;59:139–56.
10. Wolstenholme AJ, Rogers AT. Glutamate-gated chloride channels and the mode of action of the avermectin/milbemycin anthelmintics. Parasitology. 2005;131:S85–95.
11. Reinemeyer CR. Diagnosis and control of anthelmintic-resistant *Parascaris equorum*. Parasites Vectors. 2009;2:S8.
12. Cooper LG, Caffe G, Cerutti J, Nielsen MK, Anziani OS. Reduced efficacy of ivermectin and moxidectin against *Parascaris* spp. in foals from Argentina. Vet Parasitol Reg Stud Rep. 2020;20: 100388.
13. Lindgren K, Ljungvall O, Nilsson O, Ljungström BL, Lindahl C, Höglund J. *Parascaris equorum* in foals and in their environment on a Swedish stud farm, with notes on treatment failure of ivermectin. Vet Parasitol. 2008;151:337–43.
14. Martin F, Svansson V, Eydal M, Oddsdóttir C, Ernback M, Persson I, et al. First report of resistance to ivermectin in *Parascaris univalens* in Iceland. J Parasitol. 2021;107:16–22.
15. Whittaker JH, Carlson SA, Jones DE, Brewer MT. Molecular mechanisms for anthelmintic resistance in strongyle nematode parasites of veterinary importance. J Vet Pharmacol Ther. 2017;40:105–15.
16. James CE, Hudson AL, Davey MW. Drug resistance mechanisms in helminths: is it survival of the fittest? Trends Parasitol. 2009;25:328–35.
17. Njue AI, Hayashi J, Kinne L, Feng XP, Prichard RK. Mutations in the extracellular domains of glutamate-gated chloride channel alpha3 and beta subunits from ivermectin-resistant *Cooperia oncophora* affect agonist sensitivity. J Neurochem. 2004;89:1137–47.
18. McCavera S, Rogers AT, Yates DM, Woods DJ, Wolstenholme AJ. An ivermectin-sensitive glutamate-gated chloride channel from the parasitic nematode *Haemonchus contortus*. Mol Pharmacol. 2009;75:1347–55.
19. El-Abdellati A, De Graef J, Van Zeveren A, Donnan A, Skuce P, Walsh T, et al. Altered *avr-14B* gene transcription patterns in ivermectin-resistant isolates of the cattle parasites, *Cooperia oncophora* and *Ostertagia ostertagi*. Int J Parasitol. 2011;41:951–7.
20. Williamson SM, Storey B, Howell S, Harper KM, Kaplan RM, Wolstenholme AJ. Candidate anthelmintic resistance-associated gene expression and sequence polymorphisms in a triple-resistant field isolate of *Haemonchus contortus*. Mol Biochem Parasitol. 2011;180:99–105.
21. Dicker AJ, Nisbet AJ, Skuce PJ. Gene expression changes in a P-glycoprotein (*Tci-pgp-9*) putatively associated with ivermectin resistance in *Teladorsagia circumcincta*. Int J Parasitol. 2011;41:935–42.
22. Raza A, Kopp SR, Bagnall NH, Jabbar A, Kotze AC. Effects of *in vitro* exposure to ivermectin and levamisole on the expression patterns of ABC transporters in *Haemonchus contortus* larvae. Int J Parasitol Drugs Drug Resist. 2016;6:103–15.
23. Schinkel AH, Jonker JW. Mammalian drug efflux transporters of the ATP binding cassette (ABC) family: an overview. Adv Drug Deliv Rev. 2003;55:3–29.
24. Xu M, Molento M, Blackhall W, Ribeiro P, Beech R, Prichard R. Ivermectin resistance in nematodes may be caused by alteration of P-glycoprotein homolog. Mol Biochem Parasitol. 1998;91:327–35.
25. Matoušková P, Vokřál I, Lamka J, Skálová L. The role of xenobiotic-metabolizing enzymes in anthelmintic deactivation and resistance in helminths. Trends Parasitol. 2016;32:481–91.
26. Yilmaz E, Ramünke S, Demeler J, Krücken J. Comparison of constitutive and thiabendazole-induced expression of five cytochrome P450 genes in fourth-stage larvae of *Haemonchus contortus* isolates with different drug susceptibility identifies one gene with high constitutive expression in a multi-resistant isolate. Int J Parasitol Drugs Drug Resist. 2017;7:362–9.
27. Matoušková P, Lecová L, Laing R, Dimunová D, Vogel H, Raisová Stuchlíková L, et al. UDP-glycosyltransferase family in *Haemonchus contortus*: phylogenetic analysis, constitutive expression, sex-differences and resistance-related differences. Int J Parasitol Drugs Drug Resist. 2018;8:420–9.
28. Janssen IJ, Krücken J, Demeler J, Basiaga M, Kornaś S, von Samson-Himmelstjerna G. Genetic variants and increased expression of *Parascaris equorum* P-glycoprotein-11 in populations with decreased ivermectin susceptibility. PLoS ONE. 2013;8: e61635.
29. Martin F, Dube F, Karlsson Lindsjö O, Eydal M, Höglund J, Bergström TF, et al. Transcriptional responses in *Parascaris univalens* after *in vitro* exposure to ivermectin, pyrantel citrate and thiabendazole. Parasites Vectors. 2020;13:342.
30. Scare JA, Dini P, Norris JK, Steuer AE, Scoggin K, Gravatte HS, et al. Ascarids exposed: a method for *in vitro* drug exposure and gene expression analysis of anthelmintic naïve *Parascaris* spp. Parasitology. 2020;147:659–66.
31. Martin F, Eydal M, Höglund J, Tydén E. Constitutive and differential expression of transport protein genes in *Parascaris univalens* larvae and adult tissues after *in vitro* exposure to anthelmintic drugs. Vet Parasitol. 2021;298: 109535.
32. Gibson SB, Harper CS, Lackner LL, Andersen EC. The *Caenorhabditis elegans* and *Haemonchus contortus* beta-tubulin genes cannot substitute for loss of the *Saccharomyces cerevisiae* beta-tubulin gene. MicroPubl Biol. 2021. https://doi.org/10.17912/micropub.biology.000411.
33. Ondua M, Mfotie Njoya E, Abdalla MA, McGaw LJ. Investigation of anthelmintic activity of the acetone extract and constituents of *Typha capensis* against animal parasitic *Haemonchus contortus* and free-living *Caenorhabditis elegans*. Parasitol Res. 2021;120:3437–49.
34. Yates DM, Portillo V, Wolstenholme AJ. The avermectin receptors of *Haemonchus contortus* and *Caenorhabditis elegans*. Int J Parasitol. 2003;33:1183–93.
35. Stasiuk SJ, MacNevin G, Workentine ML, Gray D, Redman E, Bartley D, et al. Similarities and differences in the biotransformation and transcriptomic responses of *Caenorhabditis elegans* and *Haemonchus contortus* to five different benzimidazole drugs. Int J Parasitol Drugs Drug Resist. 2019;11:13–29.
36. Gerhard AP, Krücken J, Neveu C, Charvet CL, Harmache A, von Samson-Himmelstjerna G. Pharyngeal pumping and tissue-specific transgenic P-glycoprotein expression influence macrocyclic lactone susceptibility in *Caenorhabditis elegans*. Pharmaceuticals. 2021;14:153.
37. Janssen IJ, Krücken J, Demeler J, von Samson-Himmelstjerna G. Transgenically expressed Parascaris P-glycoprotein-11 can modulate ivermectin susceptibility in *Caenorhabditis elegans*. Int J Parasitol Drugs Drug Resist. 2015;5:44–7.
38. Cully DF, Vassilatis DK, Liu KK, Paress PS, Van der Ploeg LH, Schaeffer JM, et al. Cloning of an avermectin-sensitive glutamate-gated chloride channel from *Caenorhabditis elegans*. Nature. 1994;371:707–11.
39. Dent JA, Smith MM, Vassilatis DK, Avery L. The genetics of ivermectin resistance in *Caenorhabditis elegans*. Proc Natl Acad Sci USA. 2000;97:2674–9.
40. Gilleard JS. The use of *Caenorhabditis elegans* in parasitic nematode research. Parasitology. 2004;128:S49–70.
41. Chen S, Zhou Y, Chen Y, Gu J. fastp: an ultra-fast all-in-one FASTQ preprocessor. Bioinformatics. 2018;34:i884–90.
42. Patro R, Duggal G, Love MI, Irizarry RA, Kingsford C. Salmon provides fast and bias-aware quantification of transcript expression. Nat Methods. 2017;14:417–9.

43. Soneson C, Love MI, Robinson MD. Differential analyses for RNA-seq: transcript-level estimates improve gene-level inferences. F1000Res. 2015;4:1521.
44. Benjamini Y, Hochberg Y. Controlling the false discovery rate: a practical and powerful approach to multiple testing. J R Stat Soc Ser B (Methodol). 1995;57:289–300.
45. Chen H, Boutros PC. VennDiagram: a package for the generation of highly-customizable Venn and Euler diagrams in R. BMC Bioinform. 2011;12:35.
46. Yang J, Yan R, Roy A, Xu D, Poisson J, Zhang Y. The I-TASSER suite: protein structure and function prediction. Nat Methods. 2015;12:7–8.
47. Brenner S. The genetics of *Caenorhabditis elegans*. Genetics. 1974;77:71–94.
48. Stiernagle T. Maintenance of *C. elegans*. WormBook. 2006. p. 1–11.
49. Porta-de-la-Riva M, Fontrodona L, Villanueva A, Cerón J. Basic *Caenorhabditis elegans* methods: synchronization and observation. J Vis Exp. 2012;64: e4019.
50. Johnson JR, Ferdek P, Lian LY, Barclay JW, Burgoyne RD, Morgan A. Binding of UNC-18 to the N-terminus of syntaxin is essential for neurotransmission in *Caenorhabditis elegans*. Biochem J. 2009;418:73–80.
51. Howe KL, Bolt BJ, Shafie M, Kersey P, Berriman M. WormBase ParaSite—a comprehensive resource for helminth genomics. Mol Biochem Parasitol. 2017;215:2–10.
52. Chen N, Harris TW, Antoshechkin I, Bastiani C, Bieri T, Blasiar D, et al. WormBase: a comprehensive data resource for *Caenorhabditis* biology and genomics. Nucleic Acids Res. 2005;33:D383–9.
53. Livak KJ, Schmittgen TD. Analysis of relative gene expression data using real-time quantitative PCR and the 2(-Delta Delta C(T)) method. Methods. 2001;25:402–8.
54. Martin F, Höglund J, Bergström TF, Karlsson Lindsjö O, Tydén E. Resistance to pyrantel embonate and efficacy of fenbendazole in *Parascaris univalens* on Swedish stud farms. Vet Parasitol. 2018;264:69–73.
55. Ballesteros C, Tritten L, O'Neill M, Burkman E, Zaky WI, Xia J, et al. The effects of ivermectin on *Brugia malayi* females *in vitro*: a transcriptomic approach. PLoS Negl Trop Dis. 2016;10: e0004929.
56. Schurch NJ, Schofield P, Gierliński M, Cole C, Sherstnev A, Singh V, et al. How many biological replicates are needed in an RNA-seq experiment and which differential expression tool should you use? RNA. 2016;22:839–51.
57. Hahnel SR, Dilks CM, Heisler I, Andersen EC, Kulke D. *Caenorhabditis elegans* in anthelmintic research—old model, new perspectives. Int J Parasitol Drugs Drug Resist. 2020;14:237–48.
58. Holden-Dye L, Walker RJ. Anthelmintic drugs and nematicides: studies in *Caenorhabditis elegans*. WormBook. 2014. p. 1–29.
59. Salinas G, Risi G. *Caenorhabditis elegans*: nature and nurture gift to nematode parasitologists. Parasitology. 2018;145:979–87.
60. Jex AR, Liu S, Li B, Young ND, Hall RS, Li Y, et al. *Ascaris suum* draft genome. Nature. 2011;479:529–33.
61. Blaxter ML, De Ley P, Garey JR, Liu LX, Scheldeman P, Vierstraete A, et al. A molecular evolutionary framework for the phylum Nematoda. Nature. 1998;392:71–5.
62. International Helminth Genomes Consortium. Comparative genomics of the major parasitic worms. Nat Genet. 2019;51:163–74.
63. Viney M. The genomic basis of nematode parasitism. Brief Funct Genom. 2018;17:8–14.
64. Wang J, Gao S, Mostovoy Y, Kang Y, Zagoskin M, Sun Y, et al. Comparative genome analysis of programmed DNA elimination in nematodes. Genome Res. 2017;27:2001–14.
65. Feng XP, Hayashi J, Beech RN, Prichard RK. Study of the nematode putative GABA type-A receptor subunits: evidence for modulation by ivermectin. J Neurochem. 2002;83:870–8.
66. Paulsen IT, Brown MH, Skurray RA. Proton-dependent multidrug efflux systems. Microbiol Rev. 1996;60:575–608.
67. Yan N. Structural advances for the major facilitator superfamily (MFS) transporters. Trends Biochem Sci. 2013;38:151–9.
68. Arena JP, Liu KK, Paress PS, Frazier EG, Cully DF, Mrozik H, et al. The mechanism of action of avermectins in *Caenorhabditis elegans*: correlation between activation of glutamate-sensitive chloride current, membrane binding, and biological activity. J Parasitol. 1995;81:286–94.
69. Avery L, Horvitz HR. Effects of starvation and neuroactive drugs on feeding in *Caenorhabditis elegans*. J Exp Zool. 1990;253:263–70.
70. Geary TG, Sims SM, Thomas EM, Vanover L, Davis JP, Winterrowd CA, et al. *Haemonchus contortus*: ivermectin-induced paralysis of the pharynx. Exp Parasitol. 1993;77:88–96.
71. Gerhard AP, Krücken J, Heitlinger E, Janssen IJI, Basiaga M, Kornaś S, et al. The P-glycoprotein repertoire of the equine parasitic nematode *Parascaris univalens*. Sci Rep. 2020;10:13586.
72. De Graef J, Demeler J, Skuce P, Mitreva M, Von Samson-Himmelstjerna G, Vercruysse J, et al. Gene expression analysis of ABC transporters in a resistant *Cooperia oncophora* isolate following *in vivo* and *in vitro* exposure to macrocyclic lactones. Parasitology. 2013;140:499–508.
73. Cvilink V, Szotáková B, Krízová V, Lamka J, Skálová L. Phase I biotransformation of albendazole in lancet fluke (*Dicrocoelium dendriticum*). Res Vet Sci. 2009;86:49–55.
74. Cvilink V, Szotáková B, Vokrál I, Bártíková H, Lamka J, Skálová L. Liquid chromatography/mass spectrometric identification of benzimidazole anthelminthics metabolites formed *ex vivo* by *Dicrocoelium dendriticum*. Rapid Commun Mass Spectrom. 2009;23:2679–84.
75. Prchal L, Bártíková H, Bečanová A, Jirásko R, Vokřál I, Stuchlíková L, et al. Biotransformation of anthelmintics and the activity of drug-metabolizing enzymes in the tapeworm *Moniezia expansa*. Parasitology. 2015;142:648–59.
76. Solana HD, Rodriguez JA, Lanusse CE. Comparative metabolism of albendazole and albendazole sulphoxide by different helminth parasites. Parasitol Res. 2001;87:275–80.
77. Stuchlíková LR, Matoušková P, Vokřál I, Lamka J, Szotáková B, Sečkařová A, et al. Metabolism of albendazole, ricobendazole and flubendazole in *Haemonchus contortus* adults: sex differences, resistance-related differences and the identification of new metabolites. Int J Parasitol Drugs Drug Resist. 2018;8:50–8.
78. Laing ST, Ivens A, Butler V, Ravikumar SP, Laing R, Woods DJ, et al. The transcriptional response of *Caenorhabditis elegans* to ivermectin exposure identifies novel genes involved in the response to reduced food intake. PLoS ONE. 2012;7: e31367.
79. Jones LM, Rayson SJ, Flemming AJ, Urwin PE. Adaptive and specialised transcriptional responses to xenobiotic stress in *Caenorhabditis elegans* are regulated by nuclear hormone receptors. PLoS ONE. 2013;8: e69956.
80. Laing ST, Ivens A, Laing R, Ravikumar S, Butler V, Woods DJ, et al. Characterization of the xenobiotic response of *Caenorhabditis elegans* to the anthelmintic drug albendazole and the identification of novel drug glucoside metabolites. Biochem J. 2010;432:505–14.
81. Ménez C, Alberich M, Courtot E, Guegnard F, Blanchard A, Aguilaniu H, et al. The transcription factor NHR-8: a new target to increase ivermectin efficacy in nematodes. PLoS Pathog. 2019;15: e1007598.

Publisher's Note

II

PLOS ONE

RESEARCH ARTICLE

Transcriptomics of ivermectin response in *Caenorhabditis elegans*: Integrating abamectin quantitative trait loci and comparison to the Ivermectin-exposed DA1316 strain

Faruk Dube[1]*, Andrea Hinas[2], Nicolas Delhomme[3], Magnus Åbrink[4], Staffan Svärd[2], Eva Tydén[1]

1 Department of Biomedical Sciences and Veterinary Public Health, Division of Parasitology, Swedish University of Agricultural Sciences, Uppsala, Sweden, **2** Department of Cell and Molecular Biology, Uppsala University, Uppsala, Sweden, **3** Umeå Plant Science Centre (UPSC), Department of Forest Genetics and Plant Physiology, Swedish University of Agricultural Sciences, Umeå, Sweden, **4** Department of Biomedical Sciences and Veterinary Public Health, Section of Immunology, Swedish University of Agricultural Sciences, Uppsala, Sweden

* faruk.dube@slu.se

Citation: Dube F, Hinas A, Delhomme N, Åbrink M, Svärd S, Tydén E (2023) Transcriptomics of ivermectin response in *Caenorhabditis elegans*: Integrating abamectin quantitative trait loci and comparison to the Ivermectin-exposed DA1316 strain. PLoS ONE 18(5): e0285262. https://doi.org/10.1371/journal.pone.0285262

Editor: Raffi V. Aroian, UMass Chan: University of Massachusetts Medical School, UNITED STATES

Received: February 1, 2023

Accepted: April 18, 2023

Published: May 4, 2023

Data Availability Statement: We have made the RNA sequencing raw files available at the ENA database, accessible through the link https://www.ebi.ac.uk/ena/browser/view/ (accession number: PRJEB59331). Additionally, we have uploaded the pipeline for analysis and the necessary files for read processing, mapping, and quantification to the following GitHub repository: https://github.com/ruqse/N2IVM.

Abstract

Parasitic nematodes pose a significant threat to human and animal health, as well as cause economic losses in the agricultural sector. The use of anthelmintic drugs, such as Ivermectin (IVM), to control these parasites has led to widespread drug resistance. Identifying genetic markers of resistance in parasitic nematodes can be challenging, but the free-living nematode *Caenorhabditis elegans* provides a suitable model. In this study, we aimed to analyze the transcriptomes of adult *C. elegans* worms of the N2 strain exposed to the anthelmintic drug Ivermectin (IVM), and compare them to those of the resistant strain DA1316 and the recently identified Abamectin Quantitative Trait Loci (QTL) on chromosome V. We exposed pools of 300 adult N2 worms to IVM (10^{-7} and 10^{-8} M) for 4 hours at 20˚C, extracted total RNA and sequenced it on the Illumina NovaSeq6000 platform. Differentially expressed genes (DEGs) were determined using an in-house pipeline. The DEGs were compared to genes from a previous microarray study on IVM-resistant *C. elegans* and Abamectin-QTL. Our results revealed 615 DEGs (183 up-regulated and 432 down-regulated genes) from diverse gene families in the N2 *C. elegans* strain. Of these DEGs, 31 overlapped with genes from IVM-exposed adult worms of the DA1316 strain. We identified 19 genes, including the folate transporter (*folt-2*) and the transmembrane transporter (*T22F3.11*), which exhibited an opposite expression in N2 and the DA1316 strain and were deemed potential candidates. Additionally, we compiled a list of potential candidates for further research including T-type calcium channel (*cca-1*), potassium chloride cotransporter (*kcc-2*), as well as other genes such as glutamate-gated channel (*glc-1*) that mapped to the Abamectin-QTL.

Funding: This study was made possible through the generous support of the Swedish Research Council FORMAS, https://formas.se/en/start-page.html (grant number 2018-01049) awarded to ET and Swedish Research Council Vetenskapsrådet, https://www.vr.se/english.html (grant number 2018-05814) awarded to AH & SS. The funders had no role in study design, data collection and analysis, decision to publish, or preparation of the manuscript.

Competing interests: The authors have declared that no competing interests exist.

1 Introduction

Parasitic nematodes cause chronic and debilitating illnesses in humans and animals, as well as economic losses in livestock and agriculture [1–3]. For example, soil-transmitted helminths, infect more than one billion people and cost roughly five million disability-adjusted life years reported in 2010 [4] and plant-parasitic nematodes affecting crops cause annual economic losses of >$80 billion globally [5]. Control strategies for parasitic nematodes in domesticated or livestock animals rely on anthelmintic drugs, which cost the European ruminant livestock industry an estimated €320 million per year [6]. The three major classes of anthelmintic drugs are benzimidazoles, tetrahydropyrimidines, and macrocyclic lactones (MLs). The MLs, such as Ivermectin (IVM) and Abamectin, are the most commonly used drug class in veterinary/human medicine and agriculture due to their high efficacy, low toxicity, and broad-spectrum nature [7]. Glutamine-gated chloride ion channels (GluCls) are the primary target of MLs in nematodes. This consequently leads to the depolarization of pharyngeal muscles and hyperpolarization of body wall muscles [8]. As a result, feeding becomes impaired, and the worm experiences flaccid muscle paralysis [9, 10]. In addition, γ-aminobutyric acid (GABA) receptors have been reported as secondary targets of IVM at concentrations [11] considered therapeutically insignificant.

However, due to the widespread use of anthelmintic drugs, extensive anthelmintic drug resistance has developed in many parasitic nematode species of livestock [12]. Anthelmintic resistance has been reported in *Haemonchus contortus*, *Cooperia* spp., and *Ostertagia ostertagi* infecting sheep in Europe [13]. In addition, anthelmintic-resistant parasitic nematodes in sheep, cattle and goats have been reported in a number of countries, including Brazil, Argentina, the United States, Australia, New Zealand, and South Africa (reviewed [12]). Furthermore, there are growing concerns that mass drug administration (MDA) programs are selecting for anthelmintic resistance among helminths that infect humans [14, 15]. In recent years, there have been emerging reports of IVM resistance in human parasite *Onchocerca volvulus* in Ghana [16] and Cameroon [17]. Evidently, understanding and identifying the genetic markers underlying resistance in parasitic nematodes is necessary.

However, identification of candidate genes or gene variants that drive anthelmintic resistance in parasitic nematodes can be challenging. This is partly due to the fact that parasitic nematodes have a host-dependent life cycle, are difficult to cultivate, maintain, manipulate, and study at scale, and often lack well-annotated genomes in full chromosomes. Until now, only a few parasitic nematodes, have relatively complete chromosomal-level genomes [18–21], allowing genetic and comparative genome analyses. In comparison, the free-living nematode *Caenorhabditis elegans* is biologically simple, has a rapid 3.5-day life cycle, genetically amenable, and molecular tools for manipulation are readily available [22]. In addition, the evolutionary relationship between *C. elegans* with parasitic nematodes [23], has led to the adoption of this free-living nematode as a model for parasitic nematodes [22, 24] because it allows for comparative studies and translatable results [25].

Studies in *C. elegans* have begun to uncover IVM resistance mechanisms. For example, simultaneous mutations in *glc-1*, *avr-14*, and *avr-15* result in a ~4000-fold resistance to IVM in *C. elegans* [26]. These genes, together with *glc-2*, *glc-3*, and *glc-4*, code for the GluCls subunits, which are capable of forming diverse homomeric and heteromeric chloride channels [9, 10]. However, the discovery of IVM-resistant populations of the small-ruminant parasite *H. contortus* lacking mutations in the *glc-1*, *avr-14*, and *avr-15* genes [19, 27] suggests the existence of alternative mechanisms of resistance to MLs. Several resistance mechanisms to MLs have been proposed, including changes in gene expression in GluCl and transport protein genes [28]. For example, as previously postulated, decreased expression of drug target

genes may result in fewer drug receptors and thus reduced drug efficacy [29, 30]. Gene expression changes of transporter genes of the ATP-binding cassette family, particularly P-glycoproteins (Pgps), also known as efflux pumps, have been linked to anthelmintic drug resistance [31, 32]. This is because efflux pumps eliminate drugs from the cell, preventing them from reaching their target sites. Furthermore, increased expression of genes encoding drug metabolic enzymes, postulated to increase conversion of drugs into inactive metabolites, has been associated with resistance [33]. Collectively, this highlights the multigenic nature and multiple mechanisms of anthelmintic resistance. Although a previous microarray-based study [34] examined the effect of IVM on gene expression in *C. elegans*, the strain used was DA1316, which is highly resistant to IVM due to simultaneous mutations in three genes (*glc-1*, *avr-14*, and *avr-15*). As a result, the current study is premised on the lack of a previous transcriptomic study assessing the effect of IVM on gene expression in wild-type (N2) *C. elegans*.

In this study, we investigated gene expression in an adult *C. elegans* N2 strain exposed to IVM using an RNAseq transcriptomic approach in order to identify the underlying processes and genes involved in the response to IVM in a wild type strain. In addition, we compared our transcriptomic data with microarray data from the IVM-exposed *C. elegans* DA1316 strain [34] in order to identify genes that may be uniquely associated with IVM response in IVM-resistant strains. Additionally, we investigated the recently discovered Abamectin Quantitative Trait Loci (QTL) on chromosome V in *C. elegans* [35] to determine any potential associations between the identified genes and the QTL.

2 Materials and methods

2.1 Caenorhabditis elegans exposure and RNA extraction

Adult *C. elegans* N2 Bristol strains obtained from the Caenorhabditis Genetics Center were exposed *in vitro* to Ivermectin (IVM). We utilized IVM concentrations of 10^{-7} M and 10^{-8} M, which are within the ranges (10^{-9} M- 10^{-6} M) employed in previous studies [34, 36–40] and the 4 h exposure time was adapted from Laing et al. [34].

A detailed description of the experimental setup is described in [41]. Briefly, synchronized worms at maximum reproduction stage (76 h post L1) were incubated at 20˚ C in S-complete media supplemented with IVM in concentrations of 10^{-7} and 10^{-8} M (+ 0.025% DMSO final concentration) and 0.025% DMSO (control) for 4 h. The experiment was performed in quadruplicates (~300 worms /replicate). After exposure worms were pelleted by centrifugation, frozen in liquid nitrogen, ground with a pestle and subsequently suspended in Trizol (Invitrogen, Carlsbad, USA). Chloroform was added and the aqueous phase was advanced to NucleoSpin® RNA Plus Kit (Macherey Nagel, Düren, Germany) for RNA extraction. RNA quality and quantity checks were performed using the RNA ScreenTape kit on TapeStation 4150 (Agilent, Santa Clara, USA).

2.2 Library preparation and RNA sequencing

The SNP -& SEQ Platform, SciLifeLab Uppsala, Sweden, did the library preparation and sequencing. Using the TruSeq stranded mRNA library preparation kit with polyA selection (Illumina Inc, San Diego, USA); one microgram of RNA from each sample (biological replicate) was used to prepare sequencing libraries. From the libraries, clusters were made, and 150 cycles of paired-end sequencing were done in a single-end SP flowcell using NovaSeq 6000 equipment and v1.5 sequencing chemicals (Illumina Inc., San Diego, USA).

2.3 Read processing, mapping and quantification

Ribosomal RNA reads were assessed and filtered out using SortMeRNA (v4.3.6) [42] and rRNA databases from SILVA SSU, LSU (v111) [43] and the RFAM 5/5.8S (v11.0) [44]. Quality trimming and adapter removal was performed using Trimmomatic (v0.39) [45] with the following non-default parameters: sliding window of length four; minimum quality 20; and minimum length of 36. FastQC (v0.11.9) [46] was utilized to evaluate the quality of the resulting reads.

Expression quantification against the *C. elegans* transcriptome was performed with Salmon (v1.9.0) [47] using the entire genome (PRJNA13758, release WS283) as the decoy sequence. The transcriptome used was a concatenation of mRNA, ncRNA, and pseudogene files of PRJNA13758, release WS283 available at WormBase [48]. We have made the RNA sequencing raw files available at the ENA database, accessible through the link https://www.ebi.ac.uk/ena/browser/view/ (accession number: PRJEB59331). Additionally, we have uploaded the pipeline for analysis and the necessary files for read processing, mapping, and quantification to the following GitHub repository: https://github.com/ruqse/N2IVM.

R version 4.1.2 was utilized for all R-based analyses. Salmon output was matrix-summarized with tximport R package (v1.22.0) [49] utilizing the TxDb.Celegans.UCSC.ce11.ensGene annotation R package (v3.12.0) [50], for downstream transcript/ gene-level analysis. As a quality control measure, exploratory analysis and visualization was performed on count data.

2.4 Principal component analysis

Principal component analysis (PCA) was utilized to investigate sample variation. The variance stabilizing transformation function from the DESeq2 R package (v1.34.0) [51] was applied to count data of genes across all samples (n = 12). Since IVM exposure was performed in batches based on concentration, any batch effects were removed by removeBatchEffect function from the limma R package (v3.50.3) [52]. Using R base prcomp function, principal component analysis was performed on the variance-stabilized transformed (VST) read counts. The top two PCs that account for the most variation in the data were visualized in PCA plot for genes with non-zero read counts using the ggplot2 R package(v3.3.5) [53]. Sample clustering was determined by the enclosing ellipses implemented by the geom_mark_ellipse function in the ggforce R package (https://github.com/thomasp85/ggforce/).

2.5 Differential gene expression

Differential gene expression was determined on raw count data by DEseq function in the DESeq2 R package using the following model design, *~batch + IVM concentration*. The batch variable was to compensate for any biases caused by the batch effect. Differentially expressed genes (DEGs) were defined as those with an adjusted P-value < 0.05 and Log2foldchange (Log2FC) ≥ 0.5 or ≤ -0.5 (1.4-fold change). These cut-offs are based on recommendations by Schurch et al. [54]. Differentially expressed genes with average expression level (*baseMean*) of <20 across all samples were discarded based on the independent filtering results from DESeq2.

The metadata of DEGs such as concise description, gene ontology association, interacting gene, tissue expression and RNAi/allele phenotype observed were retrieved from WormBase using the SimpleMine tool taking DEGs gene IDs as input. To assess genes shared by each drug concentration, comparative Venn diagrams were constructed using gene IDs and the venn.diagram function of the VennDiagram R package [55]. The get.venn.partition function was utilized to acquire the gene IDs associated with each Venn diagram partition. The hypergeometric test was used to test the significance of the overlapping genes between concentrations using the R base function, phyper.

2.6 Over-representation analysis (ORA)

Over-representation analysis was performed on DEGs using all genes (19565) with a non-zero total read count as a background based on Gene Ontology (GO: Release 2021-12-15), Kyoto Encyclopedia of Genes and Genomes (KEGG: Release 2021-12-27) and TRANSFAC (Release 2021.3 classes: v2) databases. The analysis was carried out using the gost function from the gprofiler2 R package (v0.2.1) [56], with default parameters and *C. elegans* as the set organism. The output files were processed, and data visualized using ggplot2. Differentially expressed genes from enriched terms putatively involved in drug metabolism/resistance, apoptosis and transcription of regulation were retrieved, categorized, and characterized.

2.7 Comparative analysis gene expression between *C. elegans* strains N2 and DA1316 after IVM exposure

A comparative analysis of the obtained DEGs with those from a previous study [34] was performed. In that study, *C. elegans* strain (DA1316), a triple mutant of the glutamate-gated chloride channel (GluCl) subunits *avr-14*, *avr-15*, and *glc-1* was exposed to IVM 10^{-6} and 10^{-7} M for 4 h. Differential gene expression was determined by microarray assays. To reduce ambiguity prior to comparison, gene names and IDs of DEGs from the previous study were evaluated to determine if they had been renamed, merged, or divided, using the WormBase Gene Name Sanitizer tool. Only DEGs with a fold change of at least 1.4 were included in the comparison and visualized in upsetR plot using the UpSetR R package (v1.4.0) [57]. The hypergeometric test was used to test the significance of the overlapping genes between DA1316 and N2 strain using the R base function, phyper.

2.8 Analysis of IVM-induced gene expression within Abamectin-QTL on chromosome V

A recent study described quantitative trait loci (QTL) regions on chromosome V of *C. elegans* after exposure to the macrocyclic drug, Abamectin [35]. Based on genome wide association mapping, two regions were detected, left arm (VL) and right arm (VR) located at nucleotides 1,757,246–4,333,001 and 15,983,112–16,599,066, respectively. Linkage mapping approach identified three regions, VL, VR and central (VC) located at 2,629,324–3,076,312, 15,933,659–16,336,743 and 6,118,360–7,374,129, respectively. In our comparative analysis, VL and VR from the genome wide association mapping and VC from the linkage mapping were used. The BSgenome.Celegans.UCSC.ce11genome object from the BSgenome.Celegans.UCSC.ce11 R package (v1.4.2) [58] was used in this analysis. All genes in the VL, VC and VR regions were extracted using the GRanges function and subset based on our DEGs using subsetByOverlaps function. Both functions are derived from GenomicRanges R package (v1.46.1) [59]. To eliminate any chromosome length biases, the distribution/ enrichment of DEGs across all chromosomes was estimated using the Fisher's Exact Test for Count Data in R. Differentially expressed genes mapping to the QTL were subsequently identified and visualized on a karyoplot from karyoploteR R package (v1.20.3) [60].

3 Results

3.1 Transcriptomic variation amongst adult *C. elegans* worms exposed to Ivermectin

Total RNA (RIN $>$ 8) was sequenced from *C. elegans* adults at maximum reproduction exposed to IVM 10^{-7} and 10^{-8} M yielding sequencing data of 21–60 million read-pairs/sample. The used concentrations of IVM treatment were selected according to [41]. However, due to

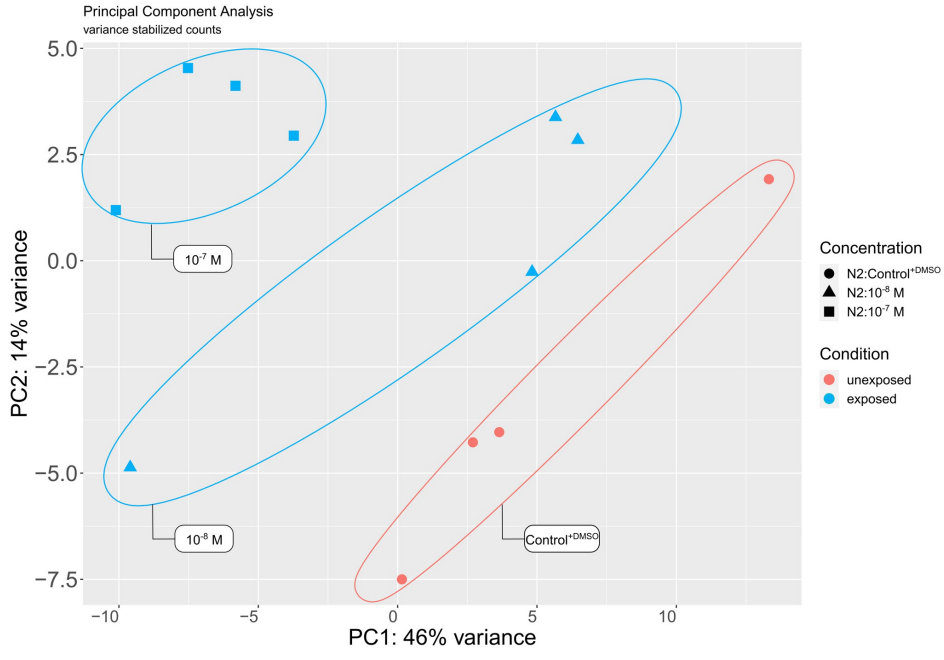

Fig 1. Variation in gene expression among worms exposed to IVM. A PCA plot of *C. elegans* N2 strain based on variance stabilized read counts from worm pools (n = 300) after exposure to IVM 10^{-7} M, 10^{-8} M or control $^{+DMSO}$. Pools are separated by both PC1 and PC2, which represent the largest variances in the data and are ellipsed by concentration/treatment.

https://doi.org/10.1371/journal.pone.0285262.g001

the very low number of differentially expressed genes in IVM 10^{-9} M, only data from IVM 10^{-7} and 10^{-8} M was used in the current study. Following quality control and evaluation with SortMeRNA and Trimmomatic, 16–42 million read-pairs/sample were obtained with a mean phred score above 33, indicating high quality reads. The read-mapping rate to the custom-built PRJNA13758 *C. elegans* transcriptome (see Methods) and the *C. elegans* genome (PRJNA13758, release WS283) as a decoy, was 97% using Salmon.

According to principal component analysis of the VST read counts, worm pools (n = 300 worms per pool), both PC1 and PC2 explained the separation by treatment condition (Fig 1).

3.2 Differential gene expression

Following DESeq2 analysis, 615 genes were differentially expressed after IVM 10^{-7} M and/or 10^{-8} M exposure (S1 Table). Of these, 76% (468 genes) had known functional annotations including GO annotations according to WormBase (release WS283). Ninety five percent (582 genes) of DEGs were exclusively detected in 10^{-7} M, 1% (8 genes) in 10^{-8} M and 4% (25 genes) showed significant (p-value = 0.00001) overlap between the two concentrations (Fig 2 & S2 Table). About 33% (201 genes) of DEGs were altered more than 2-fold, with 85 genes upregulated and 116 genes downregulated. The top ten up- and downregulated DEGs consisted of a

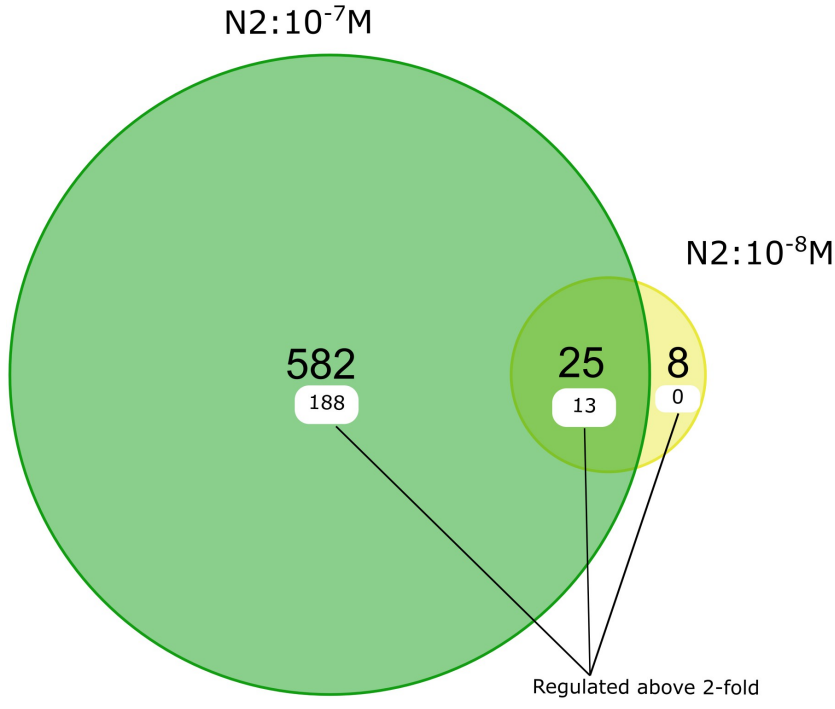

Fig 2. Differentially expressed in IVM-exposed *C. elegans* N2 strain. Venn diagrams showing the number of DEGs in *C. elegans* N2 strain between IVM concentrations 10^{-7} and 10^{-8} M based recommendations by Schurch et al. [54]. The number of genes differentially expressed above 2-fold are labelled in white.

https://doi.org/10.1371/journal.pone.0285262.g002

diverse set of genes or gene families including transmembrane transporters, and heat shock proteins (S3 Table).

To gain insights into the biological pathways underlying the differentially expressed genes, we conducted over-representation analysis on both the upregulated (Fig 3A & S4 Table) and downregulated genes (Fig 3B & S4 Table). We found that the downregulated DEGs exhibited more enrichment terms (42) compared to the upregulated genes (17). The ORA on the upregulated DEGs revealed enrichment of terms related to response to external stimulus, ABC-transport activity, and Factor: elt-3; motif: TCTTATCA (TF: M07154) based on GO, KEGG pathway, and TRANSFAC databases, respectively (Fig 3A & S4 Table). In contrast, ORA on the downregulated genes showed enrichment of terms related to metabolism of glycans, amino acids, and organic compounds, Factor: elt-3; motif: TCTTATCA (TF: M07154) among others, based on the same databases (Fig 3B & S4 Table). Differentially expressed genes from ORA terms with putative involvement in drug metabolism were explored further.

3.2.1 Differentially expressed genes encoding drug receptors. After exposure of N2 worms to IVM 10^{-7} M, the putative drug target *glc-1*, an alpha subunit of the GluCl receptor, *glc-1* was downregulated 1.4-fold. In addition, the putative drug target, *lgc-26*, a possible

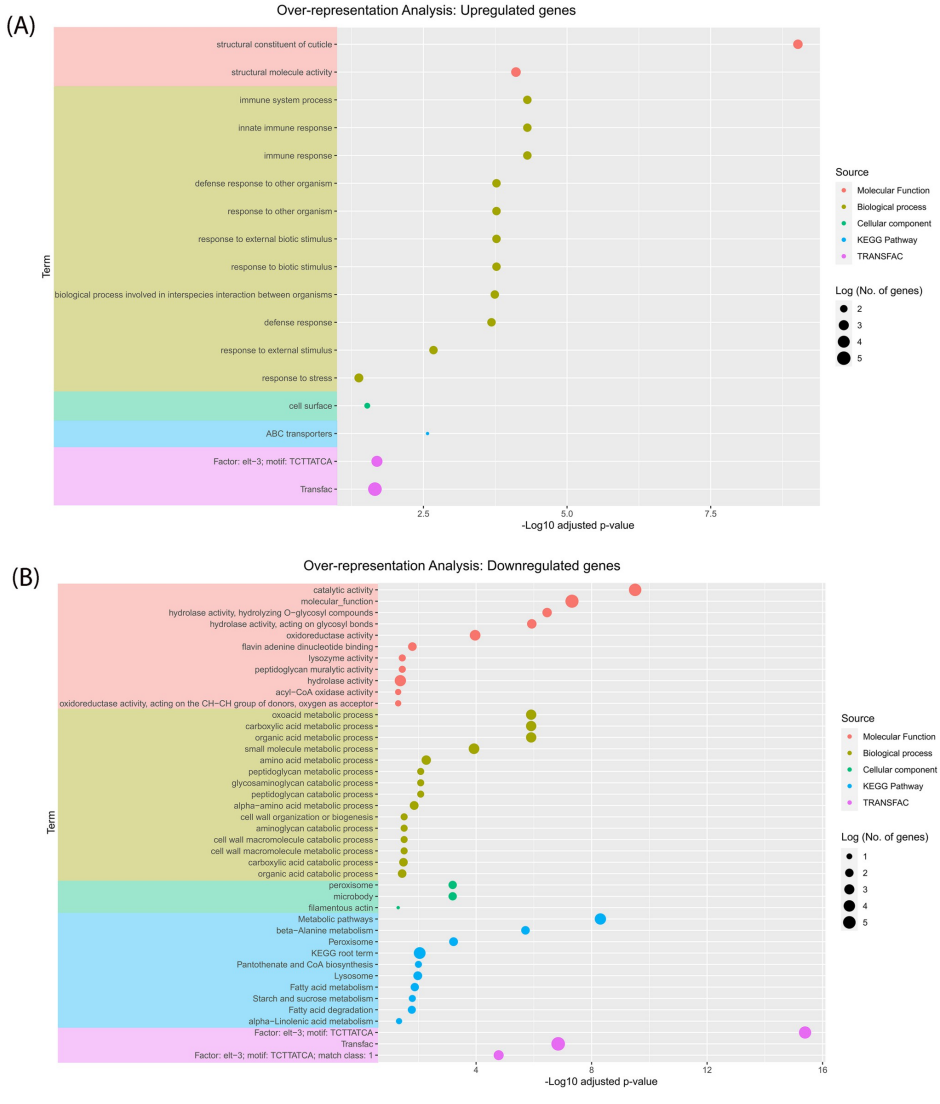

Fig 3. **A.** Biological processes underpinned by upregulated genes. An over-representation plot showing significantly enriched for terms among upregulated DEGs based on Gene ontology (molecular function, biological process and cellular component), Kyoto Encyclopedia of Genes and Genomes (KEGG), and TRANSFAC databases. The dots represent an enriched term. **B.** Biological processes underpinned by downregulated genes. An over-representation plot showing significantly enriched for terms among downregulated DEGs based on Gene ontology (molecular function, biological process and cellular component), Kyoto Encyclopedia of Genes and Genomes (KEGG), and TRANSFAC databases.

https://doi.org/10.1371/journal.pone.0285262.g003

Table 1. Upregulated genes putatively involved in IVM response in *C. elegans* N2 strain.

Category	Gene	LFC:N2:10^{-7} M[a]	-Log10 Adjusted p-value	LFC:N2:10^{-8} M[b]	-Log10 Adjusted p-value	Description[c]
Phase I metabolism	*cyp-13B2*	0.56	1.88			cytochrome P450
	cyp-33C8	1.29	7.43			cytochrome P450
	cyp-34A8	0.73	2.11			cytochrome P450
Phase II metabolism	*ugt-62*	0.81	1.55			UDP-glycosyltransferase
Ion channels	*atp-6*	1.88	34.40	2.06	46.06	ATP synthase subunit a
	best-21	0.69	1.75			chloride channel activity
	F58G6.9	1.62	1.62			copper ion transmembrane transporter activity
	kvs-5	1.10	2.84			potassium ion transmembrane transport
Solute transporters	*pgp-5*	1.83	1.38			P-glycoprotein ATP-dependent efflux pump
	pgp-6	1.15	1.93			P-glycoprotein ATP-dependent efflux pump
	pgp-9	1.52	4.61			P-glycoprotein ATP-dependent efflux pump
	folt-2	1.92	1.94			folate transporter
	pmp-4	1.05	2.11			long-chain fatty acid transporter
Transcription factors	*fkh-3*	0.52	1.71			forkhead transcription factor
	fkh-4	0.58	1.50			forkhead transcription factor
	mdl-1	0.50	2.99			basic helix-loop-helix (bHLH) protein
	nhr-17	0.55	1.75			nuclear receptor super family
	nhr-57	0.58	1.54			nuclear receptor super family
	nhr-115	1.69	1.42			nuclear receptor super family
	nhr-137	0.53	1.30			nuclear receptor super family
	tbx-33	0.58	1.83			T-box transcription factor
	tbx-38	0.99	1.33			T-box transcription factor
	zip-3	0.86	2.53			bZip transcription factor
Involved in apoptosis	*pal-1*	0.65	8.25	0.54	5.23	homeodomain protein

Alphabetically sorted upregulated genes putatively characterized as drug targets or involved in metabolite transport, xenobiotic metabolism, gene expression regulation, and apoptosis processes

[a]Log2Foldchange for Ivermectin drug concentration 10^{-7} M

[b]Log2Foldchange for Ivermectin drug concentration 10^{-8} M

[c]Full description can be found in S1 Table

https://doi.org/10.1371/journal.pone.0285262.t001

nicotinic acetylcholine receptor was downregulated 1.6-fold after exposure to IVM 10^{-7} M (Table 1). However, in IVM 10^{-8} M concentration, differential expression of the putative drug receptors was not observed.

3.2.2 Differentially expressed genes involved in Phase I and II xenobiotic metabolism. There were 11 DEGs putatively classified to be involved in Phase I metabolism, of which eight were downregulated (Table 2) and three were upregulated in IVM 10^{-7} M concentration (Table 1). Eight genes were attributed to the cytochrome P450 family, of which three genes, *cyp-33C8*, *cyp-34A8* and *cyp-13B2* were on average upregulated 1.8-fold while the rest, *cyp-33E1*, *cyp-13A5*, *cyp-25A1*, *cyp-35A2* and *cyp-34A9* were downregulated between 1.5 and 2.2-fold. Other genes involved in drug metabolism with differential expression included Flavin-containing monoxygenase, *fmo-2*, short chain dehydrogenase, *dhs-7* and aldehyde dehydrogenase *adh-5*, which were downregulated between 1.5 and 6-fold.

Table 2. Downregulated genes putatively involved in IVM response in *C. elegans* N2 strain.

Category	Gene	LFC:N2:10^{-7} M[a]	-Log10 Adj. p-value	LFC:N2:10^{-8} M[b]	-Log10 Adj. p-value	Description[c]
Drug target	*glc-1*	-0.50	2.18			alpha subunit of a glutamate-gated chloride channel
	lgc-26	-0.71	1.55			nicotinic acetylcholine receptor-like LGIC
Phase I metabolism	*alh-5*	-0.90	2.17			aldehyde dehydrogenase (NAD+) activity
	cyp-13A5	-0.74	1.85			cytochrome P450
	cyp-25A1	-0.87	1.43			cytochrome P450
	cyp-33E1	-0.54	2.35			cytochrome P450
	cyp-34A9	-1.12	6.73			cytochrome P450
	cyp-35A2	-0.99	9.22			cytochrome P450
	dhs-7	-2.60	6.50			regulation of reactive oxygen species metabolic process
	fmo-2	-1.25	6.57			flavin-containing monoxygenase
Phase II metabolism	*gst-20*	-1.02	3.67			glutathione transferase
	gst-4	-0.56	1.33			glutathione transferase
	gst-42	-0.60	4.21			glutathione transferase
	gst-6	-0.86	1.62			glutathione transferase
	gstk-2	-0.63	1.68			kappa class glutathione transferase
	ugt-11	-0.71	1.62			UDP-glycosyltransferase
	ugt-12	-0.64	1.34			UDP-glycosyltransferase
	ugt-22	-0.91	3.56			UDP-glycosyltransferase
	ugt-43	-1.61	4.48			UDP-glycosyltransferase
	ugt-44	-1.20	8.77			UDP-glycosyltransferase
Ion channels	*atp-6*	1.88	34.40	2.06	46.06	ATP synthase subunit a
	best-1	-1.29	4.21			chloride channel activity
	best-5	-1.06	2.37			chloride channel activity
	catp-1	-0.51	2.06			alpha subunit of the Na+/K+- and H+/K+-pump P-type ATPase family
	cca-1	-0.53	1.54			calcium channel alpha subunit
	F47E1.4	-0.89	1.97			sodium-independent organic anion transmembrane transporter activity
	kcc-2	-0.53	3.46			potassium chloride cotransporter
	ncx-2	-0.62	1.43			3Na[+]/1Ca[2+] exchanger
	nlr-1	-0.63	1.71			Neurexin Like receptor
	tmc-2	-0.92	1.42			mechanosensitive ion channel activity
	Y70G10A.3	-0.55	5.24			sodium-independent organic anion transmembrane transporter activity
	ZK185.5	-0.60	2.71			cation transmembrane transporter activity
Solute transporters	*aat-3*	-0.50	3.33			amino acid transporter catalytic subunit
	amt-4	-0.91	3.73			ammonium transporter protein family
	aqp-1	-1.07	3.43			aquaglyceroporin
	C13C4.6	-1.20	4.82			transmembrane transporter activity
	F11A5.9	-0.52	1.62			transmembrane transporter activity
	F17C11.12	-0.52	3.28			transmembrane transporter activity
	F23F12.13	-1.63	2.10			transmembrane transporter activity
	gem-1	-0.65	2.26			monocarboxylic acid transmembrane transporter activity
	glt-5	-0.93	4.85			glutamate/aspartate and neutral amino acid transporter
	haf-9	-0.65	2.04			half-type ATP-binding cassette (ABC) transporter
	hmit-1.3	-0.73	2.36			(H+)-dependent myo-inositol transporter
	K09C4.1	-0.92	1.33			hexose transmembrane transporter activity
	M162.5	-0.77	2.72			transmembrane transporter activity
	pept-1	-0.87	2.05			low affinity/high capacity oligopeptide transporter
	pmp-1	-0.77	1.57			ATP-binding cassette (ABC) transporter
	slc-25A29	-0.78	2.57			high-affinity L-arginine transmembrane transporter activity
	slc-28.1	-1.19	4.21			nucleoside:sodium symporter activity
	slc-36.5	-0.62	2.31			amino acid transmembrane transporter activity
	spp-1	-0.55	10.83			saposin (B) domain-containing caenopore
	swt-1	-0.50	13.61			sugar transmembrane transporter activity
	T07G12.5	-2.89	3.19			L-ascorbic acid transmembrane transporter activity
	T22F3.11	-2.81	2.22			transmembrane transporter activity
	wht-7	-1.03	4.12	-0.74	2.68	ABC-type transporter activity
	Y4C6B.3	-0.59	2.30			transmembrane transporter activity
	ZK550.2	-0.96	1.77			transmembrane transporter activity

(*Continued*)

Table 2. (Continued)

Category	Gene	LFC:N2:10^{-7} M[a]	-Log10 Adj. p-value	LFC:N2:10^{-8} M[b]	-Log10 Adj. p-value	Description[c]
Transcription factors	*bar-1*	-0.75	1.87			beta-catenin transcription coactivator
	ceh-31	-1.11	3.11			homeobox domain protein
	egl-43	-1.28	2.09			zinc finger protein
	elt-2	-0.69	6.04			GATA-type transcription factor
	fkh-6	-0.84	1.93			forkhead transcription factor
	ham-2	-0.95	1.52			C2H2 zinc finger-containing protein
	let-381	-0.95	2.15			forkhead transcription factor
	lin-22	-1.09	1.99			basic helix-loop-helix (bHLH)-containing protein
	M03D4.4	-0.79	6.49			DNA-binding transcription factor activity
	myrf-2	-0.84	4.20	-0.78	1.42	glutamine/asparagine-rich domain protein
	nhr-21	-0.77	1.52			nuclear receptor super family
	nhr-55	-1.46	3.84			nuclear receptor super family
	nhr-99	-1.04	2.21			nuclear receptor super family
	nhr-119	-0.69	1.80			nuclear receptor super family
	nhr-173	-0.89	1.51			nuclear receptor super family
	odd-2	-0.66	3.78			ODD-SKIPPED family
	pros-1	-0.97	2.24			homeodomain protein
	sta-1	-0.70	3.17			STAT family transcription factor
	tbx-2	-0.51	4.91			T-box transcription factor
	ttx-1	-0.90	1.84			OTD/OTX hoemeodomain protein
	unc-62	-0.80	1.54			Meis-class homeodomain protein
	unc-98	-0.76	2.56			C2H2 zinc finger protein
	unc-120	-0.62	3.87			MADS-box transcription factor
	unc-130	-0.64	1.82			forkhead domain transcription factor
Involved in apoptosis	*ces-1*	-1.22	8.81			C2H2-type zinc finger transcription factor
	ces-2	-0.67	2.65			basic region leucine-zipper (bZIP) transcription factor
	lec-6	-0.56	2.18			'proto' type galectin (beta-galactosyl-binding lectin)
	T05C3.6	-1.00	1.55			paralog of T05C3.2

Alphabetically sorted downregulated genes putatively characterized as drug targets or involved in metabolite transport, xenobiotic metabolism, gene expression regulation, and apoptosis processes

[a]Log2Foldchange for Ivermectin drug concentration 10^{-7} M

[b]Log2Foldchange for Ivermectin drug concentration 10^{-8} M

[c]Full description can be found in S1 Table

https://doi.org/10.1371/journal.pone.0285262.t002

Twelve DEGs putatively identified as UDP-glycosyltransferases and glutathione S-transferases involved in Phase II metabolism were enriched exclusively in IVM 10^{-7} M (Tables 1 & 2). UDP-glycosyltransferases, *ugt-62* was upregulated (Table 1) above 1.8-fold while *ugt-11*, *ugt-12*, *ugt-22*, *ugt-43* and *ugt-44* were downregulated between 1.4 and 3-fold (Table 2). In addition, glutathione S-transferases, *gst-4*, *gst-6*, *gst-20*, *gst-42* and *gstk-2* were downregulated between 1.5 and 2-fold. Only one gene, *ugt-22*, appeared in 10^{-8} M, and was downregulated 1.5-fold.

3.2.3 Differentially expressed genes involved in ion transporter activity. There were 15 DEGs putatively identified or confirmed as ion channels (Tables 1 & 2). Genes *best-1*, *best-5*, *catp-1*, *cca-1*, *F47E1.4*, *kcc-2*, *ncx-2*, *nlr-1*, *tmc-2*, *Y70G10A.3*, and *ZK185.5*, were downregulated between 1.4- and 2.4- fold (Table 2). Conversely, genes *atp-6*, *best-21*, *F58G6.9* and *kvs-5* were upregulated on average 2-fold (Table 1).

3.2.4 Differentially expressed genes involved in other solute transmembrane transporter activity. There were 30 DEGs involved in transmembrane transport and comprised of various genes and gene families (Tables 1 & 2). The DEGs consisted predominantly of P-glycoprotein efflux pumps (3 genes), other solute transporters (27 genes). Efflux pumps included,

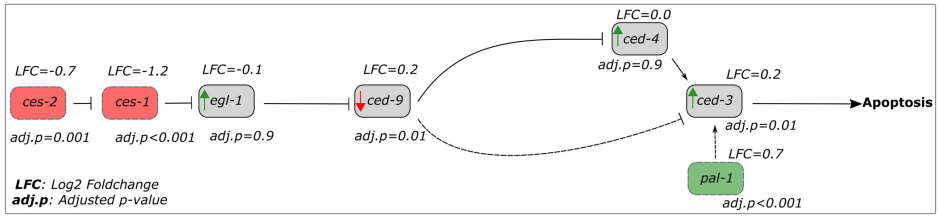

Fig 4. Adapted illustration of the genetic pathway of apoptosis from Conradt and Xue [62]. The boxes symbolize genes, where red and green boxes represent apoptotic genes that in the current study were downregulated or upregulated, respectively according to our thresholds (see Methods). Solid and dashed T-shaped lines represent repression of gene expression, whereas solid and dashed black arrows represent the opposite. Hypothetically, the green and red arrows represent the respective gene's upregulation and downregulation consequent of T-lines and black arrows.

https://doi.org/10.1371/journal.pone.0285262.g004

pgp-5, *pgp-6*, and *pgp-9*, appeared exclusively in IVM 10^{-7} M and, were all upregulated above 2-fold (Table 1). Other solute transporters included folate transporter (*folt-2*), long-chain fatty acid transporter (*pmp-1* and *pmp-4*), amino acid transporter (*aat-3*, *slc-25A29*, *slc-36.5*, *pept-1*, *glt-5*, and *slc-28.1*), myo-inositol transport (*hmit-1.3*), sugar transmembrane transporter (*swt-1*, *K09C4.1*) etc. Of these, only *folt-2* and *pmp-4* were upregulated (Table 1).

3.2.5 Differentially expressed genes involved in transcriptional regulation of xenobiotic metabolism. The differential screening identified 35 transcriptional factors (Tables 1 & 2), of these, nine were nuclear hormone receptors (NHRs) and one was a GATA-type transcription factor. These ten have been postulated to be involved in xenobiotic metabolism (see review [61]). The NHRs, *nhr-17*, *nhr-57* and *nhr-115*, *nhr-137* were upregulated between 1.4 and 3.2-fold (Table 1) whereas *nhr-21*, *nhr-55*, *nhr-99*, *nhr-119*, *nhr-121* and *nhr-173* were downregulated between 1.6 and 2.8-fold. The GATA transcription factor, *elt-2* was downregulated 1.6-fold (Table 2).

3.2.6 Differentially expressed genes involved in apoptosis. The Ivermectin concentration of 10^{-7} M was found to exhibit a greater number of differentially expressed genes (*ces-1*, *ces-2*, *lec-6*, *T05C3.6*, and *pal-1*) involved in apoptosis compared to the concentration of 10^{-8} M (*pal-1*) (Tables 1 & 2). Four of these DEGs (*ces-1*, *ces-2*, *lec-6*, and *T05C3.6*) were observed to be downregulated between 1.4 and 2.3-fold at IVM 10^{-7} M (Table 2). C2H2-type zinc finger transcription factor *ces-1* and basic region leucine-zipper (bZIP) transcription factor *ces-2* have been previously reported as repressors of the gene *egl-1*, a key activator of apoptosis in *C. elegans* [62]. The presence of caudal-type homeodomain transcription factor *pal-1*, an activator of the apoptotic gene *ced-3* (Fig 4), was detected in both IVM 10^{-7} M and 10^{-8} M and was found to be equally upregulated (~ 1.5-fold) in both concentrations (Table 1). This suggests that IVM (at 10^{-7} M and 10^{-8} M) partially activates the apoptotic machinery in the N2 *C. elegans* strain.

3.3 Comparative analysis of gene expression in the *C. elegans* strains N2 and DA1316 following exposure to IVM

We compared our transcriptomic data from the *C. elegans* strain N2 to microarray data obtained from the IVM-resistant *C. elegans* strain DA1316 in a previous study [34]. Based on our preset criteria (see Methods), 152 genes were differentially expressed in the DA1316 strain after IVM exposure for 4 h. Ninety-one percent (139 genes) of DEGs were exclusively detected in 10^{-6} M, 7% (11 genes) in10^{-7} M and 1% (2 genes) occurred in both concentrations (S1 Fig).

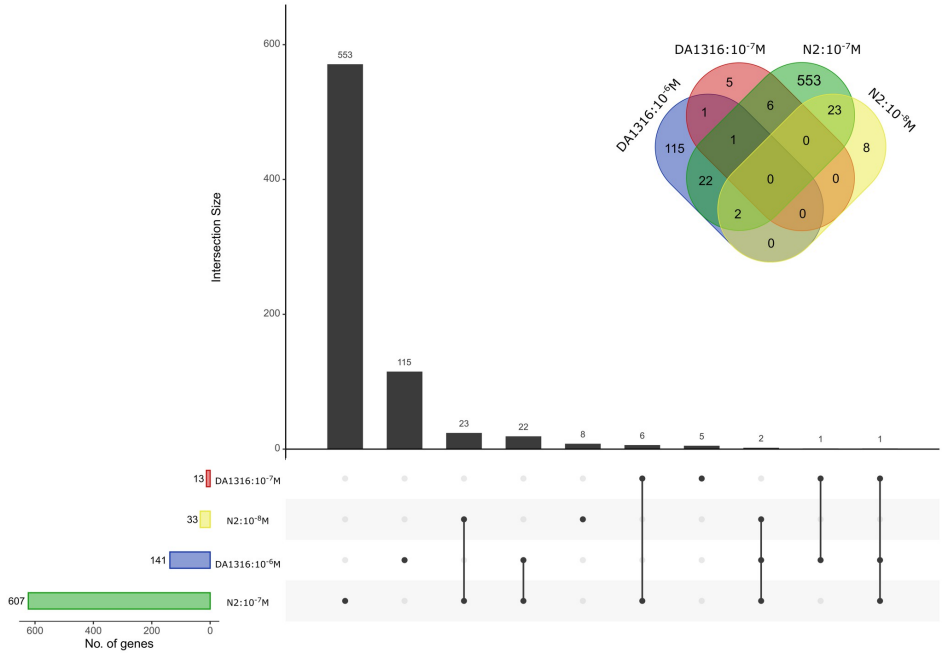

Fig 5. Differentially expressed genes in IVM-exposed *C. elegans* N2 and DA1316 strains. An UpSetR plot and Venn diagrams displaying the number of differentially expressed genes that overlap within and between *C. elegans* strains N2 and DA1316 [34] exposed to IVM 10^{-7} M, 10^{-8} M and 10^{-6} M, 10^{-7} M, respectively. The black boxes indicate the number of genes contained within each partition.

https://doi.org/10.1371/journal.pone.0285262.g005

Overall, irrespective of IVM concentration, comparison of DEGs between DA1316 and N2 strains revealed that the N2 strain showed four times more differentially expressed genes. Thirty-one genes showed significant overlap (p-value < 0.00001) between the two strains (Fig 5 & Table 3). Of these, 61% (19 genes) showed an opposite expression i.e., upregulation in one strain and downregulation in another, notably folate transporter gene, *folt-2* and putative transmembrane transporter, *T22F3.11* (Table 3 & S5 Table). Gene *folt-2* was downregulated 6-fold and 2-fold in DA1316: 10^{-6} and DA1316: 10^{-7}, respectively, and upregulated 4-fold in N2:10^{-7} M concentration (S5 Table). Similarly, *T22F3.11* was upregulated 3-fold in DA1316: 10^{-7} M and downregulated 7-fold in N2:10^{-7} M concentration. Eighteen of the 31 genes were enriched for Phase II metabolic, transmembrane transport and stress response processes. Twelve of the shared genes (*acox-1.5*, *cpt-5*, *drd-5*, *F42A10.7*, *gst-4*, *pud-1.2*, *pud-2.1*, *pud-3*, *pud-4*, *sams-1*, *ugt-12* and *ugt-22*) were downregulated in both strains. The majority of the shared DEGs (22 genes) occurred in DA1316: 10^{-6} M and N2:10^{-7} M concentrations, whereas six genes (*mtl-1*, *C23G10.11*, *scl-2*, *F21C10.10*, *T22F3.11* and *adh-1*) occurred in DA1316: 10^{-7} M and N2:10^{-7} M concentrations (Fig 5 & S5 Table).

Table 3. Overlapping differentially expressed genes between IVM-exposed *C. elegans* N2 and DA1316 strain.

Gene	LFC:N2:10^{-7} M[a]	LFC:N2:10^{-8} M[b]	LFC:DA1316:10^{-6} M[c]	LFC:DA1316:10^{-7} M[d]	Description
acox-1.5	-0.89		-0.72		acyl-CoA oxidase
adh-1	-1.30			1.07	alcohol dehydrogenase
C09B8.4	0.59		-1.20		integral component of membrane
C23G10.11	-3.60			1.23	N.A.
C35A5.3	1.29		-1.83		transmembrane transporter
cpt-5	-1.05		-0.71		acyltransferase
dod-19	0.50		-0.99		innate immune response
drd-5	-0.63		-0.84		oxidoreductase activity
F19B2.5	2.18		-1.39		ATP-dependent chromatin remodeler
F21C10.10	-0.88			1.10	N.A
F42A10.7	-0.78		-0.73		N.A.
F58G6.9	1.62		-1.72		copper ion transmembrane transport
folt-2	1.92		-2.55	-1.17	folate transporter
gst-4	-0.56		-1.41		glutathione transferase
hsp-17	2.04		-0.79		heat shock protein
msra-1	0.85		-1.08		methionine sulfoxide-S-reductase
mtl-1	-0.63			1.59	metallothioneins, small, cysteine-rich, metal-binding protein
pud-1.2	-0.96		-0.58		N.A.
pud-2.1	-0.83		-0.59		N.A.
pud-3	-2.13		-1.13		N.A.
pud-4	-0.73		-0.66		N.A.
rips-1	0.87		-1.04		S-adenosyl-L-methionine-dependent methyltransferase
sams-1	-0.84		-1.02		S-adenosyl methionine synthetase
scl-2	-0.96			1.31	sperm coating protein
T05E12.6	0.86		-1.23		N.A.
T13F3.6	1.13		-0.81		N.A.
T22F3.11	-2.81			1.44	transmembrane transport"
ugt-12	-0.64		-0.79		UDP-glycosyltransferase
ugt-22	-0.91	-0.61	-0.77		UDP-glycosyltransferase
Y94H6A.10	1.31	0.64	-1.27		N.A.
ZK228.4	2.58		-1.01		N-acetyltransferase

Alphabetically sorted differentially genes that overlap between IVM-exposed *C. elegans* N2 and DA1316 strain. Genes in bold showed an opposite expression i.e., upregulation in one strain and downregulation in another.

[a]Log2Foldchange for Ivermectin drug concentration 10^{-7} M in the N2 strain

[b]Log2Foldchange for Ivermectin drug concentration 10^{-8} M in the N2 strain

[c]Log2Foldchange for Ivermectin drug concentration 10^{-7} M in the DA1316 strain

[d]Log2Foldchange for Ivermectin drug concentration 10^{-8} M in DA1316 strain

https://doi.org/10.1371/journal.pone.0285262.t003

3.4 Ivermectin-induced DEGs are mapped within the Abamectin QTL on chromosome V

Evans et al. [35] identified three major QTL (VL, VR and VC) correlated to natural variation in Abamectin response, on chromosome V in *C. elegans*. We decided to use this information to see if any of the DEGs induced by IVM, map in the QTL regions. There was significant (adjusted $p = 0.01$) enrichment for DEGs in chromosomes X and V (S6 Table). A comparison of the DEGs of IVM-exposed *C. elegans* N2 adult worms to the QTL revealed that 45 DEGs

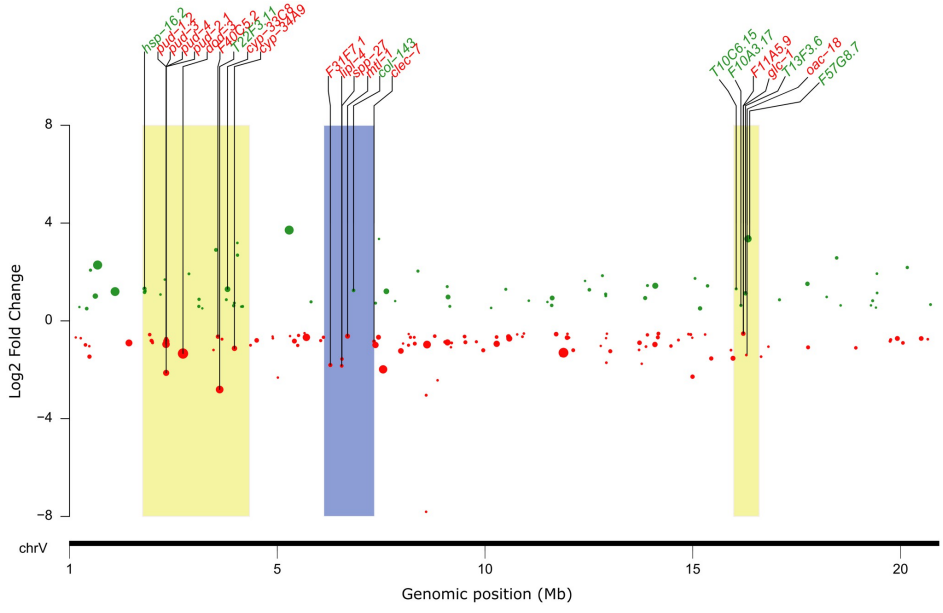

Fig 6. Differentially expressed genes of IVM-exposed *C. elegans* N2 strain map to Abamectin-QTL on chromosome V. The DEGs are represented by green (upregulated) and red (downregulated) dots, with the size of the dot representing the -log10 (*adj. p-value*) of expression, where the larger the dot, the more significantly expressed. The x-axis represents chromosome V and the y-axis represents the Log2 fold change. The karyoplot shows DEGs (labeled in green and red) mapped to abamectin-QTL VL, VC, and VR represented by yellow, blue, and yellow boxes, respectively.

https://doi.org/10.1371/journal.pone.0285262.g006

mapped to the three QTL, 51% (23 genes) were upregulated, and the majority (71%) mapped to the VL locus (Fig 6 & S7 Table). Of the 45 DEGs, nine (*folt-2*, *mtl-1*, *pud-1.2*, *pud-2.1*, *pud-3*, *pud-4*, *rips-1*, *T13F3.6* and *T22F3.11*) overlap with microarray data from IVM-resistant strain (DA1316) [34]. In addition, eight other DEGs from the DA1316 strain mapped to the QTL (S8 Table). The VL locus contained 32 DEGs (S7 Table) from N2 strain, which included seven metabolic genes (*cyp-33C8*, *cyp-34A9*, *acs-3*, *T06A1.5*, *dach-1*, *alh-5*, *cyp-34A8*), six transport-related genes (*dod-3*, *T22F3.11*, *Y39H10B.2*, *folt-2*, *Y32G9B.1*, *slc-28.1*), six stress response genes (*hsp-16.2*, *irg-1*, *hsp-16.41*, *Y73C8C.3*, *irg-2*, *Y73C8C.8*), two transcription factors (*nhr-57*, *nhr-115*), a muscle contraction regulator (*tnt-4*) and 11 others, including pud-genes (S7 Table). Genes *cyp-33C8*, *cyp-34A9*, *dod-3*, *F40C5.2*, *hsp-16.2*, *hsp-16.41*, *pud-1.2*, *pud-2.1*, *pud-3*, and *pud-4* were the ten most significantly (adjusted $p<0.001$) expressed at the VL locus. Of the 10 genes, seven (*cyp-34A9*, *dod-3*, *F40C5.2*, *pud-1.2*, *pud-2.1*, *pud-3* and *pud-4)* were down-regulated between 1.6 and 4.4-fold while the rest were upregulated on average 2.3-fold (Fig 6). Six DEGs mapped to the VC locus (Fig 6), which comprised of three stress response genes (*F31F7.1*, *mtl-1*, *clec-7*), a transport-related gene (*col-143*), a metabolic gene (*lipl-4*), and an unknown gene (S7 Table). Genes *F31F7.1*, *mtl-1*, *clec-7*, *lipl-4*, and *spp-27* were downregulated between 1.5 and 3.6-fold, with the exception of *col-143*, which was upregulated 2.4-fold (Fig 6 & S7 Table). Seven DEGs mapped to the VR locus (Fig 6) composed of a GluCl subunit (*glc-1*),

a transporter (*F11A5.9*) and five unknown genes (S7 Table). The expression of the genes *glc-1*, *F11A5.9*, and *oac-18* was decreased by 1.4-fold, 1.4-fold, and 2.6-fold, respectively. The remaining genes had 1.54- to 10-fold higher expression levels (Fig 6).

A list of candidate genes for further study (S9 Table) has been created, including genes with an opposite expression between N2 and DA1316 *C. elegans* strain, genes within Abamectin-QTL, exclusive genes in DA1316 strain, and other putative drug-responsive genes.

4 Discussion

Parasitic nematodes pose a threat to human and animal health [2, 3], while the development of resistance against MLs such as IVM exacerbates the problem [16, 17, 63]. Therefore, it is crucial to understand the molecular mechanisms underlying ML resistance. In this study, we investigated gene expression in wild-type (N2) IVM-exposed *C. elegans* adults at maximum reproduction to understand the transcriptomic response to IVM exposure. Furthermore, the transcriptomic data was compared to microarray data from the IVM-resistant *C. elegans* (DA1316) strain [34], and the recently identified Abamectin-QTL [35]. We identified 615 differentially expressed genes in the wild-type *C. elegans* (N2) strain following exposure to IVM, of which 95% occurred in the IVM 10^{-7} M concentration. Only 31 N2 strain DEGs overlapped with the IVM-resistant *C. elegans* (DA1316) strain, 19 of which, including folate transporter FOLT-2 (*folt-2*) and transmembrane transporter T22F3.11 *(T22F3.11)*, displayed an opposite expression in either strain. Eighteen of the overlapping genes were enriched for metabolic Phase II enzymes, transmembrane transport, and stress response processes. In addition, we identified 45 differentially expressed genes that mapped within the Abamectin-QTL on *C. elegans* chromosome V, nine of which overlapped with DEGs from the IVM-resistant *C. elegans* (DA1316) strain. Following comprehensive analysis we identified potential candidate genes, T-type calcium channel CCA-1 (*cca-1*), potassium chloride cotransporter KCC2 (*kcc-2*), folate transporter FOLT-2 (*folt-2*) and alpha subunit of glutamate-gated channel GluCl-1 (*glc-1*) for further investigation with possible involvement in IVM resistance.

The ML drug target *glc-1* and the putative drug target *lgc-26* encoding ion channel subunits were downregulated in the IVM 10^{-7} M concentration. The significance of *glc-1* in ML response is evident through RNAi knockdown and loss-of-function-mutations [26, 36, 64, 65]. Heterologous expression of *C. elegans glc-1* and formation of a functional chloride channel has been reported in Xenopus oocytes [66]. The role of *lgc-26* in ML response remains unknown in *C. elegans*, but other cys-loop GABA receptor members have been implicated in the ML response of parasitic nematodes. For example, *lgc-37* was upregulated in the horse roundworm parasite, *Parascaris univalens* after IVM exposure [41] and the *lgc-54* in the sheep parasite *Teladorsagia circumcincta* was reported as potential candidate in IVM resistance through genome-wide studies [67]. However, Evans, Wit [35] recently challenged this claim, as they observed that *lgc-54* mutants did not display a competitive advantage over wild-type in control conditions.

We observed a downregulation of the calcium channel alpha subunit (*cca-1*) and potassium chloride cotransporter (*kcc-2*) genes after IVM exposure. Gene *cca-1* regulates pharyngeal pumping by facilitating the effective start of action potentials by influx of calcium ions in response to marginal cell motor neuron stimulation in *C. elegans* [68, 69]. A loss of function in *cca-1* has been reported to significantly reduce pharyngeal pumping [69]. Furthermore it is established that IVM reduces pharyngeal pumping in *C. elegans* by allosterically modulating GluCl hence increased influx of chloride ions [9]. Hypothetically, a pharyngeal pump regulator such as *cca-1* would be upregulated in response to decreased pharyngeal pumping rate, however, our results showed the opposite trend. Alternatively, the downregulation of *cca-1* could

be a downstream effect, a consequence of the negative membrane potential induced by the chloride ion influx, or a defense/ protective mechanism aimed at reducing the adverse effects of IVM. Nonetheless, this highlights the importance of *cca-1* in IVM response in *C. elegans*. The *kcc-2* gene encodes a potassium chloride cotransporter, which, in conjunction with the sodium-driven chloride-bicarbonate transporter *abts-1*, mediates inhibitory GABA signaling. Mediation involves control of cellular chloride gradient to maintain membrane potential in neurons that control locomotion [70]. In addition, *kcc-2* and *abts-1* mutant of *C. elegans* were reported to exhibit paralysis after exposure to a GABA receptor agonist, muscimol [70]. Considering that IVM agonistically mediates GABA signaling through the inflow of chloride ions to cause paralysis [9], the role of *kcc-2* in IVM response is unknown and warrants exploration. Overall, these findings shed light on additional channels, such as *cca-1* and *kcc-2*, which could be investigated further as potential candidates for involvement in IVM resistance.

Seven of the 11 differentially expressed Transcription factors were downregulated and predominantly enriched for NHRs, which included *nhr-17*, *nhr-21*, *nhr-55*, *nhr-57*, *nhr-99*, *nhr-115*, *nhr-119*, *nhr-121*, *nhr-137* and *nhr-173*. Although NHRs have generally been suggested to regulate expression of detoxification genes (phase I, II and III), only a handful have experimental evidence (see review [61]). To our knowledge, none of the NHRs in the current study has been implicated in xenobiotic detoxification regulation. However, a notable example, *nhr-8* upregulation has been reported to increase expression of detoxification genes *cyp14A2*, *cyp14A5* and *cyp37B1*, and Pgp genes (*pgp-1*,*-3*,*-6*,*-9* and *-13*) resulting in the reduced IVM efficacy [71]. Recent work by Guerrero et al. [72] emphasized this phenomenon, demonstrating *nhr-8* role in upregulation of Pgp genes (*pgp-3*, *-5*, *-11* and *-13*) in the presence of the drug tunicamycin. The GATA-type transcription factor, *elt-2* was downregulated in the current study. The proposed genes regulated by *elt-2* in *C. elegans* include those involved in protection against xenobiotic compounds: CYPs, GSTs, and UGTs such as *ugt-22* [73]. While it is conceivable that this downregulation of *elt-2* might explain the previously described downregulation of *ugt-22*, it is unclear why *elt-2* is downregulated in the presence of a xenobiotic such as IVM.

In this study, an analysis of putative apoptotic genes showed that four out of the five genes identified were downregulated, including C2H2-type zinc finger transcription factor *ces-1* and basic region leucine-zipper (bZIP) transcription factor *ces-2*. These genes have been previously shown to act as repressors of the key apoptotic activator *egl-1* under anti-apoptotic conditions. Under pro-apoptotic conditions, *egl-1* represses *ced-9*, thereby activating the pro-apoptotic genes *ced-3* and *ced-4*, hence apoptosis. The downregulation of *ces-1* and *ces-2* in this study is indicative of *egl-1* being liberated and subsequently able to repress *ced-9*, thereby activating the pro-apoptotic genes *ced-3* and *ced-4*, leading to apoptosis [62]. Additionally, caudal-type homeodomain transcription factor *pal-1*, a reported activator of *ced-3* [74], was found to be upregulated. To further support the pro-apoptotic response hypothesis, genes *ces-1*, *ces-2*, and *pal-1* were predominantly present in the highest IVM concentration (10^{-7} M), in which all worms were previously reported to be immobile [41]. While these findings suggest that IVM at concentrations of 10^{-7} M and 10^{-8} M partially activates the apoptotic machinery in the N2 *C. elegans* strain, it is important to note that other mechanisms involving above genes may also be at play as not all relevant apoptotic genes were detected in the data.

Our second objective was to compare *C. elegans* strains N2 (wild-type) and DA1316 (IVM-resistant) following IVM exposure. Comparing the RNAseq and microarray data from the N2 and DA1316 strains, respectively, revealed that the N2 strain had four times the number of differentially expressed genes with only a 4% (31 genes) overlap between the two strains. Nineteen of these overlapped genes displayed an opposite expression and may have a role in IVM metabolism or resistance. For example, the folate transporter *folt-2*, whose expression was

reduced 6-fold and 2-fold in the resistant DA1316 strain, but increased 4-fold in the sensitive N2 strain, may be involved in the import of IVM. Another potential candidate is the transmembrane transporter *T22F3.11*, whose expression increased by 3-fold in the resistant strain, but decreased 7-fold in the sensitive N2 strain, suggesting a role in IVM efflux. In addition, genes are that are exclusively expressed in the resistant strain could also be an important group for further exploration. Overall, further studies are needed to confirm the role of these genes in IVM response. Twelve of the 31 overlapping genes were downregulated, including four pud-genes, *pud-2.1*, *pud-3*, and *pud-4*. Pud-genes are unique to *Caenorhabditis* spp. without known orthologues in other nematodes and their function remains elusive. In spite of that, Cui et al. [75] reported slow growth and hypersensitivity to cadmium of *C. elegans* after *pud-4* (*F15E11.12*) RNAi knockdown. Another study reported downregulation of *pud-1.2* and *pud-4* following viral infection of *C. elegans* [76]. Other overlapping genes such as *hsp-17* encoding a heat shock protein, exhibited inverted regulation in either strain. Gene *hsp-17*, a stress responder, was downregulated 1.7-fold in DA1316 and upregulated 4-fold in N2 strain. This re-emphasizes the inherent sensitivity of the N2 strain to IVM than its resistant or tolerant counterpart. The discrepancy in gene expression between the two studies could be attributable to strain, technique, life-stage, or IVM concentration. Strain differences may account for most of the difference in DEGs, since N2 is more sensitive to IVM than resistant or tolerant strains [34, 77]. Thus, the N2 strain may have more elevated cellular and biological processes, which could account for the increase in DEGs. Overall, we speculate that pud-genes may be universal stress responders exclusively in *C. elegans*.

As a final objective, we mapped the 615 DEGs derived from the IVM-exposed *C. elegans* to the recently identified Abamectin-QTL [35]. We identified 45 DEGs that corresponded to the QTL regions and compared them to the proposed list of candidate genes from the QTL [35], but only two genes, putative folate transporter (*folt-2*) and *dod-3*, between the two data sets overlapped. Gene *folt-2* supposedly participates in the active uptake of folate [78], a B-class vitamin central in the synthesis of nucleotides and amino acids [79]. Like other eukaryotes, *C. elegans* are intrinsically deficient in folate [80], and therefore rely on dietary sources such as OP50 *E. coli*. In our data, *folt-2* was upregulated, which may be caused by restriction in dietary intake due IVM-induced decreased pharyngeal pumping [9]. This could lead to folate deficiency in the worm. Whether this folate deficiency triggers upregulation of *folt-2* remains unclear and therefore entails further study. In contrast, the function *dod-3* and its role ML response is unknown. Overall, the role of *folt-2*, *dod-3* and other 43 genes that corresponded to the Abamectin-QTL in ML response is unknown and prompts further investigation.

In conclusion, we have profiled the transcriptomes of adult wild-type (N2) *C. elegans* after exposure to different IVM concentrations and revealed predominantly downregulated diverse sets of genes. Some genes overlapped with a previous microarray study on IVM-resistant *C. elegans* while others mapped to recently described abamectin-QTL. Based on this, we have a compiled a list of potential candidate genes for further investigation. Although Abamectin and Ivermectin (IVM) belong to the same subgroup of avermectins, it is important to exercise caution when making comparisons between the two drugs. While Abamectin serves as a precursor drug for IVM, the pharmacokinetics of these drugs have been reported to be considerably different [81, 82]. These differences have been attributed, in part, to variations in the drugs' lipophilicity [83]. Future studies employing quantitative genetics approaches, such as identifying IVM-QTL and corresponding candidate genes, validated through the use of near-isogenic lines, mutant strains, and transcriptomic profiling, would provide more detailed information.

Supporting information

S1 Fig. Differential gene expression in IVM-exposed *C. elegans* DA1316 strain. Venn diagrams showing the number of DEGs in *C. elegans* DA1316 strain between IVM concentrations 10^{-6} M and 10^{-7} M.
(TIF)

S1 Table. Differential gene expression in *C. elegans* (N2) at 10^{-7} M or 10^{-8} M IVM.
(XLSX)

S2 Table. Differential gene expression in *C. elegans* (N2) at 10^{-7} M compared to 10^{-8} M IVM.
(XLSX)

S3 Table. Top 10 up—and downregulated differentially expressed genes in *C. elegans* (N2) at 10^{-7} M and 10^{-8} M IVM.
(DOCX)

S4 Table. Over-representation analysis of IVM-exposed *C. elegans* (N2) differentially expressed genes.
(XLSX)

S5 Table. Differential gene expression in *C. elegans* DA1316 vs N2 after IVM exposure.
(XLSX)

S6 Table. Enrichment analysis of the differentially expressed genes from IVM-exposed *C. elegans* (N2) across all chromosomes.
(XLSX)

S7 Table. Differentially expressed genes from IVM-exposed *C. elegans* (N2) strain mapped to Abamectin-QTL.
(XLSX)

S8 Table. Differentially expressed genes from IVM-exposed *C. elegans* (DA1316) strain mapped to Abamectin-QTL.
(XLSX)

S9 Table. A list of potential candidate genes for further investigation.
(XLSX)

Acknowledgments

We would like to thank the Science for Life Laboratory (SciLifeLab) for providing sequencing services and Swedish National Infrastructure for Computing (SNIC) at UPPMAX for enabling computations and data handling resources. Shweta Roy's contributions were invaluable to the success of the experimental setup.

Author Contributions

Conceptualization: Faruk Dube, Andrea Hinas, Magnus Åbrink, Staffan Svärd, Eva Tydén.

Data curation: Faruk Dube.

Formal analysis: Faruk Dube, Andrea Hinas, Nicolas Delhomme, Magnus Åbrink, Staffan Svärd, Eva Tydén.

Funding acquisition: Andrea Hinas, Staffan Svärd, Eva Tydén.

Investigation: Faruk Dube.

Methodology: Faruk Dube, Andrea Hinas, Nicolas Delhomme, Magnus Åbrink, Staffan Svärd, Eva Tydén.

Project administration: Andrea Hinas, Eva Tydén.

Resources: Eva Tydén.

Software: Faruk Dube, Nicolas Delhomme.

Supervision: Andrea Hinas, Nicolas Delhomme, Magnus Åbrink, Staffan Svärd, Eva Tydén.

Validation: Faruk Dube, Andrea Hinas, Nicolas Delhomme, Magnus Åbrink, Staffan Svärd, Eva Tydén.

Visualization: Faruk Dube.

Writing – original draft: Faruk Dube, Magnus Åbrink.

Writing – review & editing: Faruk Dube, Andrea Hinas, Nicolas Delhomme, Staffan Svärd, Eva Tydén.

References

1. Coyne DL, Cortada L, Dalzell JJ, Claudius-Cole AO, Haukeland S, Luambano N, et al. Plant-Parasitic Nematodes and Food Security in Sub-Saharan Africa. Annu Rev Phytopathol. 2018; 56:381–403. https://doi.org/10.1146/annurev-phyto-080417-045833 PMID: 29958072
2. Gilleard JS, Kotze AC, Leathwick D, Nisbet AJ, McNeilly TN, Besier B. A journey through 50 years of research relevant to the control of gastrointestinal nematodes in ruminant livestock and thoughts on future directions. Int J Parasitol. 2021; 51(13–14):1133–51. https://doi.org/10.1016/j.ijpara.2021.10.007 PMID: 34774857
3. Veesenmeyer AF. Important Nematodes in Children. Pediatr Clin North Am. 2022; 69(1):129–39. https://doi.org/10.1016/j.pcl.2021.08.005 PMID: 34794670
4. Pullan RL, Smith JL, Jasrasaria R, Brooker SJ. Global numbers of infection and disease burden of soil transmitted helminth infections in 2010. Parasit Vectors. 2014; 7:37. https://doi.org/10.1186/1756-3305-7-37 PMID: 24447578
5. Nicol JM, Turner SJ, Coyne DL, Nijs Ld, Hockland S, Maafi ZT. Current Nematode Threats to World Agriculture. In: Jones J, Gheysen G, Fenoll C, editors. Genomics and Molecular Genetics of Plant-Nematode Interactions. Dordrecht: Springer Netherlands; 2011. p. 21–43.
6. Charlier J, Rinaldi L, Musella V, Ploeger HW, Chartier C, Vineer HR, et al. Initial assessment of the economic burden of major parasitic helminth infections to the ruminant livestock industry in Europe. Preventive Veterinary Medicine. 2020; 182:105103. https://doi.org/10.1016/j.prevetmed.2020.105103 PMID: 32750638
7. Shoop WL, Mrozik H, Fisher MH. Structure and activity of avermectins and milbemycins in animal health. Vet Parasitol. 1995; 59(2):139–56. https://doi.org/10.1016/0304-4017(94)00743-v PMID: 7483237
8. Pemberton DJ, Franks CJ, Walker RJ, Holden-Dye L. Characterization of glutamate-gated chloride channels in the pharynx of wild-type and mutant Caenorhabditis elegans delineates the role of the subunit GluCl-alpha2 in the function of the native receptor. Mol Pharmacol. 2001; 59(5):1037–43. https://doi.org/10.1124/mol.59.5.1037 PMID: 11306685
9. Wolstenholme AJ, Rogers AT. Glutamate-gated chloride channels and the mode of action of the avermectin/milbemycin anthelmintics. Parasitology. 2005; 131 Suppl:S85–95. https://doi.org/10.1017/S0031182005008218 PMID: 16569295
10. Wolstenholme AJ, Neveu C. The avermectin/milbemycin receptors of parasitic nematodes. Pestic Biochem Physiol. 2022; 181:105010. https://doi.org/10.1016/j.pestbp.2021.105010 PMID: 35082033
11. Feng XP, Hayashi J, Beech RN, Prichard RK. Study of the nematode putative GABA type-A receptor subunits: evidence for modulation by ivermectin. J Neurochem. 2002; 83(4):870–8. https://doi.org/10.1046/j.1471-4159.2002.01199.x PMID: 12421359

12. Ahuir-Baraja AE, Cibot F, Llobat L, Garijo MM. Anthelmintic resistance: is a solution possible? Exp Parasitol. 2021; 230:108169. https://doi.org/10.1016/j.exppara.2021.108169 PMID: 34627787

13. Geurden T, Hoste H, Jacquiet P, Traversa D, Sotiraki S, Frangipane di Regalbono A, et al. Anthelmintic resistance and multidrug resistance in sheep gastro-intestinal nematodes in France, Greece and Italy. Veterinary Parasitology. 2014; 201(1):59–66. https://doi.org/10.1016/j.vetpar.2014.01.016 PMID: 24560365

14. Vercruysse J, Levecke B, Prichard R. Human soil-transmitted helminths: implications of mass drug administration. Curr Opin Infect Dis. 2012; 25(6):703–8. https://doi.org/10.1097/QCO.0b013e328358993a PMID: 22964945

15. Humphries D, Nguyen S, Boakye D, Wilson M, Cappello M. The promise and pitfalls of mass drug administration to control intestinal helminth infections. Curr Opin Infect Dis. 2012; 25(5):584–9. https://doi.org/10.1097/QCO.0b013e328357e4cf PMID: 22903231

16. Osei-Atweneboana MY, Awadzi K, Attah SK, Boakye DA, Gyapong JO, Prichard RK. Phenotypic evidence of emerging ivermectin resistance in Onchocerca volvulus. PLoS Negl Trop Dis. 2011; 5(3):e998. https://doi.org/10.1371/journal.pntd.0000998 PMID: 21468315

17. Nana-Djeunga HC, Bourguinat C, Pion SD, Bopda J, Kengne-Ouafo JA, Njiokou F, et al. Reproductive status of Onchocerca volvulus after ivermectin treatment in an ivermectin-naïve and a frequently treated population from Cameroon. PLoS Negl Trop Dis. 2014; 8(4):e2824.

18. Doyle SR, Tracey A, Laing R, Holroyd N, Bartley D, Bazant W, et al. Genomic and transcriptomic variation defines the chromosome-scale assembly of Haemonchus contortus, a model gastrointestinal worm. Commun Biol. 2020; 3(1):656. https://doi.org/10.1038/s42003-020-01377-3 PMID: 33168940

19. Doyle SR, Illingworth CJR, Laing R, Bartley DJ, Redman E, Martinelli A, et al. Population genomic and evolutionary modelling analyses reveal a single major QTL for ivermectin drug resistance in the pathogenic nematode, Haemonchus contortus. BMC Genomics. 2019; 20(1):218. https://doi.org/10.1186/s12864-019-5592-6 PMID: 30876405

20. Ghedin E, Wang S, Spiro D, Caler E, Zhao Q, Crabtree J, et al. Draft genome of the filarial nematode parasite Brugia malayi. Science. 2007; 317(5845):1756–60. https://doi.org/10.1126/science.1145406 PMID: 17885136

21. Cotton JA, Bennuru S, Grote A, Harsha B, Tracey A, Beech R, et al. The genome of Onchocerca volvulus, agent of river blindness. Nat Microbiol. 2016; 2:16216. https://doi.org/10.1038/nmicrobiol.2016.216 PMID: 27869790

22. Salinas G, Risi G. Caenorhabditis elegans: nature and nurture gift to nematode parasitologists. Parasitology. 2018; 145(8):979–87. https://doi.org/10.1017/S0031182017002165 PMID: 29208057

23. Harder A. Chapter Three—The Biochemistry of Haemonchus contortus and Other Parasitic Nematodes. In: Gasser RB, Samson-Himmelstjerna GV, editors. Advances in Parasitology. 93: Academic Press; 2016. p. 69–94.

24. Hahnel SR, Dilks CM, Heisler I, Andersen EC, Kulke D. Caenorhabditis elegans in anthelmintic research—Old model, new perspectives. Int J Parasitol Drugs Drug Resist. 2020; 14:237–48. https://doi.org/10.1016/j.ijpddr.2020.09.005 PMID: 33249235

25. Wit J, Dilks CM, Andersen EC. Complementary Approaches with Free-living and Parasitic Nematodes to Understanding Anthelmintic Resistance. Trends in Parasitology. 2021; 37(3):240–50. https://doi.org/10.1016/j.pt.2020.11.008 PMID: 33317926

26. Dent JA, Smith MM, Vassilatis DK, Avery L. The genetics of ivermectin resistance in *Caenorhabditis elegans*. Proc Natl Acad Sci U S A. 2000; 97(6):2674–9.

27. Rezansoff AM, Laing R, Gilleard JS. Evidence from two independent backcross experiments supports genetic linkage of microsatellite Hcms8a20, but not other candidate loci, to a major ivermectin resistance locus in Haemonchus contortus. Int J Parasitol. 2016; 46(10):653–61. https://doi.org/10.1016/j.ijpara.2016.04.007 PMID: 27216082

28. Whittaker JH, Carlson SA, Jones DE, Brewer MT. Molecular mechanisms for anthelmintic resistance in strongyle nematode parasites of veterinary importance. J Vet Pharmacol Ther. 2017; 40(2):105–15. https://doi.org/10.1111/jvp.12330 PMID: 27302747

29. Williamson SM, Storey B, Howell S, Harper KM, Kaplan RM, Wolstenholme AJ. Candidate anthelmintic resistance-associated gene expression and sequence polymorphisms in a triple-resistant field isolate of Haemonchus contortus. Mol Biochem Parasitol. 2011; 180(2):99–105. https://doi.org/10.1016/j.molbiopara.2011.09.003 PMID: 21945142

30. El-Abdellati A, De Graef J, Van Zeveren A, Donnan A, Skuce P, Walsh T, et al. Altered avr-14B gene transcription patterns in ivermectin-resistant isolates of the cattle parasites, Cooperia oncophora and Ostertagia ostertagi. Int J Parasitol. 2011; 41(9):951–7. https://doi.org/10.1016/j.ijpara.2011.04.003 PMID: 21683704

31. Dicker AJ, Nisbet AJ, Skuce PJ. Gene expression changes in a P-glycoprotein (Tci-pgp-9) putatively associated with ivermectin resistance in Teladorsagia circumcincta. Int J Parasitol. 2011; 41(9):935–42. https://doi.org/10.1016/j.ijpara.2011.03.015 PMID: 21683705

32. Raza A, Kopp SR, Bagnall NH, Jabbar A, Kotze AC. Effects of in vitro exposure to ivermectin and levamisole on the expression patterns of ABC transporters in Haemonchus contortus larvae. Int J Parasitol Drugs Drug Resist. 2016; 6(2):103–15.

33. James CE, Hudson AL, Davey MW. Drug resistance mechanisms in helminths: is it survival of the fittest? Trends Parasitol. 2009; 25(7):328–35. https://doi.org/10.1016/j.pt.2009.04.004 PMID: 19541539

34. Laing ST, Ivens A, Butler V, Ravikumar SP, Laing R, Woods DJ, et al. The transcriptional response of Caenorhabditis elegans to Ivermectin exposure identifies novel genes involved in the response to reduced food intake. PLoS One. 2012; 7(2):e31367. https://doi.org/10.1371/journal.pone.0031367 PMID: 22348077

35. Evans KS, Wit J, Stevens L, Hahnel SR, Rodriguez B, Park G, et al. Two novel loci underlie natural differences in Caenorhabditis elegans abamectin responses. PLoS Pathog. 2021; 17(3):e1009297. https://doi.org/10.1371/journal.ppat.1009297 PMID: 33720993

36. Ardelli BF, Stitt LE, Tompkins JB, Prichard RK. A comparison of the effects of ivermectin and moxidectin on the nematode Caenorhabditis elegans. Vet Parasitol. 2009; 165(1–2):96–108. https://doi.org/10.1016/j.vetpar.2009.06.043 PMID: 19631471

37. Ghosh R, Andersen EC, Shapiro JA, Gerke JP, Kruglyak L. Natural variation in a chloride channel subunit confers avermectin resistance in Caenorhabditis elegans. Science. 2012; 335(6068):574–8.

38. Ménez C, Alberich M, Kansoh D, Blanchard A, Lespine A. Acquired Tolerance to Ivermectin and Moxidectin after Drug Selection Pressure in the Nematode *Caenorhabditis elegans*. Antimicrob Agents Chemother. 2016; 60(8):4809–19.

39. Yilmaz E, Gerst B, McKay-Demeler J, Krücken J. Minimal modulation of macrocyclic lactone susceptibility in Caenorhabditis elegans following inhibition of cytochrome P450 monooxygenase activity. Exp Parasitol. 2019; 200:61–6. https://doi.org/10.1016/j.exppara.2019.03.017 PMID: 30946841

40. Zain MM, Yahaya ZS, Him NA. The Effect of Macrocyclic Lactones-Ivermectin Exposure on Egg Hatching and Larval Development of Caenorhabditis elegans. Trop Life Sci Res. 2016; 27(supp1):3–8. https://doi.org/10.21315/tlsr2016.27.3.1 PMID: 27965734

41. Dube F, Hinas A, Roy S, Martin F, Åbrink M, Svärd S, et al. Ivermectin-induced gene expression changes in adult Parascaris univalens and Caenorhabditis elegans: a comparative approach to study anthelminthic metabolism and resistance in vitro. Parasit Vectors. 2022; 15(1):158. https://doi.org/10.1186/s13071-022-05260-4 PMID: 35513885

42. Kopylova E, Noé L, Touzet H. SortMeRNA: fast and accurate filtering of ribosomal RNAs in metatranscriptomic data. Bioinformatics. 2012; 28(24):3211–7. https://doi.org/10.1093/bioinformatics/bts611 PMID: 23071270

43. Quast C, Pruesse E, Yilmaz P, Gerken J, Schweer T, Yarza P, et al. The SILVA ribosomal RNA gene database project: improved data processing and web-based tools. Nucleic Acids Res. 2013; 41(Database issue):D590–6. https://doi.org/10.1093/nar/gks1219 PMID: 23193283

44. Griffiths-Jones S, Bateman A, Marshall M, Khanna A, Eddy SR. Rfam: an RNA family database. Nucleic Acids Res. 2003; 31(1):439–41. https://doi.org/10.1093/nar/gkg006 PMID: 12520045

45. Bolger AM, Lohse M, Usadel B. Trimmomatic: a flexible trimmer for Illumina sequence data. Bioinformatics. 2014; 30(15):2114–20. https://doi.org/10.1093/bioinformatics/btu170 PMID: 24695404

46. de Sena Brandine G, Smith AD. Falco: high-speed FastQC emulation for quality control of sequencing data. F1000Res. 2019; 8:1874. https://doi.org/10.12688/f1000research.21142.2 PMID: 33552473

47. Patro R, Duggal G, Love MI, Irizarry RA, Kingsford C. Salmon provides fast and bias-aware quantification of transcript expression. Nat Methods. 2017; 14(4):417–9. https://doi.org/10.1038/nmeth.4197 PMID: 28263959

48. Davis P, Zarowiecki M, Arnaboldi V, Becerra A, Cain S, Chan J, et al. WormBase in 2022-data, processes, and tools for analyzing Caenorhabditis elegans. Genetics. 2022; 220(4). https://doi.org/10.1093/genetics/iyac003 PMID: 35134929

49. Soneson C, Love MI, Robinson MD. Differential analyses for RNA-seq: transcript-level estimates improve gene-level inferences. F1000Res. 2015; 4:1521. https://doi.org/10.12688/f1000research.7563.2 PMID: 26925227

50. Team BC MB. TxDb.Celegans.UCSC.ce11.ensGene: Annotation package for TxDb object(s) 2019 [https://bioconductor.org/packages/TxDb.Celegans.UCSC.ce11.ensGene/.

51. Love MI, Huber W, Anders S. Moderated estimation of fold change and dispersion for RNA-seq data with DESeq2. Genome Biol. 2014; 15(12):550. https://doi.org/10.1186/s13059-014-0550-8 PMID: 25516281

52. Ritchie ME, Phipson B, Wu D, Hu Y, Law CW, Shi W, et al. limma powers differential expression analyses for RNA-sequencing and microarray studies. Nucleic Acids Res. 2015; 43(7):e47. https://doi.org/10.1093/nar/gkv007 PMID: 25605792

53. Wickham H. ggplot2: Elegant Graphics for Data Analysis. New York, NY: Springer; 2009.

54. Schurch NJ, Schofield P, Gierliński M, Cole C, Sherstnev A, Singh V, et al. How many biological replicates are needed in an RNA-seq experiment and which differential expression tool should you use? Rna. 2016; 22(6):839–51. https://doi.org/10.1261/rna.053959.115 PMID: 27022035

55. Chen H, Boutros PC. VennDiagram: a package for the generation of highly-customizable Venn and Euler diagrams in R. BMC Bioinformatics. 2011; 12(1):35.

56. Kolberg L, Raudvere U, Kuzmin I, Vilo J, Peterson H. gprofiler2—an R package for gene list functional enrichment analysis and namespace conversion toolset g:Profiler. F1000Res. 2020; 9.

57. Conway JR, Lex A, Gehlenborg N. UpSetR: an R package for the visualization of intersecting sets and their properties. Bioinformatics. 2017; 33(18):2938–40. https://doi.org/10.1093/bioinformatics/btx364 PMID: 28645171

58. TBD T. BSgenome.Celegans.UCSC.ce11: Full genome sequences for Caenorhabditis elegans (UCSC version ce11). 2016.

59. Lawrence M, Huber W, Pagès H, Aboyoun P, Carlson M, Gentleman R, et al. Software for computing and annotating genomic ranges. PLoS Comput Biol. 2013; 9(8):e1003118. https://doi.org/10.1371/journal.pcbi.1003118 PMID: 23950696

60. Gel B, Serra E. karyoploteR: an R/Bioconductor package to plot customizable genomes displaying arbitrary data. Bioinformatics. 2017; 33(19):3088–90. https://doi.org/10.1093/bioinformatics/btx346 PMID: 28575171

61. Hartman JH, Widmayer SJ, Bergemann CM, King DE, Morton KS, Romersi RF, et al. Xenobiotic metabolism and transport in Caenorhabditis elegans. J Toxicol Environ Health B Crit Rev. 2021; 24(2):51–94. https://doi.org/10.1080/10937404.2021.1884921 PMID: 33616007

62. Conradt B, Xue D. Programmed cell death. WormBook. 2005:1–13. https://doi.org/10.1895/wormbook.1.32.1 PMID: 18061982

63. Kaplan RM. Biology, Epidemiology, Diagnosis, and Management of Anthelmintic Resistance in Gastrointestinal Nematodes of Livestock. Vet Clin North Am Food Anim Pract. 2020; 36(1):17–30. https://doi.org/10.1016/j.cvfa.2019.12.001 PMID: 32029182

64. Ardelli BF, Prichard RK. Inhibition of P-glycoprotein enhances sensitivity of Caenorhabditis elegans to ivermectin. Veterinary Parasitology. 2013; 191(3):264–75. https://doi.org/10.1016/j.vetpar.2012.09.021 PMID: 23062691

65. Cook A, Aptel N, Portillo V, Siney E, Sihota R, Holden-Dye L, et al. Caenorhabditis elegans ivermectin receptors regulate locomotor behaviour and are functional orthologues of Haemonchus contortus receptors. Molecular and Biochemical Parasitology. 2006; 147(1):118–25. https://doi.org/10.1016/j.molbiopara.2006.02.003 PMID: 16527366

66. Cully DF, Vassilatis DK, Liu KK, Paress PS, Van der Ploeg LHT, Schaeffer JM, et al. Cloning of an avermectin-sensitive glutamate-gated chloride channel from Caenorhabditis elegans. Nature. 1994; 371(6499):707–11. https://doi.org/10.1038/371707a0 PMID: 7935817

67. Choi YJ, Bisset SA, Doyle SR, Hallsworth-Pepin K, Martin J, Grant WN, et al. Genomic introgression mapping of field-derived multiple-anthelmintic resistance in Teladorsagia circumcincta. PLoS Genet. 2017; 13(6):e1006857. https://doi.org/10.1371/journal.pgen.1006857 PMID: 28644839

68. Shtonda B, Avery L. CCA-1, EGL-19 and EXP-2 currents shape action potentials in the Caenorhabditis elegans pharynx. J Exp Biol. 2005; 208(Pt 11):2177–90. https://doi.org/10.1242/jeb.01615 PMID: 15914661

69. Steger KA, Shtonda BB, Thacker C, Snutch TP, Avery L. The Caenorhabditis elegans T-type calcium channel CCA-1 boosts neuromuscular transmission. J Exp Biol. 2005; 208(Pt 11):2191–203.

70. Bellemer A, Hirata T, Romero MF, Koelle MR. Two types of chloride transporters are required for GABA (A) receptor-mediated inhibition in Caenorhabditis elegans. Embo j. 2011; 30(9):1852–63.

71. Ménez C, Alberich M, Courtot E, Guegnard F, Blanchard A, Aguilaniu H, et al. The transcription factor NHR-8: A new target to increase ivermectin efficacy in nematodes. PLoS Pathog. 2019; 15(2):e1007598. https://doi.org/10.1371/journal.ppat.1007598 PMID: 30759156

72. Guerrero GA, Derisbourg MJ, Mayr FA, Wester LE, Giorda M, Dinort JE, et al. NHR-8 and P-glycoproteins uncouple xenobiotic resistance from longevity in chemosensory *Caenorhabditis elegans* mutants. Elife. 2021; 10.

73. McGhee JD, Fukushige T, Krause MW, Minnema SE, Goszczynski B, Gaudet J, et al. ELT-2 is the predominant transcription factor controlling differentiation and function of the Caenorhabditis elegans intestine, from embryo to adult. Dev Biol. 2009; 327(2):551–65.

74. Maurer CW, Chiorazzi M, Shaham S. Timing of the onset of a developmental cell death is controlled by transcriptional induction of the Caenorhabditis elegans ced-3 caspase-encoding gene. Development. 2007; 134(7):1357–68.

75. Cui Y, McBride SJ, Boyd WA, Alper S, Freedman JH. Toxicogenomic analysis of Caenorhabditis elegans reveals novel genes and pathways involved in the resistance to cadmium toxicity. Genome Biol. 2007; 8(6):R122. https://doi.org/10.1186/gb-2007-8-6-r122 PMID: 17592649

76. Chen K, Franz CJ, Jiang H, Jiang Y, Wang D. An evolutionarily conserved transcriptional response to viral infection in Caenorhabditis nematodes. BMC Genomics. 2017; 18(1):303. https://doi.org/10.1186/s12864-017-3689-3 PMID: 28415971

77. Menzel R, Bogaert T, Achazi R. A systematic gene expression screen of Caenorhabditis elegans cytochrome P450 genes reveals CYP35 as strongly xenobiotic inducible. Arch Biochem Biophys. 2001; 395 (2):158–68. https://doi.org/10.1006/abbi.2001.2568 PMID: 11697852

78. Balamurugan K, Ashokkumar B, Moussaif M, Sze JY, Said HM. Cloning and functional characterization of a folate transporter from the nematode Caenorhabditis elegans. Am J Physiol Cell Physiol. 2007; 293 (2):C670–81. https://doi.org/10.1152/ajpcell.00516.2006 PMID: 17475669

79. Stokstad ER. Historical perspective on key advances in the biochemistry and physiology of folates. Folic acid metabolism in health and disease. 1990;13.

80. Brzezińska A, Wińska P, Balińska M. Cellular aspects of folate and antifolate membrane transport. Acta Biochim Pol. 2000; 47(3):735–49. PMID: 11310973

81. Gokbulut C, Karademir U, Boyacioglu M, McKellar QA. Comparative plasma dispositions of ivermectin and doramectin following subcutaneous and oral administration in dogs. Vet Parasitol. 2006; 135(3–4):347–54. https://doi.org/10.1016/j.vetpar.2005.10.002 PMID: 16280198

82. Al-Azzam SI, Fleckenstein L, Cheng KJ, Dzimianski MT, McCall JW. Comparison of the pharmacokinetics of moxidectin and ivermectin after oral administration to beagle dogs. Biopharm Drug Dispos. 2007; 28(8):431–8. https://doi.org/10.1002/bdd.572 PMID: 17847063

83. Lespine A. Lipid-like properties and pharmacology of the anthelmintic macrocyclic lactones. Expert Opin Drug Metab Toxicol. 2013; 9(12):1581–95. https://doi.org/10.1517/17425255.2013.832200 PMID: 24050513

Acta Universitatis Agriculturae Sueciae

Doctoral Thesis No. 2024:11

Parascaris univalens poses a lethal intestinal threat to foals through potential ruptures from high infestations. Control relies on anthelmintic drugs like ivermectin, but resistance exacerbated by frequent first year treatments challenges effectiveness. Research into underlying genetics is vital yet hindered by ethical, financial and technical obstacles. This thesis examined using the model nematode *Caenorhabditis elegans* to study anthelmintic resistance via transcriptomics and gene networks. Despite differing responses, commonalities in engaged gene families support *C. elegans* as a useful initial model, though targeted parasite research is crucial for fully elucidating resistance mechanisms.

Faruk Dube received his doctoral studies in the Department of Animal Biosciences. He earned his master's degree in Infection Biology from Uppsala University in Sweden, and his bachelor's degree in Biomedical Laboratory Technology was obtained from Makerere University in Uganda.

Acta Universitatis Agriculturae Sueciae presents doctoral theses from the Swedish University of Agricultural Sciences (SLU).

SLU generates knowledge for the sustainable use of biological natural resources. Research, education, extension, as well as environmental monitoring and assessment are used to achieve this goal.

ISSN 1652-6880
ISBN (print version) 978-91-8046-286-0
ISBN (electronic version) 978-91-8046-287-7